UNIVERSITY OF CALIFORNIA

Los Angeles

Molecular and Epigenetic Regulation of

Stem Cell Self-Renewal and Differentiation

A dissertation submitted in partial satisfaction of the

requirements for the degree Doctor of Philosophy

in Oral Biology

by

Peng Deng

2017

ABSTRACT OF THE DISSERTATION

Molecular and Epigenetic Regulation of

Stem Cell Self-Renewal and Differentiation

by

Peng Deng

Doctor of Philosophy in Oral Biology

University of California, Los Angeles, 2017

Professor Cun-Yu Wang, Chair

Mesenchymal stem cells (MSCs) are capable of differentiating into osteoblasts and adipocytes, and the dysregulation of MSC lineage specification may lead to the imbalance between bone mass and fat tissue, which finally result in osteoporosis. Our previous study has shown the critical role of KDM4B in promoting osteogenic differentiation and reducing adipogenic differentiation of MSCs in vitro, but the in vivo function of KDM4B remains to be investigated. In this study, Global deletion of Kdm4b and deletion of Kdm4b in mesenchymal progenitors, but not in mature osteoblasts, enhanced age-related bone loss and adipose accumulation in mouse bone marrow. Deletion of Kdm4b in mesenchymal progenitors also promoted bone loss and adipose accumulation induced by estrogen deficiency respectively. Restoration of KDM4B successfully

reinstated ALP activity, mineralization and expression of osteogenic-related genes, and inhibited adipogenesis of BMSCs from Prx1-Cre;Kdm4b$^{fl/fl}$ mice. Furthermore, Kdm4b was required for the self-renewal of mouse MSCs, as determined by colony formation assay and serial transplantation assay. Collectively, Kdm4b was required for bone homeostasis by promoting osteogenic differentiation and reducing adipogenic differentiation of MSCs in vivo. Kdm4b was also required for self-renewal of MSCs. Targeting KDM4B may facilitate the prevention and therapy of osteoporosis, and also be used in MSC-based bone regeneration. In addition, we reported an efficient ex vivo culture protocol to derive functional MSCs from human ESCs by inhibition of NFκB. We found inhibition of NFκB promoted loss of the pluripotent markers during differentiation of human ESCs, and increased expression of mesenchymal lineage markers. Microarray analysis revealed that the genes regulated by inhibition of NFκB signaling are associated with developmental process and cell differentiation during human ESC differentiation. Finally, the purified MSCs showed multipotency in vitro. Our data provides key insights into the role of NFκB in mesenchymal lineage specification of human ESCs and provide a novel method for generation of MSCs.

The dissertation of Peng Deng is approved.

Aghaloo Tara

Guoping Fan

Reuben Kim

Cun-Yu Wang, Committee Chair

University of California, Los Angeles

2017

TABLE OF CONTENT

Chapter 1

Chapter 2

LIST OF FIGURES

LIST OF TABLES

ACKNOWLEDGEMENTS

This dissertation would not have been possible without the generous support and help from the many people throughout my PhD program. First and foremost, I would like to thank Dr Cun-Yu Wang for his mentorship, advice, insight, as well as all the help. I would also like to thank him for providing me with generous support regarding my tuition. I would like to thank my committee members Dr Aghaloo Tara, Dr Guoping Fan, Dr Reuben Kim, Dr Jiaoti Huang, for their experimental advice, insightful comments, guidance, and encouragement. It is truly a great honor to have them as my committee members. I would like to thank Dr Qianming Chen for his support and care.

My accomplishments today are all the result from the superb faculty support at School of Dentistry, UCLA. I would like to thank Dr. Wen Yuan Shi, PhD advisor, for his constant care and advice. Many thanks to Ms Megan Scott and Mr Matthew Dingman at the Oral Biology department for their patience in helping me circumventing countless difficult administrative situations.

I want to thank all the current and past members of Wang Lab for the stimulating work discussions and support. I especially would like to thank Dr Bo Yu, Dr Quan Yuan, Dr Dr Jiong Li, Dr Yongxin Yu, Dr Demeng Chen, Dr Yingduan Cheng for their significant contributions towards the project described here.

Lastly, I would like to acknowledge my wife and my family for their accommodation and support during my studies. I could not have made it to here without you.

BIOGRAPHICAL SKETCH	
NAME Deng, Peng CHS 33-030, UCLA Los Angeles, CA 90095	**POSITION TITLE** Graduate Student Researcher (GSR) in Division of Oral Biology and Medicine

EDUCATION/TRAINING

INSTITUTION	DEGREE or Position	MM/YY	FIELD OF STUDY
Sichuan University, School of life science	B.S.	09/2006 - 06/2010	Life Science
Sichuan University, School of Stomatology			Oral Biology and Medicine
University of California, Los Angeles, School of Dentistry	Visiting researcher	05/2011 - 04/2013	Oral Biology and Medicine
University of California, Los Angeles, School of Dentistry	Graduate Student (GSR)	09/2013 - now (11/2014 - now)	Oral Biology and Medicine

Positions

Position and Employment

2013-now   Graduate Student, Division of Oral Biology and Medicine, UCLA School of Dentistry

2015-now   GSR, Division of Oral Biology and Medicine, UCLA School of Dentistry

Other Experience and Professional Memberships

2014-now   (Student) Member, American Association for the Advancement of Science (AAAS)

Publications

1. **Deng P**, Zhou C, Alvarez R, Hong C, Wang CY. Inhibition of IKK/NF-κB Signaling Enhances Differentiation of Mesenchymal Stromal Cells from Human Embryonic Stem Cells. *Stem Cell Reports*. 2016 Apr 12;6(4):456-65. doi: 10.1016/j.stemcr.2016.02.006.

2. **Deng P**, Chen QM, Hong C, Wang CY. Histone methyltransferases and demethylases: regulators in balancing osteogenic and adipogenic differentiation of mesenchymal stem cells. *Int J Oral Sci*. 2015 Dec 18;7(4):197-204. doi: 10.1038/ijos.2015.41.

3. Lee HL, Yu B, **Deng P,** Wang CY, Hong C. Transforming Growth Factor-β-Induced KDM4B Promotes Chondrogenic Differentiation of Human Mesenchymal Stem Cells. *Stem Cells*. 2016 Mar;34(3):711-9. doi: 10.1002/stem.2231.

4. Chen, D., Wu, M., Li, Y., Chang, I., Yuan, Q., Salvo, EM., **Deng, P.**, et al. Targeting BMI1+ Cancer Stem Cells Overcomes Chemoresistance and Inhibits Metastases in Squamous Cell Carcinoma. Cell Stem Cell. 2017. DOI: http://dx.doi.org/10.1016/j.stem.2017.02.003

5. Li, J., Guo, Y., Feng, X., Wang, Z., Wang, Y.**, Deng, P.**, & Chen, Q.. Receptor for activated C kinase 1 (RACK1): a regulator for migration and invasion in oral squamous cell carcinoma cells. *Journal of cancer research and clinical oncology*, 2012*138*(4), 563-571.

6. Li, Jing, Changyang Gong, Xiaodong Feng, Xikun Zhou, Xiaoping Xu, Liang Xie, Ruinan Wang, **Peng Deng**, et al. "Biodegradable thermosensitive hydrogel for SAHA and DDP delivery: therapeutic effects on oral squamous cell carcinoma xenografts." *PloS one* 7, no. 4 (2012): e33860.

CHAPTER 1

Histone Demethylases KDM4B promotes osteogenesis and reduces adipogenesis, and is required for self-renewal of Mesenchymal Stromal Cells

1. INTRODUCTION

Osteoporosis is a skeletal disorder characterized by compromised bone strength predisposing a person to an increased risk of fracture as defined by the NIH Consensus Development Panel. To date, osteoporosis is most common bone disease affecting 9 million people worldwide. In United States, approximately 1.5 million osteoporotic fractures occur annually, including around 700,000 vertebral fractures, 300,000 hip fractures, 250,000 wrist fractures, and 300,000 fractures at other sites[1]. Osteoporosis is usually diagnosed by measuring bone mineral density (BMD), and several clinical risk factors have been identified as contributing to fracture risk, such as age, premature menopause, prior fragility fracture, the use of oral corticosteroids, and excess alcohol consumption[2].

The human skeleton is a dynamic organ where bone mass is controlled a delicate process, bone remodeling. Bone remodeling is a life-long process, which occurs in distinct areas of bone known as basic multicellular units (BMUs)[3]. Within BMUs, bone resorption by osteoclasts and bone formation by osteoblasts are tightly coupled in a delicate balance to maintain homeostasis of bone mass. However, in certain physiological conditions and various diseases, bone resorption outpaces bone formation that shifts the balance to a negative outcome, and results in a net bone loss (also known as osteopenia), which may eventually develops osteoporosis[4]. For instance, by about the fifth decade of life, age-related bone loss begins in both men and women.

The term MSC was originally used to describe a hypothetical multipotent progenitor derived from embryonic mesenchymal tissues with the ability of self-renewal to maintain the homeostasis of

skeletal tissues[5]. However, questions rise about the existence of a common mesenchymal progenitor. First, the "inducible" multipotency does not mean that the precursor cells are also "determined" to spontaneous differentiation into all the skeletal tissues *in vivo*[6]. Secondly, the heterogeneity of mesenchymal stromal cells from different tissues has been observed in proliferation rate, mutlipotency in vitro, and the ability to generate ectopic bone[7, 8]. In addition, bone and muscle derive from different precursors during embryonic development[9]. All the considerations demand an unequivocal identification of MSCs in vivo, and a lineage tracing approach to study their fate map. To facilitate the exchange of data among investigators, Mesenchymal and Tissue Stem Cell Committee proposed the minimal criteria of MSCs[10]. First, MSC must be plastic-adherent when maintained in standard culture conditions. Second, MSC must express CD105, CD73 and CD90, and lack expression of CD45, CD34, CD14 or CD11b, CD79alpha or CD19 and HLA-DR surface molecules. Third, MSC must differentiate to osteoblasts, adipocytes and chondroblasts in vitro.

In this study, MSCs refers to heterogeneous cell populations with capacity for self-renewal and multipotency of differentiation, which can give rise to multiple lineages, including osteoblasts and adipocytes. As the progenitor of osteoblasts, the commitment to osteoblasts and self-renewal capacity of MSCs are critical for the maintenance of bone homeostasis. In addition, MSCs are considered to be of great promise for regenerative medicine. MSCs were originally isolated from bone marrow, and then have been found in many other adult tissues, such as adipose tissues, although characteristics of MSCs from different tissue origins exhibited different capacities in colony-formation capacity, proliferation rate, and differentiation potential[11]. Understanding of the molecular mechanisms in regulation of MSC lineage specification will promote MSCs to differentiate into the desired cell types for tissue repair, instead of other cell types. In this paper,

we mainly focused on the molecular mechanism regulation of osteogenic and adipogenic differentiation of MSCs, as well as regulation of self-renewal of MSCs.

Several cell surface single markers and combinations of these markers have been proposed to identify MSCs and to isolate MSCs, such as PDGFRα (platelet-derived growth factor receptor alpha), Sca-1 (stem cell antigen-1), αSMA (alpha-smooth muscle actin), Nestin, LepR (leptin receptor) and so on[12-15]. And It is widely accepted that MSCs are negative for the expression of hematopoietic lineage markers, such as CD45 (also known as the leukocyte common antigen (LCA)), Ter119 (lymphocyte antigen 76). However, to date, there is no single, unique marker that identifies MSCs or excludes all the other lineages. On the other hand, the overlay among different marker-defined populations has been observed. For instance, Nes-GFP$^+$ cells comprise both PDGFRα$^+$ and PDGFRα$^-$ cells. And LepR+ cells are positive with PDGFRα, but include Sca-1$^+$ and Sca-1$^-$ cells[15].

1.1 Regulation of MSC Lineage Specification

The differentiation of MSCs is a highly controlled process involves multiple mechanisms, which can be regulated at several levels, such as expression of key transcription factors, activities of related signaling pathway, and at epigenetic levels. The osteogenic differentiation of MSCs can be categorized into three steps: commitment to sublineage progenitors, differentiation into pre-osteoblasts/pre-adipocytes and maturation of osteoblasts/adipocytes[16, 17]. Subsequently, mature osteoblasts get entombed in osteoid (unmineralized bone matrix) to become osteocytes. The adipogenic differentiation of MSCs also involves several stages as defined previously, including mesenchymal precursors, committed pre-adipocytes, growth-arrested pre-adipocytes, mitotic clonal expansion, terminal differentiation into lipid-laden and insulin-responsive adipocytes [18, 19].

A reverse relationship between osteogenic differentiation and adipogenic differentiation of MSCs has been long suggested. For instance, accumulation of adipose tissue in bone marrow has been observed in parallel with bone loss during aging[20, 21]. All the bone marrow is red and contains cells for blood formation at birth. With age, hematopoietic marrow is progressively replaced by fatty marrow with a higher conversion in the appendicular skeleton. By the age of 25 years, approximately 40% hematopoietic marrow was replaced with fat in the axial skeleton, rib, sternums, and metaphysis of femora and humeri[21, 22]. In contrast, during treatment of osteoporosis, intermittent administration of parathyroid hormone (PTH) increases bone mass, and reduced bone marrow adipose tissue (MAT). This negative correlation has been found in cell culture and animal models[23], indicating the osteogenic differentiation of MSCs is switched to differentiation into adipocyte lineages[24].

1.1.1 Transcription Factors Governing Osteogenesis and Adipogenesis of MSCs

Runt-related transcription factor 2 (RUNX2) is a member of the runt family, and is considered as the master transcription factor that directs MSC fate toward osteoblasts. RUNX2 was discovered as a DNA binding protein at the promoter of osteocalcin (bone gamma-carboxyglutamate protein, BGLAP). In human, mutations in the RUNX2 gene are also associated with cleidocranial dysplasia[25]. Both mutation of Runx2 at C-terminal and deletion of RUNX2 in MSCs caused a severe skeletal defect, and led to death at birth, indicating Runx2 is required for osteogenic differentiation of MSC and bone formation[26, 27]. It was further confirmed in cell culture and bone repair that Runx2 transduced MSCs exhibited increased osteogenic differentiation potential *in vitro* and enhanced bone formation in skull defects *in vivo*[28]. Interestingly, Runx2 transgenic mice that overexpressed Runx2 in osteoblasts using type I collagen promoter showed osteopenia with multiple bone fractures. In Runx2 transgenic mice, although neonatal osteoblasts were increased,

their maturation and function was impaired in matrix production and mineralization[27, 29]. In a word, Runx2 is essential for differentiation of MSC into osteoblasts, but overexpression of Runx2 severely impaired maturation of osteoblasts.

Osterix (OSX/SP7), a zinc finger-containing transcription factor, is another essential osteogenic master regulator. Osx is expressed in osteoblasts of all endochondral and membranous bones. As *Nakashima et al.* reported, Osx-deficient mice did not form bone *in vivo*, indicating Osx is required for bone formation. MSCs in Osx-deficient mice exhibited impaired differentiation into osteoblasts and did not deposit bone matrix, despite having normal levels of Runx2. In contrast, Osx expression was down-regulated in Runx2 null mice, indicating that OSX is activated downstream of RUNX2.

There are also several Homeobox (HOX) genes that have been implicated in osteogenesis. HOX genes encode a large family of homeodomain-containing transcription factors, and play an important role in anterior-posterior axis patterning and the developmental fate of cells[30]. For instance, distal-less homeobox 5 (DLX5) was found to induce RUNX2 and OSX expression when treated with bone morphogenetic protein 2 (BMP2)[31]. Interestingly, although Osx is a downstream target of Runx2, the DLX5-mediated Osx upregulated could be independent of Runx2 in mouse myogenic C2C12 cells[32]. In addition, Homeobox A10 (HOXA10) is expressed in the presomitic mesoderm during embryogenesis, which develops into the axial skeleton[33, 34]. HOXA10-specific regulatory elements can be found at promoters at Runx2 and Runx2 target genes, such as BGLAP, alkaline phosphatase (ALP), and bone sialoprotein (BSP)[33].

Like the role of Runx2 in osteogenesis, Pparγ (peroxisome proliferator-activated receptor gamma) is considered as a master transcription factor of adipogenesis. As a member of the nuclear receptor superfamily, Pparγ are capable of forming heterodimers with the retinoid X receptor, and regulate

the expression of target genes in a ligand-dependent manner. Pparγ is expressed at high levels in white and brown adipose tissue, where it plays an essential role in many different biological processes including adipogenesis, glucose homeostasis, and insulin sensitivity. Due to adipocyte hypertrophy, heterozygous Pparγ-deficient mice were reported to be protected from the development of insulin resistance under a high-fat diet[35]. Similarly, patients with heterozygous mutations in the ligand-binding domain of PPARγ showed severe insulin resistance[36]. Using adipose-specific PPAR knockout mice model, Jones et al. found that these mice exhibited diminished weight gain despite hyperphagia, and did not develop insulin resistance[37]. In particular, no factor has been found that can promote adipogenesis in the absence of PPARγ, highlighted the critical role in regulation of adipogenesis[38].

Three members of CCAAT/enhancer-binding protein (C/EBP) family (C/EBPα, -β, -δ) also play an important role in promoting adipogenesis of MSCs. C/EBPα is expressed at late stages during adipogenesis, and is required for differentiation of white adipose tissue in mice[39]. Cell culture studies also showed show that C/EBPα is sufficient to induce differentiation of preadipocytes into mature adipocytes. C/EBPα directly promoted the transcription of adipose specific genes, such as the fatty acid-binding protein (FABP), stearyl CoA desaturase (SCD1), and the insulin-responsive glucose transporter 4 (Glut4). Although C/EBPβ and C/EBPδ single knockout mice had only slightly smaller white fat pads compared to wild type controls, adipose tissue was significantly reduced in double knockout mice. Compared to C/EBPα, C/EBPβ and C/EBPδ seem to be more important for differentiation of brown adipocytes. The interscapular brown adipose tissue (BAT) in wild-type mice contained many lipid droplets by 20 h after birth, whereas C/EBPβ and C/EBPδ single knockout mice did not accumulate any droplets[40, 41].

1.1.2 Signaling pathways Governing Osteogenesis and Adipogenesis of MSCs

There are multiple signaling pathways regulating lineage specification of MSCs, such as Wnt (wingless-type MMTV integration site) signaling, BMP (bone morphogenetic protein) signaling, Hedgehog signaling, NELL-1(NEL-like protein 1) signaling, and IGF (insulin-like growth factor) signaling. In this paper, we mainly focus on Wnt signaling and BMP signaling that was found to be related to KDM4B functions.

Wnt signaling plays an essential role in proliferation, stem cell differentiation, and self-renewal. Wnt signaling is classified into canonical Wnt signaling (β-catenin-dependent) and non- canonical Wnt signaling (β-catenin-independent). Generally, canonical Wnt signaling initiates with the binding of Wnt ligands, such as Wnt3a and Wnt10b, to the frizzled receptors (Frz), which subsequently induces complex formation with coreceptors, low-density lipoprotein receptor (LRP5/6) and intracellular proteins Disheveled (DSH). Activated DSH then inhibits the Axin (axis inhibition protein)/GSK3 (glycogen synthase kinase 3)/APC (adenomatosis polyposis coli) complex, which lead to β-catenin accumulation in nuclei. The role of canonical Wnt signaling in bone formation has been well-established in both animal models and patients[42]. For instance, loss-of-function mutations of LRP5 gene cause pseudo-glioma syndrome, which is characterized by a low bone mass phenotype. In addition, mutations in Wnt antagonist sclerostin (SOST) gene induced skeletal disorders such as sclerosteosis that is featured with increased bone mass[43], while treatments with anti-sclerostin antibodies increased BMD by enhancing bone formation and inhibiting bone resorption in Phase II clinical trials[44]. Mechanistically, canonical WNT signaling was found to promote MSC osteogenic differentiation by directly stimulating Runx2 expression[45]. Moreover, non-canonical Wnt signaling has recently been found to promote osteogenesis[46]. Transgenic Wnt4 mice exhibited significant increased bone mass compare to controls[47].

On the other hand, Wnt signaling family has been found to inhibit adipogenesis of MSCs. Activation of canonical Wnt signaling induced by Wnt10b treatment and ectopic overexpression of Wnt1 inhibited PPARγ expression and almost completely blocked adipogenic differentiation of 3T3-L1 preadipocytes[19, 48, 49]. Conversely, treatment with DKK1, an antagonistic inhibitor of Wnt signaling, promoted adipogenesis[48]. However, although the inhibitory effect of Wnt signaling on adipogenesis has been proved more than 15 years, the mechanisms by which Wnt signaling regulate expression of PPARγ and C/EBPα remains largely unknown. Interestingly, although upregulation of PPARγ suppressed β-catenin signaling[50], overexpression of PPARγ and/ or C/EBPα could not Wnt/β-catenin mediated inhibition of adipogenesis[51], indicating Wnt signaling may inhibit adipogenesis independent on PPARγ and/ or C/EBPα at different stages of adipogenesis.

BMPs are members of the transforming growth factor-beta (TGF-β) superfamily and play a major role in bone formation and skeletal development. More than 20 BMP genes has been found in human genome, in which BMP2, -6, -7 and -9, promote osteogenic differentiation of MSCs both *in vitro* and *in vivo*[52]. Knockout of specific BMPs often leads to a variety of skeletal anomalies, suggesting the critical important role of BMP signaling in skeletal development[53, 54]. Smad1 is the major downstream mediator of BMP signaling, while osteoblast-specific deletion of Smad1 resulted in an osteopenic phenotype, and impaired osteoblastic differentiation and proliferation. Consistently, overexpression of noggin, a well-established antagonist of BMPs, also led to osteopenia[55, 56]. Mechanistically, Dlx5 is an early response gene in response to BMP2 treatment and could be a direct target of BMP-signaling[31]. BMP-signaling can also directly induce runx2 expression[57].

Several BMP family members, such as BMP2, -4, -9, also promote adipogenesis. For example, BMP-2 enhanced adipogenic differentiation of murine 3T3-L1 preadipocytes in in synergy with activator of PPARγ, rosiglitazone[58]. BMP2 and BMP4 induced commitment of C3H10T1/2 pluripotent stem cells into adipocytes. Interestingly, overexpression of BMPr1A or BMPr1B promoted adipogenic commitment of C3H10T1/2 cells, while overexpression of a negative receptor dominant-negative-BMPr1A inhibited adipogenic commitment induced by BMP2/4. Conversely, depletion of Smad4, the co-regulator in the BMP/SMAD signaling, disrupted commitment by the BMP2/4[59]. These findings indicate a critical role of BMP signaling in adipogenesis. Haka et al. also reported that BMP2 may also induce PPARγ expression and adipogenesis by MAPK signaling in C3H10T1/2 cells[60].

1.2 Epigenetic Regulation

The term "epigenetic regulation" refers to inheritable changes in gene expression without altering the DNA sequence, such as DNA methylation, histone modification and small non-coding RNA-associated regulation[61]. In eukaryotic cells, chromatin structure is highly dynamic, regulated in large part by histone modifications, such as histone acylation and methylation[62]. Histone methylation usually takes place at lysine residues of histones. Specifically, the lysine residues can be unmodifed (me0), mono- (me1), di- (me2) or trimethylated (me3). The resulting histone methylation levels are important in regulating transcription factors' access to the promoters of target genes by regulating chromatin structure[63]. Major methylation sites are located in the tail histones H3 and H4, such as H3K4, H3K9, H3K27, H3K36 and H4K20[64]. In general, methylation at H3K4 and H3K36 is associated with transcriptional activation, while methylation at H3K9 and H3K27 is related to transcriptional repression. The role of mono-methylation at H4K20 could be either transcriptional activation or repression[64, 65].

Although it has been five decades since histone methylation's discovery[66], its correlation with gene regulation was only established recently[67]. Recent studies have highlighted histone methylation states as an important modulator in stem cell differentiation[63]. Regulation of these methylation states is tightly controlled by the opposing activities of histone lysine methyltransferases (KMTs) and histone lysine demethylases (KDMs)[65], which are recruited to specific histone lysine residues and are responsible for the establishment and regulation of histone methylation and demethylation, respectively. The SET domain-containing family and the Jumonji C (JmjC) domain-containing family represent the major KMTs and KDMs[63, 65].

1.2.1 SET domain-containing Histone Methyltransferases

The evolutionarily conserved SET(Su(var)3–9, Enhancer-of-zeste, Trithorax) domain functions as the catalytic domain of KMTs by transferring a methyl group from s-adenosylmethionine to the ε-amine on the side chain of histone lysine residues[65]. These SET domain-containing KMTs seem to be particularly sensitive to posttranslational methylation at target lysine sites. Although it has been five decades since histone methylation's discovery[66], its correlation with gene regulation was only established recently[67].

EZH2 (Enhancer of zeste homologue 2), also known as KMT6A, catalyzes the addition of methyl groups to H3K27[68]. EZH2 inhibits osteogenesis of MSCs. Suppression of EZH2 by CDK1 (cyclin dependent kinase 1) results in MSC differentiation to osteoblasts[69]. Likewise, chemical enzymatic inhibition and siRNA knockdown studies also show that EZH2 is a negative regulator of osteogenesis of MSCs[70]. A genome-wide screen of polycomb target genes demonstrates that EZH2 is present on osteogenesis-related genes in non-differentiated MSCs, such as RUNX2 and TCF7 (transcription factor 7)[68, 69]. Mechanistically, EZH2 expression is down-regulated under osteogenic inductive conditions and disassociates from the promoter RUNX2[71]. Conversely, a recent study on

10

NCCs (neural crest cells) reported that EZH2 is required for neural crest-derived bone formation. As a result of conditional ablation of EZH2 in NCCs, the formation of multiple skeletal elements was inhibited and severe craniofacial defects were caused[72]. It is likely that EZH2 has different tissue-specific functions in osteogenesis. In regard to adipogenesis, EZH2 methyltransferase activity is required for adipogenesis. Deletion of EZH2 in brown preadipocytes leads to decrease of H3K27me3 on the promoters of Wnt genes, resulting in severe defects in adipogenesis. These differentiation defects could be rescued by ectopic EZH2 and inhibitors of Wnt/β-catenin signaling. This suggests that EZH2 promotes adipogenesis by repression of Wnt genes[73]. In addition to Wnt/β-catenin signaling, MITR (myocyte enhancer factor-2 interacting transcriptional repressor) also prevents adipogenesis by inhibiting the transcriptional activity of PPAR-γ. EZH2 is present at the MITR promoter, where it inhibits MITR expression in adipocytes. Dissociation of EZH2 from the MITR promoter increases MITR expression and inhibits adipogenesis, while simultaneously enhancing the osteogenic differentiation of MSCs[74].

SETDB1 (SET domain bifurcated 1) is another well-known KMT that inhibits osteogenic differentiation and adipogenesis of MSCs. Lawson et al. found that mesenchymal deletion of Setdb1 led to long bone defects and significant decrease in trabecular bone in both embryos and postnatal Setdb1-deficient mice[75, 76]. They also observed impaired osteoblastic activity in Setdb1-deficient MSCs from bone marrow with hyperactivity of Runx2. Consistently, knockdown of Setdb1also enhances Runx2-mediated gene transcription *in vitro,* which may be caused by the decrease of H3K9me3 in the promoters of Runx2 target genes[75]. Although Runx2 is necessary for osteoblast differentiation, when transgenically over-expressed it can inhibit osteoblast maturation[77]. Collectively, Setdb1 inhibits osteogenic differentiation of MSCs, but it is required for normal skeletal formation due to its ability to repress hyperactive Runx2-mediated transcription.

On the other hand, Setdb1 is down-regulated by PPAR-γ in rodent models of obesity, such as high-fat feeding mice and the genetically predisposed obese ob/ob mice. A similar down-regulation of Setdb1 is observed in adipogenic differentiation of MSCs *in vitro*, while siRNA-mediated knockdown of Setdb1promotes adipogenesis with up-regulated expression of PPAR-γ, C/EBPα (CCAAT/enhancer binding protein alpha) and other adipogenesis related genes[78].

There are also several other SET domain-containing KMTs that regulate lineage specification of MSCs, such as MLL1 (Myeloid/lymphoid or mixed-lineage leukaemia 1), MLL3, MLL4. For instance, MEFs isolated from MLL3-null mice show striking defects in adipogenesis. Upon adipogenic induction, MLL3 and MLL4 are recruited to the promoter of aP2 (adipocyte protein 2),an adipogenic marker gene, in a time-dependent manner[79]. In addition, MLL3 and MLL4 can form a complex with PTIP (Pax transactivation domain-interacting protein). PTIP-deficient MEFs, white preadipocytes, and brown preadipocytes all exhibit impaired adipogenic potential, with decreased enrichment of PTIP and MLL4 on the PPAR-γ promoter[80]. Collectively, MLL3 and MLL4 facilitate adipogenesis through their KMT activity to promote PPARγ and aP2 expression. Additionally, although additional KMTs have been identified in association with osteogenesis and adipogenesis[74, 81, 82], further investigation to explore their underlying mechanism is necessary. In summary, there is increasing evidence showing that SET domain-containing KMTs are essential for MSC differentiation (Table 1).

Table 1. The role of SET domain-containing KMTs in regulation of osteogenesis and adipogenesis (shaded) of MSCs.

KMTs	Specificity	target	Finding	reference
SETDB1	H3K9	Runx2target genes	SETDB1 inhibits osteogenesis.	[75, 76]
		PPAR-γ target genes	SETDB1inhibits adipogenesis.	[78]
EZH2	H3K27	Runx2, TCF7, OC	EZH2 inhibits osteogenesis.	[69, 71]
		Wnt genes, MITR	EZH2 promotes adipogenesis.	[73, 74]
SETD8	H4K20	PPAR-γ and PPAR-γ target genes	SETD8 promotes adipogenesis.	[83, 84]
MLL1	H3K4	Not known	Mice with SET domain mutated MLL1exhibit skeletal defects.	[85, 86]
MLL3, MLL4	H3K4	PPAR-γ, aP2	MLL3 and MLL4 are promotes adipogenesis.	[79, 80]

1.2.1 JmjC domain-containing Histone Methyltransferases

KDMs are capable of removing methyl groups from histone lysine residues, and this reversibility of KMTs was first discovered in 2004[87]. To date, more than 30 histone demethylases have been identified, while JmjC domain-containing KMTs represent the largest class of potential histone demethylases and act by catalyzing the removal of mono-, di-, tri-methyl residues via a 2OG-Fe(II)-dependent dioxygenase reaction[88, 89]. On the basis of emerging findings, JmjC domain-

containing KDMs have been recognized and shown to play crucial roles in transcription regulation, stem cell differentiation, and animal development[88, 90, 91].

JHDM1 (JmjC domain-containing histone demethylase 1), also known as KDM2 cluster, catalyzes the removal of tri-methyl marks at H3K4, as well as mono- and di-methyl marks at H3K36[92-94]. Recently, KDM2A and KDM2B were reported to regulate MSC differentiation by associating with the BCOR (BCL-6 co-repressor) complex[94-96]. KDM2B represses expression of AP-2α (activating enhancer binding protein 2α) by removing the H3K4me3 and H3K36me2 marks in the its promoter[95]. In addition, KDM2A and the BCOR complex are reported to inhibit osteogenesis by increasing histone H3K4/36 methylation in the EREG (epiregulin) promoter, thereby repressing EREG transcription. EREG is required for expression of osteogenic related genes, such as OSX (osterix) and DLX2 (distal-less homeobox 5)[96]. In addition, although depletion of KDM2A in SCAP (stem cells from apical papilla) enhances adipogenic differentiation in vitro[94], the effect of KDM2A on adipogenic differentiation is still not fully understood.

KDM4B is a member of KDM4 cluster, also known as the JMJD2 subfamily, which can catalyze the removal of di- and tri-methyl marks at H3K9 and H3K36[97, 98]. Five functional KDM4 member genes have been identified in the human genome, of which KDM4A-C are broadly expressed in human tissues, while KDM4D and KDM4E are specifically enriched in the human testes[97, 99]. Partly because they have redundant roles, Kdm4c or Kdm4d knockout mice are viable without gross abnormalities[99, 100]. However, conditional deletion of Kdm4b was recently reported to delay mammary gland development in mice[101], while Kdm4a is required for skeletal muscle differentiation and neural crest specification[102, 103]. More recently, KDM4B was reported to enhance osteogenic differentiation of human MSCs[104]. In the bone marrow of aging mice, Kdm4b expression is reduced, accompanying decreased osteogenesis. Knockdown of KDM4B by shRNA

inhibits osteogenic differentiation in human bone marrow-derived MSCs. Conversely, over-expression of KDM4B enhances osteogenesis. After subcutaneous transplantation of MSCs with an HA scaffold, KDM4B is also required for MSC-mediated bone formation *in vivo*. Mechanistically, KDM4B was found to remove the H3K9me3marks in the promoter of DLX5 (distal-less homeobox 5), activating its expression during osteogenesis. The role of KDM4 member genes in adipogenesis is still controversial. Ye et al. reported that knockdown of KDM4B by shRNA enhanced adipogenic differentiation of MSCs and increased the expression of PPAR-γ and CD36[105]. These results indicate that KDM4B inhibits adipocyte lineage specification from MSCs. However, Kdm4b was also found to act as a co-factor of C/EBPβ to promote differentiation of preadipocytes[106]. Kdm4b with C/EBPβ is recruited to the promoters of the target genes of C/EBPβ, such as Cdc45l (cell division cycle 45 homolog), Mcm3 (mini-chromosome maintenance complex component 3), Gins1 (GINS complex subunit 1) and Cdc25c (cell division cycle 25 homolog c). By removing the H3K9me3 marks, Kdm4b facilitates C/EBPβ target gene expression[106]. It is possible that the conflicting effects are caused by opposing functions of KDM4B at different stages of adipogenesis.

The KDM6 cluster contains three member genes, KDM6A, KDM6B, and UTY, which catalyzes the removal of di- and tri-methyl marks at H3K27[90, 107]. Both KDM6A and KDM6B promote osteogenic differentiation of MSCs. Although Hemming et al. reported that transcription levels of KDM6A are down-regulated during osteogenesis of human bone marrow MSCs[71], siRNA-mediated knockdown of KDM6A inhibits osteogenesis. Conversely, retroviral-mediated over-expression of KDM6A enhances the potential of MSCs to differentiate into mineral forming osteoblasts and ectopic bone formation *in vivo[71]*. Over-expression of KDM6A results in a decrease in H3K27me3 at both RUNX2 and OC (osteocalcin) transcription start sites, which subsequently

increases the expression of RUNX2 and OC. KDM6B is recruited to the promoters of BMP (bone morphogenetic protein) and HOX (homeobox) genes, which each promote the osteogenic differentiation of MSCs. In terms of adipogenesis, KDM6A and KDM6B are both reported to inhibit adipogenic differentiation of MSCs. Under adipogenic differentiation conditions, enforced over-expression of KDM6A results in decreased mRNA level of PPAR-γ, C/EBPα and adiposin. Knockdown of KDM6A shows an increase in lipid formation[71], and depletion of KDM6B facilitates adipogenesis and promotes PPAR-γ and CD36 expression.

Several other KDMs have also been reported to regulate MSC differentiation. NO66 catalyzes the removal of mono-, di- and tri-methyl marks at H3K4, as well as di- and tri-methyl marks at H3K36[108], which has been found in all the developing bones[108]. Under osteogenic inductive conditions, NO66 interacts with OSX to inhibit OSX transcriptional activity[108, 109]. Both NO66 and OSX can be found present in the promoter of BSP (bone sialoprotein), promoting demethylation of H3K4me3 and H3K36me3 to repress BSP expression. A structural study showed that the hinge domain-dependent oligomerization of NO66 is essential for the interaction with OSX[109]. RBP2 (retinol binding protein 2), also known as KDM5A, catalyzes removal of themono-, di- and tri-methyl marks at H3K4[110, 111]. KDM5A, also known as RBP2 (retinol binding protein 2), catalyzes removal of the mono-, di- and tri-methyl marks at H3K4[110, 111]. RBP2 was found to repress osteogenesis in Soas-2 cells (a human osteogenic sarcoma cell line)[112] and adipose-derived MSCs by repression of RUNX2-mediated transcriptional activity[81]. Depletion of RBP2 increased expression levels of osteogenic related genes, promoted bone formation after subcutaneous transplantation in *vivo*. In addition, RBP2 was shown to inhibit adipogenesis of preadipocytes, and depletion of RBP2 in preadipocytes enhanceed lipid formation *in vitro[112]*. It is possible that RBP2 exert inhibitory effects during both osteogenic and adipogenic differentiation[113, 114]. JHDM1E, also

known as PHF2 (plant homeodomain finger 2), catalyzes the removal of di-methyl marks at H3K9[115]. Deletion of Phf2 in adipose tissue results in a 50% reduction in WAT, while BAT appears normal. Mechanistically, Phf2 was found to be a co-activator of C/EBPα and to be recruited to the promoter of C/EBP responsive elements[116].

Collectively, these findings have revealed an important role of JmjC family genes in regulation of the balance between osteogenic differentiation and adipogenic differentiation of MSCs (Table 2). In contrast to KMTs, JmjC domain-containing KDMs control transcriptional activity by removing the methylation marks at the specific histone lysine residues. It seems that the methyltransferase activity of SET domain-containing KMTs is specific to one target site, while JmjC domain-containing KDMs exhibit more redundancy and tissue specificity. However, the underlying mechanisms of JmjC family genes in adipogenesis remains not well understood.

Table 2. The role of JmjC domain-containing KDMs in regulation of osteogenesis and adipogenesis (shaded) of MSCs.

KMTs	Specificity	target	Finding	reference
KDM2A	H3K4me3, H3K36me1/2	EREG	KDM2A inhibits osteogenesis.	96
		Not known	KDM2A inhibits adipogenesis.	94
KDM2B	H3K4me3, H3K36me1/2	AP-2α	KDM2B inhibits osteogenesis.	95
KDM4B	H3K9me2/3 H3K36me2/3	DLX5	KDM4B promotes osteogenesis.	105
		Not known	KDM4B inhibits adipocyte lineage specification from human bone marrow-derived MSCs.	105

		C/EBPβ target genes	KDM4B promotes adipogenesis by catalyzing demethylation of H3K9me3in the promoter of C/EBPβ target genes in preadipocytes.	[106]
KDM4C	H3K9me2/3, H3K36me2/3	Not known	KDM4C is required for adipogenesis from preadipocytes.	[117]
KDM6A	H3K27me2/3	RUNX2, OC	KDM6A promotes osteogenesis.	[71]
		Not known	KDM6A inhibits adipogenesis.	[71]
KDM6B	H3K27me2/3	BMP and HOX genes	KDM6B promotes osteogenesis.	[105]
		Not known	KDM6B inhibits adipogenesis.	[105]
NO66	H3K4me1/2/3, H3K36me2/3	OSX target genes	NO66 inhibits osteogenesis.	[108, 109, 118]
RBP2	H3K4me1/2/3	Runx2 target genes	RBP2 inhibits osteogenesis.	[81]
		Not known	RBP2 inhibits adipogenesis from preadipocytes.	[112]
PHF2	H3K9me2	C/EBP response elements	PHF2 promotes adipogenesis.	[116]

1.3 Self-renewal of MSCs

In addition to differentiation potential, self-renewal is another essential capacity of stem cells. Transplantation assay of hematopoietic stem cell (HSC) serves as the paradigm for defining postnatal stem cells[119]. In the ideal serial transplantation assay, a single HSC can reconstitute

multi-lineage hematopoiesis in lethally irradiated recipient mice. Accordingly, to define the MSCs with skeletogenic potential, self-renewal and multipotency should be probed at a single cell level, and through in vivo transplantation experiments[120].

Although the multiple differentiation potentials of MSCs have been recognized for a long time, the self-renewal capacity of MSCs has recently been demonstrated[121, 122]. In general, the self-renewal capacity of MSCs is usually defined by the generation of a heterotopic ossicles *in vivo*, the miniature bone organs that include the hematopoietic microenvironment[121]. *In vitro*, colony-forming assay is usually used to assess the self-renewal capacity of MSCs. Primary MSCs isolated from bone marrow can proliferate and undergo several passages. At early passages, MSCs are spindle-like in morphology and small in size with high proliferation rate and great differentiation potential. After a long period of expansion, MSCs lose their ability of self-renewal and differentiation, and become large and flatten[123]. The aging of MSCs has also been observed in vivo. Several studies have shown that MSCs from older donors exhibited a slower proliferation rate and a decrease in their differentiation to osteoblasts[124, 125]. However, the molecular mechanisms regulating self-renewal of MSCs remains largely unknown. Recently, emerging evidence has revealed that MSCs express Sox2 ((sex determining region Y)-box 2) and Nanog, which may contribute to the maintenance of MSCs at undifferentiated stage[126-128].

1.3.1 Transcription Factors in Self-renewal of MSCs

SOX2 is a member of the Sox HMG box family of transcription factors. The function of SOX2 in maintenance of pluripotency and regulation of self-renewal was first identified in embryonic stem cells (ESCs). Sox2 is also a critical factor for the reprogram of somatic cells to induced pluripotent stem cells (iPSCs) Induction of pluripotent stem cells from mouse embryonic and adult fibroblast cultures by defined factors[129]. Recent studies have revealed that SOX2 is required for self-renewal

of MSCs[130-132]. In MSCs, SOX2 expression was downregulated upon osteogenic differentiation[133]. In the osteoblast lineage, overexpressing of Sox2 increased sphere formation capacity and inhibited osteoblast differentiation[134]. Deletion of Sox2 by Cre-expressing virus caused a significant loss of colony-forming ability, which strongly support that Sox2 maintains stemness[135]. In addition, YAP1 (Yes Associated Protein 1) and BMI1 were identified as SOX2 target in maintenance of MSCs by the same group[130, 135].

Nanog is a homeodomain transcription factor that is also required for maintenance of ESCs and induction for iPSCs[129, 136]. NANOG was detected in NANOG in proliferating cells in cultured human adult MSCs[137]. Overexpression of NANOG enhanced the proliferation, colony formation capacity, and differentiation potential along the chondrogenic and osteogenic lineages but reduced adipogenic differentiation in MSCs derived from human bone marrow[138]. In addition, Nanog upregulated genes involved in cell cycle, DNA replication, and DNA damage repair[139]. However, the *in vivo* role Nanog in regulation of MSC self-renew remains to be investigated.

OCT4, one of the three central transcription factor in regulation of maintenance of pluripotency in ESCs, has also been reported to be regulate self-renewal of MSC *in vitro*[126, 138]. Expression of Oct4 decreased after spontaneous differentiation in MSCs. However, knockout of Oct4 has little effect on the ability of MSCs in colony formation and differentiation into bone, fat, or cartilage[140], indicating that Oct4 may not be a critical factor that directly regulate self-renewal of MSCs.

1.3.3 Epigenetic regulation of Self-Renewal of MSCs

Dnmt1 (DNA methyltransferases 1) is a major DNA methyltransferase that catalyzes the transfer of methyl groups to specific CpG structures in DNA. It is responsible for maintaining methylation status during DNA replication. Inactivation of Dnmt1 in mice led to loss of genomic imprinting and early embryonic lethality[141]. Although Dnmt1 is dispensable for maintenance of embryonic

stem cell, it has been reported to maintain the progenitor state in constantly replenished somatic tissues, such as mammalian epidermis[142, 143]. In MSCs, Dnmt1 is a direct target of NANOG and OCT4. OCT4 and NANOG promote Dnmt1 expression through direct binding to its promoter, thereby leading to repressed spontaneous differentiation of MSCs[126].

Emerging evidence has recently revealed that heterochromatin architecture alteration with massive histone methylation changes may function as a driver of human aging[144]. WRN (Werner syndrome ATP-dependent helicase) plays roles in DNA replication and telomere maintenance. Deficiency of WRN protein led to Werner syndrome (WS), a premature aging disorder. Although ESCs-*WRN*$^{-/-}$ expressed pluripotency markers, and were able to differentiate into MSCs, the MSCs derived from WRN-null ESCs showed features of a global loss of H3K9me3 and premature cellular aging, indicating histone methylation status is critical for self-renewal of MSCs[144].

In addition to histone methylation, histone H3 acetylation also plays a key role in regulating MSC aging and differentiation[145]. bFGF (basic fibroblast growth factor) promoted MSC proliferation and suppressed the spontaneous osteogenic differentiation, with corresponding changes in histone H3 acetylation in Oct4 and Sox2. Interestingly, treatment with HDAC (histone deacetylases) inhibitors downregulated polycomb group genes (PcGs) as BMI1, EZH2 and SUZ12 (SUZ12 polycomb repressive complex 2 Subunit), and upregulated JMJD3, which may induce changes in histone methylation status in MSCs[146, 147].

Taken together, epigenetic regulation played a critical role in regulation of MSC differentiation and self-renewal. Specifically, KDM4B promoted osteogenic differentiation and inhibited adipogenic differentiation of MSCs. But the *in vivo* function of KDM4B in regulation of lineage specification of MSCs and bone homeostasis remains to be investigated. On the other hand, KDM4B expression may influence self-renewal of MSCs by regulating global histone methylation

status in MSCs. Hence, in this study, we investigated the effect of Kdm4b knockout on bone mass

in mice model and the role of KDM4B in regulation of MSC self-renewal.

2. METHODS AND MATERIALS

Mice and genotyping primers

Mice used in this study included Kdm4b^{fl/fl} mice, CMV-Cre mice, *Prx1-Cre* mice [148], Lepr-Cre mice[149], Ocn-Cre mice[150], and loxp-tdTomato mice[151]. To obtain a defined genetic background, all mice were backcrossed six times onto a C57BL/6 background, and housed in the Division of Laboratory Animal Medicine (DLAM) at the University of California, Los Angeles (UCLA). We established a sample size of at least 8 mice per group in all experiments. The mice were randomly assigned to the groups including sham, OVX and PTH (1-34) injection. Bones and blood samples were collected post procedures as indicated. ELISAs were performed with a mouse P1NP ELISA kit and a CTx ELISA kit (both from Immunodiagnostic Systems). All procedures were approved by the University Committee on Use and Care of Animals at UCLA. The primers for *Kdm4b* are: forward, 5'-ACCCAGGACTGATGTTCACA-3'; reverse, 5'-GAAAGAAGACCTG AGCTGTC-3'; the primers for *Cre* are: forward, 5'-GCATTACCGGTCGATGCAAC GAGTGATGAG-3'; reverse, 5'-GAGTGAACGAACCTGGTCGAAATCAGTGCG-3'; the primers for *tdTomato* are: forward, 5'- CGAGGCGGATCACAAGCAATA-3'; reverse, 5'-TCAATGGGCGGGGGTCGTT-3'.

µCT Analysis

Femurs were dissected, fixed overnight in 10% neutral buffered formalin for 24 h, and stored in 70% ethanol. The specimens were placed into a cylindrical holder (16.5 mm in diameter) with the long axis of the femur perpendicular to the X-ray source, and scanned at 55 kVp and 70 µA on a Scanco µCT40 scanner (Scanco Medical). The regions of interest were defined as the areas between 0.3 mm and 0.4 mm proximal to the growth plate in the distal femurs. µCT Evaluation Program V4.4A (Scanco Medical) with a threshold of 220 was used for analysis of all scans. To

evaluate the MAT in tibias, samples were stained with osmium tetroxide, and scanned as previously described[152, 153]. A threshold of 400 was used for analysis of osmium tetroxide-stained MAT in tibias.

Tetracycline double labeling and histomorphometric analysis

To examine the rate of bone formation, mice were injected intraperitoneally with 5 mg/kg body mass tetracycline (Sigma-Aldrich, USA) dissolved in physiological saline solution on day 0 and day 7. Samples were collected 3 days post the second injection, fixed 10% neutral buffered formalin for 24 h, dehydrated in 30% sucrose for 2 days, and sectioned without decalcification (8 µm) in Bone Histomorphometric Laboratory at UCLA. Mineral apposition rate (MAR) and bone formation rate (BFR) were measured as previously described[47, 154]. After toluidine blue staining, osteoblasts were identified as plump cuboidal cells with a perinuclear clear zone lining the osteoid surface.

Immunostaining and TRAP staining

After scanning, the specimens were decalcified in 10% ethylenediaminetetraacetic acid (EDTA, PH 7.4, Fisher) for 2 weeks, and were sectioned (5 µm) for staining as previously described[155]. The slides were incubated at 65 ℃ for 2 hrs, dewaxed with xylene (Fisher), and rehydrated through gradient ethanol into water. Immunostaining was performed using a DAKO Envision Plus Kit (DakoCytomation California, USA) according to manufacturers' instructions. Antibodies used included rabbit polyclonal anti-FABP4 (1:200, Abcam). To perform osteoclast quantification, TRAP staining was then performed using a TRAP kit from Sigma-Aldrich according to manufacturers' instructions.

For tdTomato-expressing samples, bones were fixed in 4% paraformaldehyde, decalcified in 10% EDTA (PH 7.4) for 2 weeks, and dehydrated in 30% sucrose for at least 2 days in dark. After

frozen section, slides were washed with PBS twice, blocked in PBS with 10% horse serum for 30 minutes, and then stained with rabbit anti-FABP4 (1:200, Abcam) overnight at 4°C. Cy2 affiniPure donkey anti-rabbit IgG andibody (Jackson ImmunoResearch, USA) was used as secondary antibodies (1:200, Invitrogen). After being extensively washed with PBS, the slides were stained with DAPI (49,69-diamidino-2-phenylindole) and mounted with antifade mounting medium (Thermo Fisher Scientific). Images were taken and analyzed using an Olympus IX-51 microscope.

Cell culture

Intact bone marrow was isolated from the long bones by flushing and subjected to enzymatic digestion with Collagenase Type I (3 mg/mL; Worthington) and Dispase (4 mg/mL; Roche Diagnostics) as described previously[156]. For CFU-F assays, the digested cells were plated in 6-well plates at a density of 1 x 10^6 cells/well, and cultured in a humidified 5% CO2 incubator at 37 °C in DMEM supplemented with 15% FBS and 1% penicillin/streptomycin (Invitrogen). CFU-F colonies were stained with 0.5% Crystal violet (Sigma-Aldrich) in 4% Paraformaldehyde (Santa Cruz, USA), and counted after 10 days of culture. For *in vitro* differentiation, the digested cells were cultured for 2 weeks and passaged 2-3 times with trypsin for expansion. To induce osteogenesis, cells were cultured in osteogenic induction medium containing 100 µM ascorbic acid, 2 mM β-glycerophosphate and 10 nM dexamethasone. To induce adipogenesis, cells were cultured in adipogenic induction medium containing 1 µM dexamethasone, 10 µg/mL insulin, 0.5 mM 3-isobutyl-1-methylxanthine, and 0.2 mM indomethacin (All from Sigma).

For primary culture of bone marrow macrophages, we isolated bone marrow cells from femurs, and treated the cells with 100 ng/ml macrophage colony-stimulating factor (M-CSF; R&D systems) for 2 days. For further induction of osteoclastogenesis, the osteoclast precursors with 100 ng/ml

mouse RankL (R&D systems) for 3 days. Wnt3a (100ng/ml), BMP2 (100 ng/ml), PTH (100 μM), and vehicle controls were added into the medium as indicated.

ALP, ARS, and Oil Red O staining

For ALP staining, cells were fixed with 70% ethanol for 15 min and incubated with a mix of 0.25% naphthol AS-BI phosphate (Sigma-Aldrich) and 0.75% Fast Blue BB salt (Sigma- Aldrich) dissolved in 0.1 M Tris buffer (pH 9.6) for 20 min. For quantitative determination of ALP activity, 20 μL cell extract was incubated with a mix of 50 μL ALP stabilizing buffer (Sigma-Aldrich) and 50 μL pNPP liquid substrate (Sigma-Aldrich) for 20 min at 37 ℃. The absorbance was then read at OD405 nm on a microplate reader (Bio-Rad). For ARS staining, after 2–3 weeks of osteogenic induction, the cells with fixed with 70% ethanol for 1 hour and stained with 1% Alizarin red solution (PH 4.2, Sigma-Aldrich). The stained cultures were then destained by 10% Cetylpyridinium chloride solution (PH 7), and absorbance of the solution was read at 562 nM. To detect the lipid droplet formation, Oil Red O staining was performed with a kit form Diagnostic Biosystems according to the manufacturer's instructions, after 2-3 weeks of differentiation.

Viral infection and Luciferase assay

To overexpress KDM4B in BMSCs, cells was plated, allowed to attach overnight, and then infected with retroviruses expressing KDM4B in the presence of polybrene for 6 hrs (8 μg/ml, Sigma-Aldrich). Resistant cells were selected and overexpression was confirmed by western blot analysis. For luciferase assay, MSCs were infected with lentiviruses expressing TOPflash luciferase reporters (System Biosciences). Luciferase activity was measured using a Dual-luciferase Reporter Assay System (Invitrogen) as described previously after wnt3a treatment for 2 days.

Reverse Transcription-PCR (RT-PCR) and RNA-seq

Total RNA was extracted using Trizol reagents (Invitrogen) according to the manufacturer's instructions. 2-µg aliquots of RNAs were used to generate cDNA with random hexamers and reverse transcriptase (New England Biolabs, UK). Quantitative PCR (QPCR) then performed reactions using the QuantiTect SYBR Green PCR kit (Qiagen) and the CFX96 Touch™ Real-Time PCR Detection System (Bio-Rad). The primers for *Gapdh* are: forward, 5'-ACAACTTTGGCATTGTGGAA-3'; reverse, 5'- GATGCAGGGATGATGTTCTG-3'. The primers for Runx2 are: forward, 5'-TCCACAAGGACAGAGTCAGATTACAG-3'; reverse, 5'-CAGAAGTCAGAGGTGGCAGTGTCATC-3'. The primers for Sp7 are: forward, 5'-ATGGCGTCCTCTCTGCTTG-3'; reverse, 5'-TGAAAGGTCAGCGTAT GGCTT-3'. The primers for *Bglap* are: forward, 5'- CTGACCTCACAGATGCCAAGC-3'; reverse, 5'-TGGTCTGATAGCTCGTCACAAG-3'. The primers for *Alp* are: forward, 5'-CACGGCCATCCTATATGGTAA-3'; reverse, 5'-GGGCCTGGTAGTTGTTGTGA-3'. The primers for *Col1a1* are: forward, 5'-TAGGCCATTGTGTATGCAGC-3'; reverse, 5'-ACATGTTCAGCTTTGTGGACC-3'. The primers for *Spp1* are: forward, 5'-ATCTCACCATTCGGATGAGTCT-3'; reverse, 5'-TGTAGGGACGATTGGAGTGAAA-3'. The primers for *CD36* are: forward, 5'-ATGGGCTGTGATCGGAACTG-3'; reverse, 5'-GTCTTCCCAATAAGCATGTCTCC-3'. The primers for *C/EBPα* are: forward, 5'-GTCACTGGTCAACTCCAGCA-3'; reverse, 5'-TGGACAAGAACAGCAACGAG-3'. The primers for *FABP4* are: forward, 5'-AAGGTGAAGAGCATCATAACCCT-3'; reverse, 5'-TCACGCCTTTCATAACACATTCC-3'. The primers for *Pparγ* are: forward, 5'-AACTGGATGACAGTGACATTTCCC-3'; reverse, 5'-CCCCTCCTGCAACTTCTCAAT-3'. The primers for *Axin2* are: forward, 5'-AACCTATGCCCGTTTCCTCTA-3'; reverse, 5'-

GAGTGTAAAGACTTGGTCCACC-3'. The primers for *DKK1* are: forward, 5'-CTCATCAATTCCAACGCGATCA-3'; reverse, 5'-GCCCTCATAGAGAACTCCCG-3'.

For RNA-seq experiments, RNA was isolated using RNeasy Mini Kit (Qiagen) from three biological replicates of primary MSCs from Prx1-Cre; Kdm4b^{fl/fl} mice and control mice, and MSCs induced for osteogenesis for 4 days. Total RNA was then purified with Dynabeads™ mRNA Purification Kit (Invitrogen). RNA-seq libraries were constructed using Stranded mRNA-Seq Kit (Kapa Biosystems), and sequenced using an illumina HiSeq 3000 sequencer at the Technology Center for Genomics & Bioinformatics (TCGB) core in UCLA.

Western blot assay

Cells were collected and lysed in CelLytic™ MT Cell Lysis Reagent (Sigma-Aldrich) containing protease inhibitor cocktail (Pierce Biotechnology) on ice for 30 min, and centrifuged at 18,000 g for 15 min at 4 °C. Aliquots of the lysates were separated on a 7.5% - 12.5% sodium dodecyl sulfate-polyacrylamide gel, and then transferred onto nitrocellulose membranes (Bio-Rad). The membrane was incubated with primary antibodies overnight 4 °C, followed by a horseradish peroxidase-conjugated secondary antibody. Protein bands were detected with an enhanced chemiluminescence western blotting detection kit Thermo Fisher Scientific. The following antibodies were used: mouse anti-α-tubulin (1:10000, Sigma-Aldrich), rabbit anti-Flag (1:2000, Sigma-Aldrich).

Chromatin Immunoprecipitation (ChIP)

ChIP assay was performed using a ChIP assay kit (Upstate Biotechnology, USA) following the manufacturer's instructions. Briefly, cells were treated with 3'-dithiobispropionimidate solution (10 mM) for 10 min at room temperature, followed by incubation in 1% formaldehyde for 15 min in a 37 °C water bath for cross-linking. Nuclei were extracted as previous described[157], and lysed.

Immunoprecipitation was performed with Dynabeads Protein A/G (Thermo Fisher Scientific), and the precipitated DNA was quantified with QPCR. Data was expressed as the percentage of input DNA. The following antibodies were used: rabbit anti-KDM4B (Bethyl Laboratories, USA), mouse anti-H3K9me2 (Abcam, UK), rabbit anti-H3K9me3 (Abcam), anti-mouse IgG (Abcam), anti-rabbit IgG (Cell Signaling Technology).

Serial Transplantation

In the initial transplantation, MSCs from bone marrow of *Prx1-Cre;Kdm4b*$^{wt/wt}$*;tdTomato* and *Prx1-Cre;Kdm4b*$^{fl/fl}$*;tdTomato* mice by mechanical and enzymatic dissociation as stated above, respectively. After 2-3 passages for expansion, 100 µl of cell suspension with approximately 1 x 10^6 cells were incubated with scaffolds at 37 °C for 6 hrs, and then transplanted subcutaneously at the dorsal sites of nude mice (n=8). 6 weeks after transplantation, the scaffolds were explanted and digested to give rise to cells for secondary transplantation. Again, 6 weeks after secondary transplantation, the scaffolds were fixed with 4% paraformaldehyde, decalcified by 10% EDTA (PH 7.4), and were subjected to frozen section. Representative sections were stained with H&E. Images were taken, and SPOT 4.0 software (Diagnostic Instruments, Michigan, USA) was used to measure the area of mineralized tissue and adipose tissue versus total area. Expression of TdTomato was detected and considered as an evidence that the newly formed bone tissue and adipose tissue were generated by MSCs from MSCs from bone marrow of *Prx1-Cre;Kdm4b*$^{wt/wt}$*;tdTomato* and *Prx1-Cre;Kdm4b*$^{fl/fl}$*;tdTomato* mice during the serial transplantation.

Statistical analyses

For single comparisons, an unpaired two-tailed Student's t-test was used. And the statistical significance of differences among more than two groups was calculated using one-way ANOVAs.

The statistical significance of differences between treatments in the OVX experiments, PTH administration, and in vitro differentiation experiments were assessed using two-way ANOVAs followed by post hoc tests. Data shown are representative of at least three independent experiments and are represented as mean $\pm$ SEM. A p value < 0.05 was considered to be statistically significant. *, $p < 0.05$; **, $p < 0.01$; ***, $p < 0.001$.

3. RESULT

3.1 Global deletion of *Kdm4b* enhanced age-related bone loss and adipose accumulation in mouse bone marrow

To explore the *in vivo* role of *Kdm4b* in regulation of lineage specification of MSCs, we examined the effects of *Kdm4b* knockout on bone mass and bone marrow fat (BMF) during aging by global deletion of *Kdm4b*. The loxp sites in the Kdm4b[fl] allele surround the fifth exon, which contains the Jumonji domain (JMJD) of *Kdm4b* [158, 159]. Micro-computed tomography (μCT) analysis revealed that bone mineral density (BMD) and the bone volume/tissue volume ratio (BV/TV) of Kdm4b-/- mice was significantly lower compared to WT littermates at 7 and 12 months of age (Figure 1A). Of note, *Kdm4b-/-*mice exhibited comparable bone mass to the controls at 3 months of age, indicating an important role of *Kdm4b* in inhibiting age-related bone loss. Histomorphometric analysis further showed decreased osteoblasts in *Kdm4b-/-* mice at 7 and 12 months of age, compared to WT mice (Figure 1B). However, the osteoclasts were not affected by *Kdm4b* deletion during observed time, as determined by TRAP (tartrate-resistant acid phosphatase) staining (Figure 1C). Taken together, Global deletion of Kdm4b enhanced age-related bone loss by reducing osteoblasts.

A reverse correlation between osteogenesis and adipogenesis of MSCs has been long suggested, and recent studies have revealed the existence of regulated marrow fat tissue (rMAT) [16, 160]. Next, we found that significantly increased numbers of bone marrow adipocytes, and the area taken by adipose tissue in bone marrow of *Kdm4b-/-* mice as compared to littermate controls (Figure 1D).
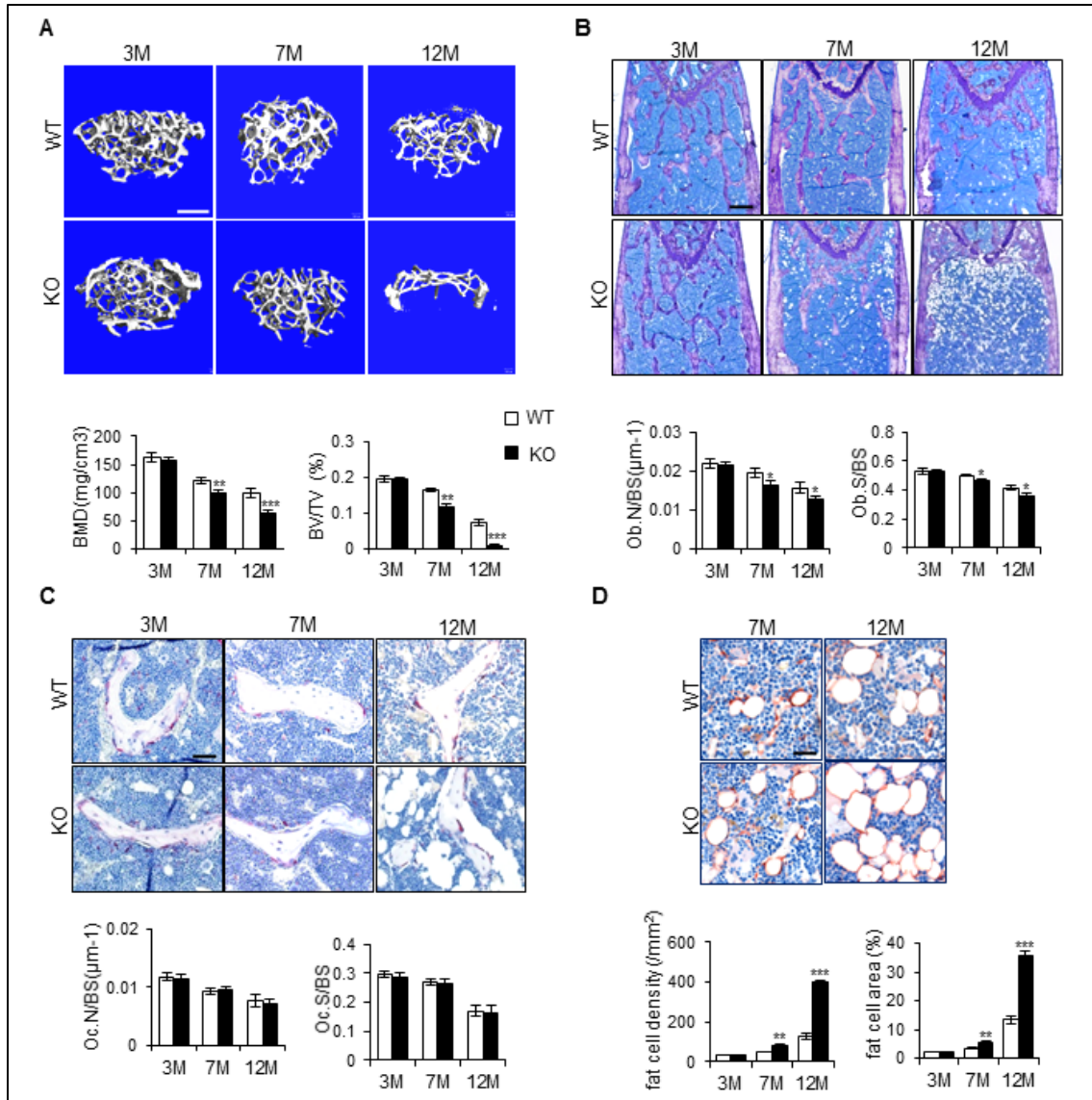
Figure 1. Global deletion of *Kdm4b* enhanced age-related bone loss and adipose accumulation in mouse bone marrow. (A) μCT analysis of trabecular bone in femurs of *Kdm4b-/-* and sex-matched littermate controls. Bar indicates 400 μm. Bone mineral density (BMD) and BV/TV (bone volume/total volume) were analyzed. (B) Toluidine blue-stained bone sections from 3-, 7, and 12-month-old *Kdm4b-/-* and littermates. Bar indicates 400 μm. Osteoblast number (Ob.N) and osteoblast surface (Ob.S) were normalized to the bone surface (BS), respectively. (C) Trap staining of trabecular bone in femurs of *Kdm4b-/-* and sex-matched littermate controls. Bar indicates 50 μm. Osteoclast number (Oc.N) and osteoclast surface (Oc.S)

were normalized to the BS, respectively. (D) Representative fatty acid binding protein 4 (FABP4) staining in femur sections and quantification of the adipocyte per millimeter^2. Bar indicates 40 μm.

To further test whether the enhanced age-related bone loss and adipose accumulation was caused by imbalanced differentiation potential of MSCs in *Kdm4b-/-* mice, we isolated the MSCs as previously reported and induced the MSCs to undergo osteogenic differentiation and adipogenic differentiation, respectively [161]. As evidenced by alkaline phosphatase activity assay and Alizarin red staining, primary MSCs from *Kdm4b-/-* mice demonstrated decreased osteogenic potential, in response to osteogenic stimulus (OS) (Figure 2A). qRT-PCR assay also showed reduced mRNA expression of the osteogenic-related genes, such as transcription factors *Sp7* and *Runx2*, and mineralization markers *Col1a1*, *Alpl*, *Spp1* and *Ocn* in primary MSCs from *Kdm4b-/-* mice, 7 days after induction (Figure 2B). On the other hand, MSCs from *Kdm4b-/-* mice exhibited enhanced adipogenic potential, as determined by Oil Red O staining and expression of adipogenic-related genes, such as *Ap2*, *CD36*, *Pparγ*, *C/EBPα* (Figure 2C, 2D).
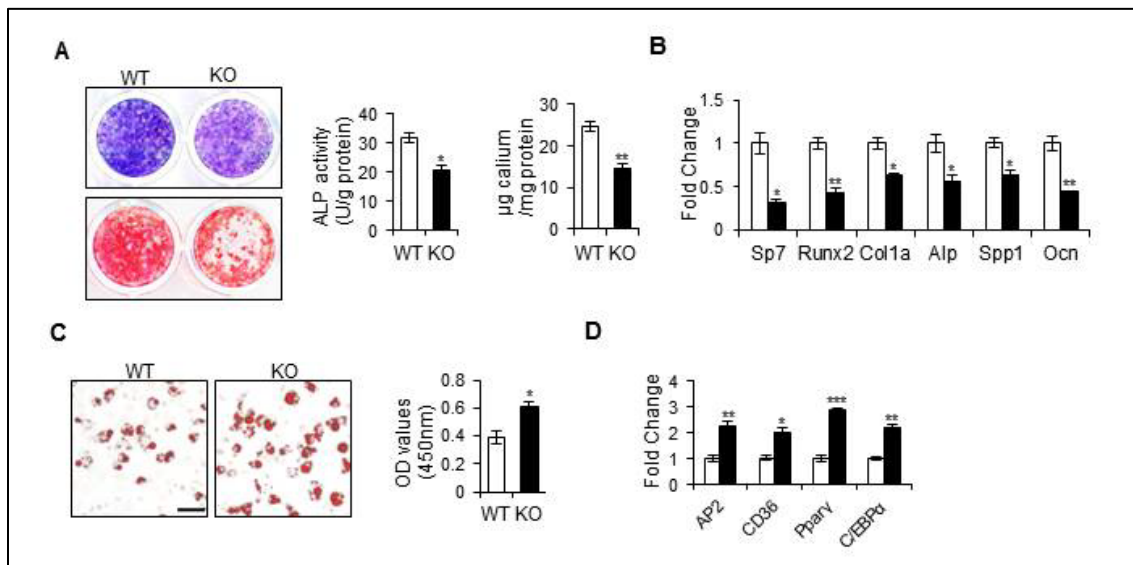
Figure 2. Global deletion of *Kdm4b* reduced osteogenic differentiation and promoted adipogenic differentiation of primary mBMSCs. (A) Alkaline phosphatase (ALP) activity assay and Alizarin Red S (ARS) staining of mBMSCs from *Kdm4b-/-* and littermate controls in response to osteogenic stimulus (OS). (B)

qRT-PCR analysis of expression of osteogenic-related genes in mBMSCs from *Kdm4b-/-* and littermate controls in response to OS. (C) Oil Red O staining of mBMSCs from *Kdm4b-/-* and littermate controls in response to adipogenic stimulus (AS). Bar indicates 80 μm. (D) qRT-PCR analysis of expression of adipogenic-related genes in mBMSCs from *Kdm4b-/-* and littermate controls in response to AS.

3.2 Deletion of *Kdm4b* in mesenchymal progenitors enhanced age-related bone loss and adipose accumulation in mouse bone marrow

To investigate if the enhanced age-related bone loss and adipose accumulation in mouse bone marrow was caused by loss of function of KDM4B in mesenchymal progenitors, We conditionally deleted *Kdm4b* from bone marrow MSCs by generating *Prx1-Cre;Kdm4b$^{fl/fl}$* mice. Consistent to global deletion of kdm4b, we found a significant decrease in bone mass in *Prx1-Cre;Kdm4b$^{fl/fl}$* mice (Figure 2A) at 12-month old, as determined by μCT analysis. Histomorphometric analysis revealed osteoblasts were decreased in *Prx1-Cre;Kdm4b$^{fl/fl}$* mice at 12 months of age, while osteoclasts were not affected (Figure 2B, 2C). In addition, we also observed significant upregulation of rMAT in the bone marrow of *Prx1-Cre;Kdm4b$^{fl/fl}$* mice at 12 months of age, compared to the littermate controls (Figure 2D).

Figure 3. Deletion of Kdm4b in mesenchymal progenitors enhanced aged-related bone loss and adipose accumulation. (A) µCT analysis of trabecular bone in femurs of *Prx1-Cre;Kdm4b^{fl/fl}* and sex-matched littermate controls (*Prx1-Cre;Kdm4b+/+ or Kdm4b^{fl/fl}*). Bar indicates 400 µm. .BMD and BV/TV were analyzed. (B) Toluidine blue-stained bone sections from 3- and 12-month-old *Prx1-Cre;Kdm4b^{fl/fl}* mice and littermates. Bar indicates 500 µm. Ob.N and Ob.S were normalized to the BS, respectively. (C) Trap staining of trabecular bone in femurs of *Prx1-Cre;Kdm4b^{fl/fl}* and sex-matched littermate controls. Bar indicates 40 µm. Oc.N and Oc.S were normalized to the BS, respectively. (D) Representative images show FABP4 staining in femur sections and quantification of the adipocyte per millimeter^2. Bar indicates 30 µm.

We isolated primary MSCs from the femur of *Prx1-Cre;Kdm4b^{fl/fl}* mice and littermate controls. Consistently, the primary MSCs from *Prx1-Cre;Kdm4b^{fl/fl}* mice exhibited decreased osteogenic potential and enhanced adipogenic potential (Data not shown).

To investigate whether KDM4B regulates the function of mature osteoblasts, we conditionally deleted *Kdm4b* in mature osteoblasts by generating *Ocn-Cre;Kdm4b^{fl/fl}* mice. We assessed the trabecular bone parameters of *Ocn-Cre;Kdm4b^{fl/fl}* mice and littermate controls at 3- and 12-month-old, but no significant difference was observed (Figure 3A-3C). And histomorphometric analysis showed that the osteoblast and osteoclast counts were comparable in the *Ocn-Cre;Kdm4b^{fl/fl}* mice and littermate controls (Figure 3D, 3E). In addition, as evidenced by adipocyte numbers and area, deletion of *Kdm4b* in mature osteoblasts contributed barely to the accumulation of adipose tissue in aged mice (Figure 3F). Taken together, these findings indicate KDM4B is critical for the differentiation of MSCs to osteoblasts, but not for the function of matured osteoblasts.
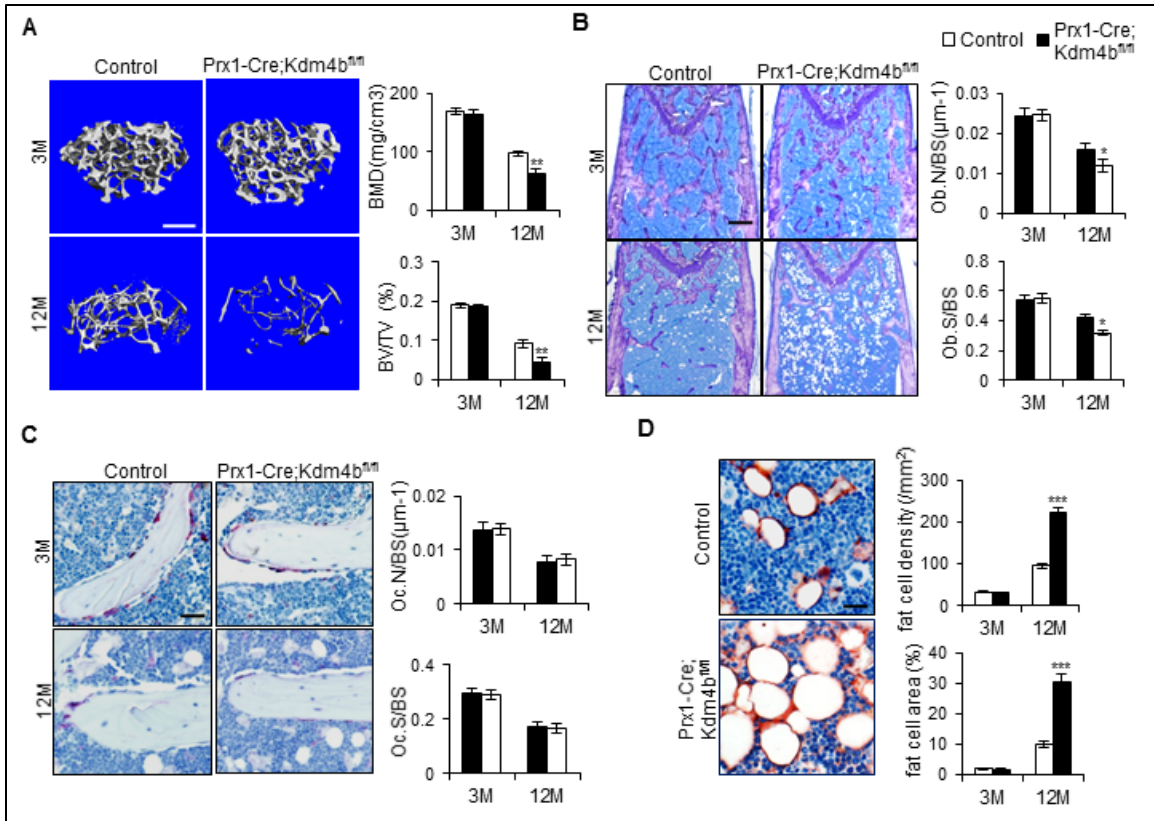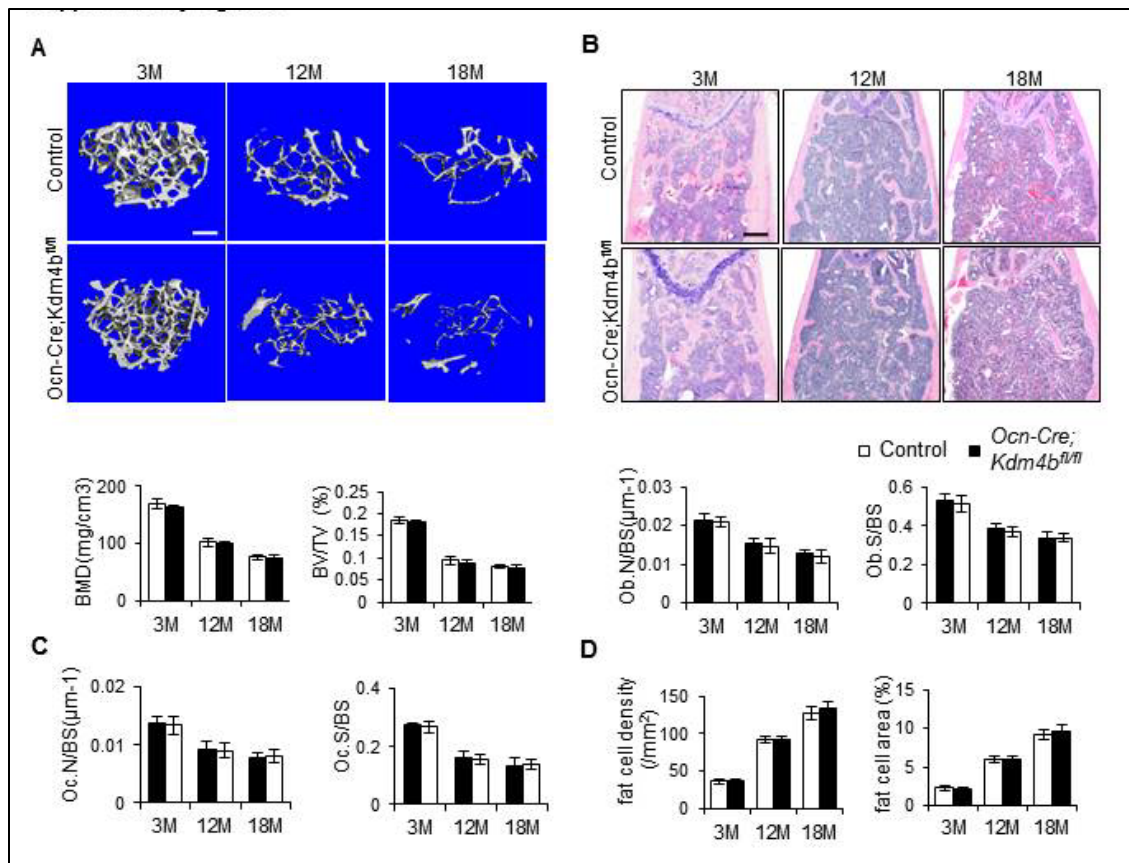

Figure 4. Deletion of Kdm4b in mesenchymal progenitors had little effect on age-related bone loss and adipose accumulation. (A) μCT analysis of trabecular bone in femurs of *Ocn-Cre;Kdm4b^{fl/fl}* and sex-

matched littermates (*Ocn-Cre;Kdm4b+/+ or Kdm4b^{fl/fl}*). Bar indicates 400 μm. BMD and BV/TV (bone volume/total volume) of trabecular bone in femurs of *Ocn-Cre;Kdm4b^{fl/fl}* and littermate controls. (B) H&E stained bone sections from 3- and 12-month-old *Ocn-Cre;Kdm4b^{fl/fl}* mice and littermates, and histomorphometric analysis of Oc.N and Oc.S. Bar indicates 500 μm. (C) Histomorphometric analysis of Ob.N and Ob.S. (D) Quantification of the adipocyte per millimeter^2.

3.3 Deletion of *Kdm4b* in mesenchymal progenitors enhanced bone loss and adipose accumulation induced by estrogen deficiency

To mimic the pathogenesis of osteoporotic bone loss, we performed ovariectomy (OVX) surgery on the female *Prx1-Cre;Kdm4b^{fl/fl}* mice and littermate controls at 2-month old, and the tissues were collected 5 weeks post-operation. Using μCT analysis, We found noticeable trabecular bone loss in littermate mice, compared to sham controls; and bone loss in *Prx1-Cre;Kdm4b^{fl/fl}* mice was even markedly higher, compared to littermates (Figure 3A). Further, toluidine blue staining showed significantly lower osteoblast number and osteoblast surface in *Prx1-Cre;Kdm4b^{fl/fl}* mice following OVX, compared to littermate controls (Figure 3B). However, the elevated osteoclast number and osteoclast surface, induced by OVX, were not affected by deletion of *Kdm4b* in mesenchymal progenitors (Figure 3C). On the other hand, histology analysis revealed a significant increase in adipocyte numbers and the area taken by adipose tissue in *Prx1-Cre;Kdm4b^{fl/fl}* mice following OVX, compared to littermate controls (Figure 3D). Collectively, these results indicate Kdm4b is a key factor that inhibits development of osteoporosis by promoting osteoblastic differentiation from mesenchymal progenitors.
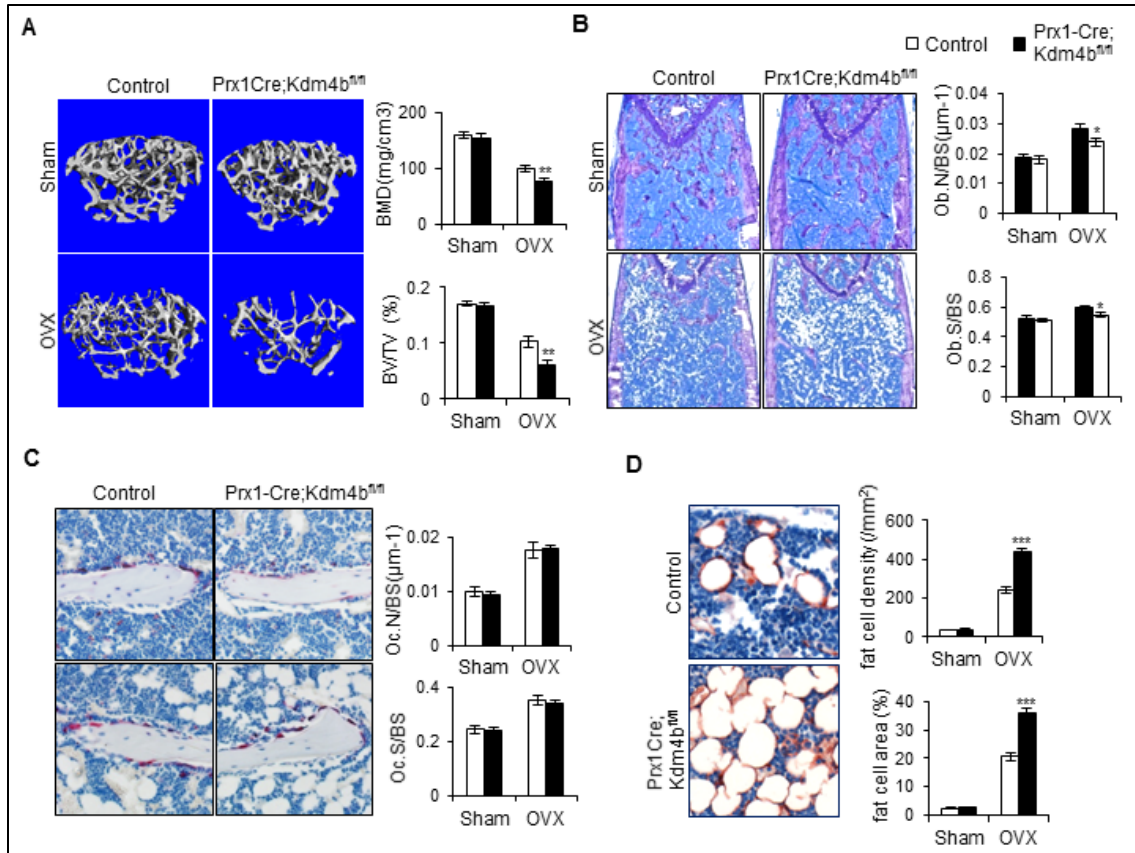
Figure 5. Deletion of Kdm4b in mesenchymal progenitors enhanced bone loss and adipose accumulation induced by estrogen deficiency. (A) μCT analysis of trabecular bone in femurs of *Prx1-Cre;Kdm4b^fl/fl^* and littermates after sham and OVX surgery, respectively. BMD and BV/TV were analyzed. (B) Toluidine blue-stained bone sections from *Prx1-Cre;Kdm4b^fl/fl^* mice and littermates after sham and OVX surgery, respectively. Ob.N and Ob.S were normalized to the BS, respectively. (C) Trap staining of trabecular bone in femurs of *Prx1-Cre;Kdm4b^fl/fl^* and littermate controls after sham and OVX surgery, respectively. Oc.N and Oc.S were normalized to the BS, respectively. (D) Representative images showed FABP4 staining in femur sections and quantification of the adipocyte per millimeter^2.

To investigate whether osteoblasts and adipocytes come from same mesenchymal progenitors, we generated *Prx1-Cre;Kdm4b^fl/fl^;tdTomato* mice that expressed tdTomato in the Prx1-Cre recombined cells, including mesenchymal progenitors and sublineages. We found osteocytes and

osteoblasts lining on the trabecular bone surface were expressing tdTomato (Figure 6A), and the Fabp4-expressing adipocytes in bone marrow were also positive with tdTomato. OVX was then performed on *Prx1-Cre;Kdm4b^{wt/wt};tdTomato* mice and *Prx1-Cre;Kdm4b^{fl/fl};tdTomato* mice. We found tdTomato+ adipocytes in *Prx1-Cre;Kdm4b^{fl/fl};tdTomato* mice are significantly more, compared to the *Prx1-Cre;Kdm4b^{wt/wt};tdTomato* mice following OVX (Figure 6B, 6C). Giving the osteoblasts in *Prx1-Cre;Kdm4b^{fl/fl}* mice was less than littermate controls, these results indicate that deletion of Kdm4b in mesenchymal progenitors shifts the lineage specification of mesenchymal progenitors from osteogenic differentiation to adipogenic differentiation.
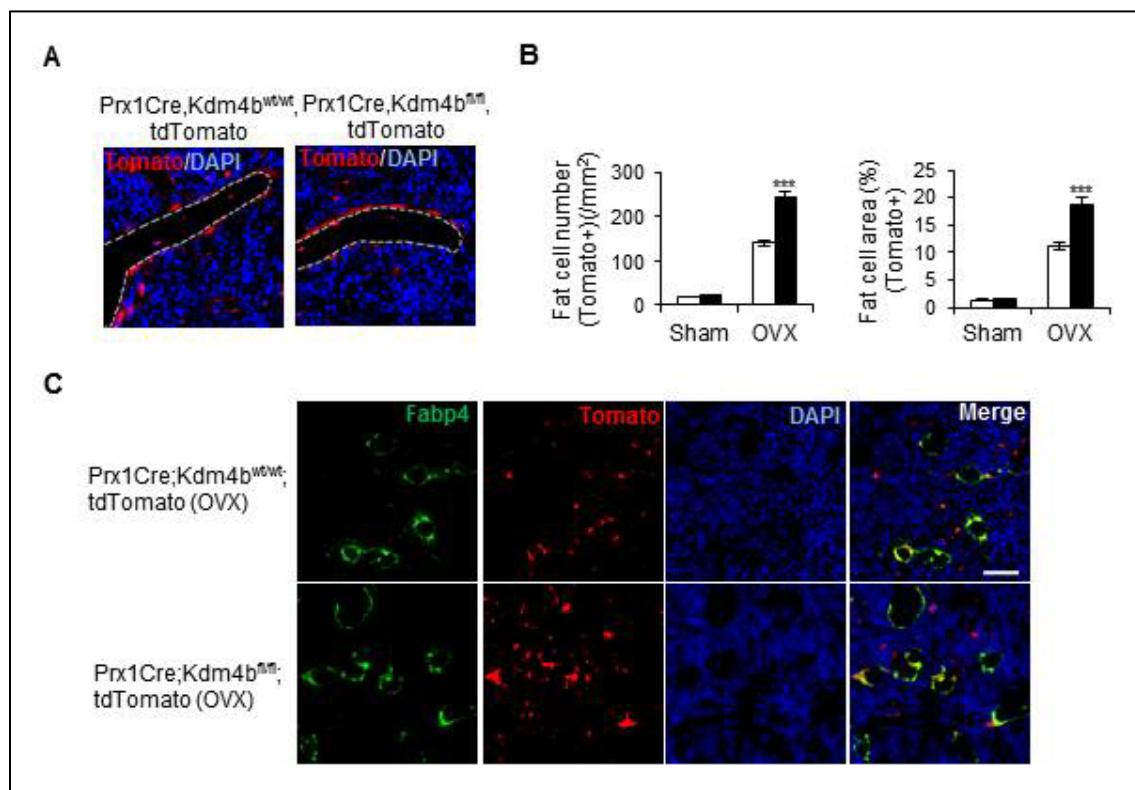
Figure 6. Prx1-labbled mesenchymal progenitors give rise to both bone and fat lineages in bone marrow. cells. (A) osteoblasts and osteocytes expressed tdTomato. (B) Quantification of the tomato-expressing adipocyte per millimeter^2. (C) Representative images show FABP4 staining in femur sections after OVX surgery. Bar indicates 40 μm.

3.4 Overexpression of Kdm4b and pharmacological inhibition of H3K9me2 reinstated osteogenesis, and inhibited adipogenesis of BMSCs from *Prx1-Cre;Kdm4b^{fl/fl}* mice, respectively.

To further conform if the change in osteogenesis and adipogenesis of MSCs was induced by loss of enzymatic function of KDM4B, we performed rescue experiment by introducing Flag-tagged *KDM4B* into MSCs from *Prx1-Cre;Kdm4b^{fl/fl}* mice (Figure 7A). As expected, the restoration of KDM4B successfully reinstated ALP activity, mineralization and expression of osteogenic-related genes in primary MSCs from *Prx1-Cre;Kdm4b^{fl/fl}* mice (Figure 7B, 7C). Restoration of KDM4B also inhibited the adipogenic differentiation of primary MSCs from *Prx1-Cre;Kdm4b^{fl/fl}* mice (Figure 7D, 7E).

Figure 7. Overexpression of Kdm4b reinstated osteogenesis, and inhibited adipogenesis of BMSCs from *Prx1-Cre;Kdm4b^{fl/fl}* mice. (A) Western blot analysis shows overexpression of Flag-tagged KDM4B in primary mBMSCs from *Prx1-Cre;Kdm4b^{fl/fl}* mice. (B) ALP activity assay and ARS staining of *Kdm4b-/-* mBMSCs *after*

40

transfection with KDM4B *overexpressing retroviruses and empty vector control* in response to OS. (C) qRT-PCR analysis of expression of osteogenic-related genes in *Kdm4b-/-* mBMSCs *after transfection with Kdm4b overexpressing retroviruses and empty vector control* in response to OS. (D) Oil Red O staining of *Kdm4b-/-* mBMSCs *after transfection* in response to AS. (E) qRT-PCR analysis of expression of adipogenic-related genes in *Kdm4b-/-* mBMSCs *after transfection* in response to AS.

In addition, we tried to inhibit the H3K9me2 levels enhanced by deletion of *Kdm4b* with small chemical inhibitor, A366 [162]. The inhibitory effect of A366 on H3K9m3 level in MSC from *Prx1-Cre;Kdm4b$^{fl/fl}$* mice and controls was confirmed by western blot (Figure 8A). Treatment with A366 slightly enhanced ALP activity and mineralization of wild-type MSCs (Figure 8B). More importantly, A366 treatment successfully rescued the decreased osteogenesis of MSCs from *Prx1-Cre;Kdm4b$^{fl/fl}$* mice (Figure 8B). On the other hand, adipogenic differentiation of MSCs from *Prx1-Cre;Kdm4b$^{fl/fl}$* mice and controls was dramatically suppressed by A366 treatment （Figure 8C, 8D）. Taken together, the function of KDM4B that removes the H3K9me2 and/or H3K9me3 marks played a critical role in promoting osteogenesis and reducing adipogenesis of MSCs.
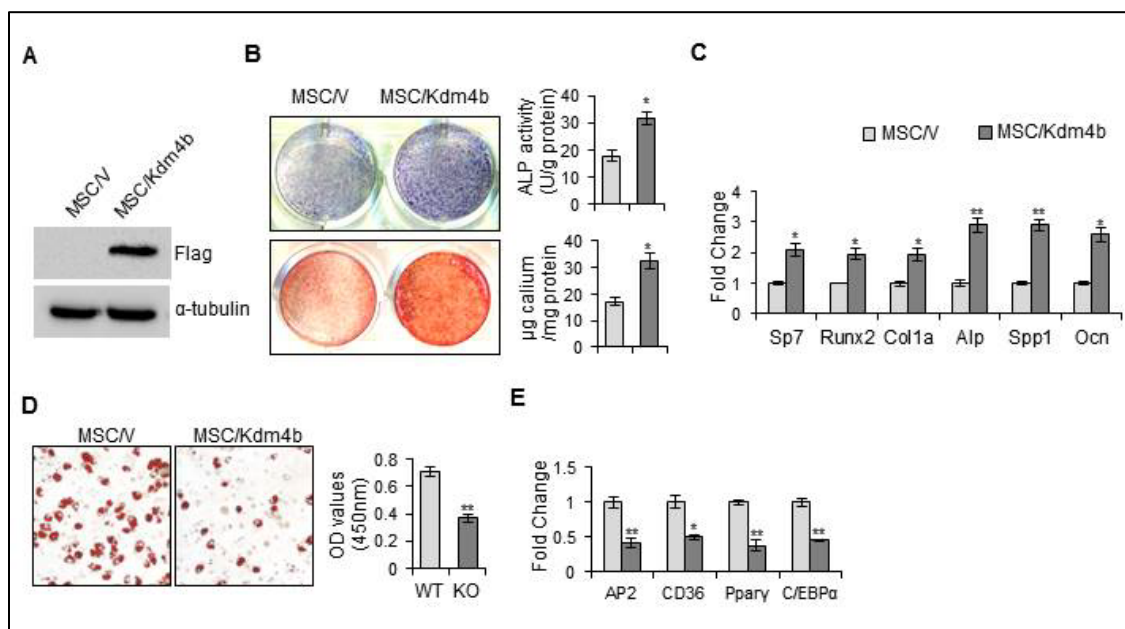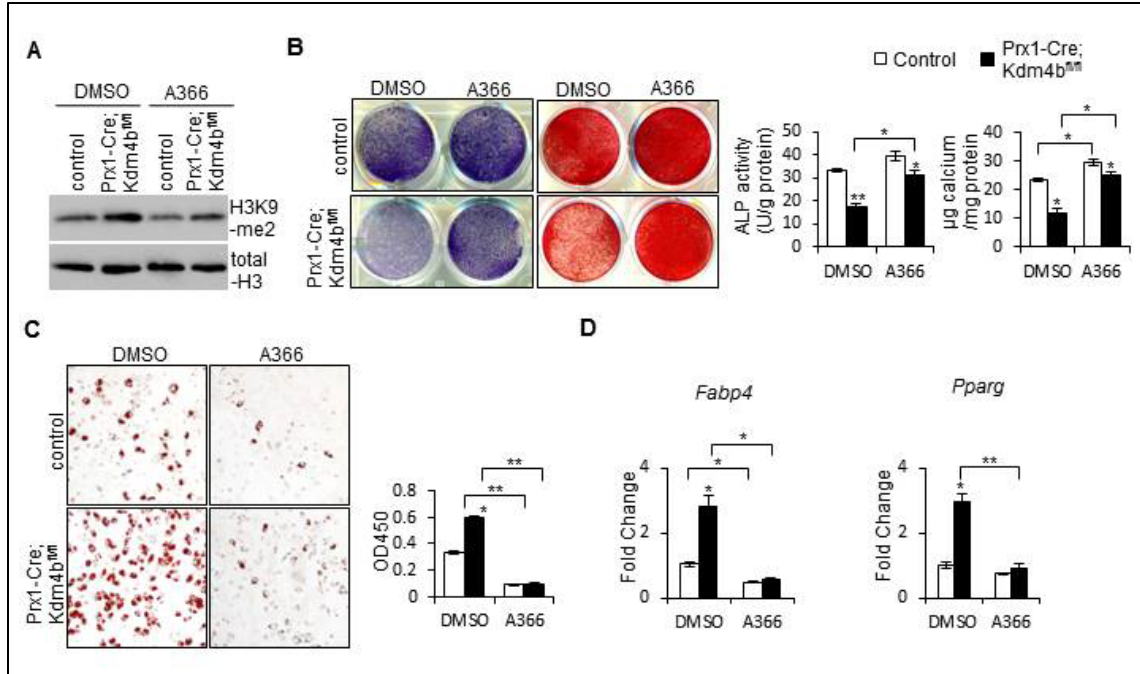
Figure 8. Pharmacological inhibition of H3K9me2 reinstated osteogenesis, and inhibited adipogenesis of BMSCs from *Prx1-Cre;Kdm4b^{fl/fl}* mice. (A) Western blot analysis shows inhibition of H3K9me2 in primary mBMSCs by H3K9me2 inhibitor A366. (B)ALP activity assay and ARS staining of mBMSCs treated with A366 and DMSO in response to OS. (C) Oil Red O staining of treated with A366 and DMSO in response to AS. (D) qRT-PCR analysis of expression of adipogenic-related genes in mBMSCs with A366 and DMSO in response to AS.

3.5 KDM4B is required for activation of wnt signaling and expression of osteogenic-related genes induced by wnt3a

Next, we sought to investigate the molecular mechanism by which *Kdm4b* regulate the lineage specification of mesenchymal progenitors. Total RNA were isolated from primary MSCs from *Prx1-Cre;Kdm4b^{fl/fl}* mice and littermate controls, respectively, and RNA-seq was performed to assess the involved signaling pathways and genes. Genes that were downregulated by 1.5 folds in primary MSCs from *Prx1-Cre;Kdm4b^{fl/fl}* mice in presence of OS for 4 days, were selected for Gene ontology (GO) analysis, which revealed these genes were related to skeletal system development

(Figure 9A) [163, 164]. KEGG analysis further showed Wnt signaling and BMP signaling, which are critical for osteogenesis, are affected by deletion of *Kdm4b* in primary MSCs (Figure 9B, Table 1). Gene set enrichment analysis (GSEA) further revealed that deletion of Kdm4b downregulated Wnt signaling related genes (Figure 9C)[165]. Since we had reported that KDM4B is required for BMP-induced osteogenesis in human MSCs, we investigated the effect of *Kdm4b* knockout on Wnt signaling transduction in primary MSCs. Luciferase reporter containing TEF/LCF binding sites was transfected into primary MSCs from *Prx1-Cre;Kdm4b^{fl/fl}* mice and littermate controls, respectively. We found that Wnt signaling significantly suppressed by deletion of *Kdm4b* in response to overnight wnt3a treatment (Figure 9D). Consistently, the expression of downstream genes *Axin2* and *DKK1* was also inhibited in *Kdm4b* deleted primary MSCs, when treated with wnt3a (Figure 9E, 9F).
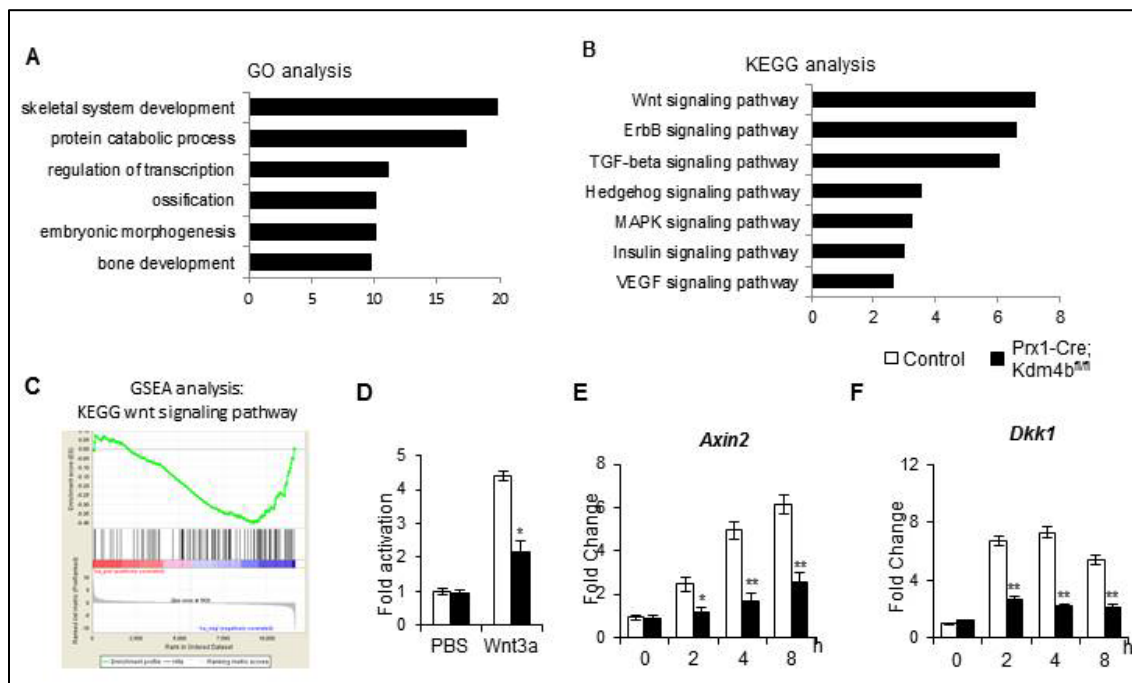
Figure 9. KDM4B is required for activation of wnt signaling. (A) Go analysis of genes downregulated by 1.5 folds in primary MSCs from *Prx1-Cre;Kdm4b^{fl/fl}* mice. (B) KEGG pathway analysis of genes

downregulated by 1.5 folds in primary MSCs from *Prx1-Cre;Kdm4b^{fl/fl}* mice. (C) GSEA revealed that deletion

of Kdm4b downregulated Wnt signaling related genes. (D) Luciferase reporter assay containing TEF/LCF

binding sites in wnt3a treated primary MSCs from *Prx1-Cre;Kdm4b^{fl/fl}* mice and littermates. (E, F) qRT-PCR

analysis of expression of Wnt target genes (Axin2, DKK1) in Wnt3a treated primary MSCs from *Prx1-*

Cre;Kdm4b^{fl/fl} mice and littermates.

Table 3. KEGG analysis revealed that deletion of Kdm4b downregulated Wnt signaling related genes. The

genes downregulated more than 1.5 folds were shown in the list.

GENE	FPKM		Fold Change
	Control	Prx1-Cre;Kdm4b^{fl/fl}	（Prx1-Cre;Kdm4b^{fl/fl}/contorl）
APC	8.65054	4.50888	0.521225265
CCND2	89.7542	55.9644	0.623529595
CSNK1A1	123.595	65.3907	0.529072373
CSNK2A1	43.6257	26.1681	0.599832209
CTNNB1	240.042	152.614	0.635780405
CUL1	53.3896	31.9673	0.598755188
DAAM1	5.07208	2.86402	0.564663807
DVL3	12.2218	6.97503	0.570703988
EP300	14.2298	9.23324	0.648866463
FBXW11	31.2358	20.4447	0.654527817
FZD1	33.0212	9.90758	0.300036946
FZD3	0.850885	0.211596	0.248677553
FZD5	13.3127	4.75013	0.356811916

FZD8	10.7895	3.69788	0.342729506
GSK3B	21.7972	13.4462	0.616877397
LRP6	20.2416	10.4728	0.51738993
MAPK8	3.59528	2.27372	0.632418059
NFAT5	10.0084	4.94359	0.493944087
NFATC3	18.9068	10.0643	0.532311126
NFATC4	13.1687	5.25406	0.398980917
PLCB1	1.39441	0.59875	0.429393077
PORCN	10.0627	4.14335	0.411753307
PPP2R5E	15.0845	7.71459	0.511424973
PPP3CB	20.9198	12.2643	0.586253215
PPP3R1	102.712	57.426	0.559097282
PRICKLE2	1.18828	0.564292	0.474881341
PRKCA	6.23553	2.58004	0.413764347
RAC3	21.9881	14.6372	0.665687349
ROCK2	35.5115	18.4681	0.520059699
SFRP2	23.3259	1.4691	0.062981493
SMAD2	10.0203	6.05496	0.604269333
SMAD3	9.03863	4.35555	0.481881657
SMAD4	28.4069	18.1766	0.639865666
TBP	11.2734	7.4937	0.664724041
TCF7	1.09027	0.34247	0.314114852
TM4SF19	0.969236	0.589513	0.608224416
VANGL1	3.09351	1.27491	0.412124092
VANGL2	1.31899	0.37018	0.280654137

WNT10B	1.25235	0.261483	0.208793868
WNT5A	10.2278	2.64652	0.258757504
WNT5B	0.862578	0.384679	0.445964307
WNT9A	2.78656	0.645211	0.231543911

3.6 KDM4B is required for *Runx2* expression induced by Wnt3a and BMP2 by removing H3K9me3 at *Runx2* promoter.

Runx2 was considered as the master transcription factor for osteogenesis[166, 167]. As previous suggested, Wnt signaling and BMP signaling can synergistically activate expression of *Runx2*[168]. Here, we found that deletion of *Kdm4b* significantly inhibited expression of *Runx2* induced by treatment with wnt3a, BMP2, and wnt3a and BMP2, respectively (Figure 10A). Chip assay further revealed β-catenin, Smad1, and Kdm4b was recruited to the promoter of Runx2 in response to wnt3a and BMP2 treatment (Figure 10B, 10C-10E). Conversely, H3K9me3, a repressive histone modification, was removed from the *Runx2* promoter regain in response to wnt3a and BMP2 treatment in primary MSCs (Figure 10C). However, the H3K9me3 levels in MSCs from *Prx1-Cre;Kdm4b^{fl/fl}* mice was significantly higher, compared to MSCs from the littermates, and remained unchanged when treated with wnt3a and BMP2 (Figure 10C). To further test whether β-catenin, Smad1, and Kdm4b functions as in a complex, re-Chip assay was performed, and we found that DNA fragments containing Runx2 promoter regions can be successfully pulled down by primary IP with β-catenin antibody, following secondary IP with Samd1 or Kdm4b antibody (Figure 10G). These results indicate KDM4B may function in the same complex with β-catenin and Smad1to activate Runx2 expression.
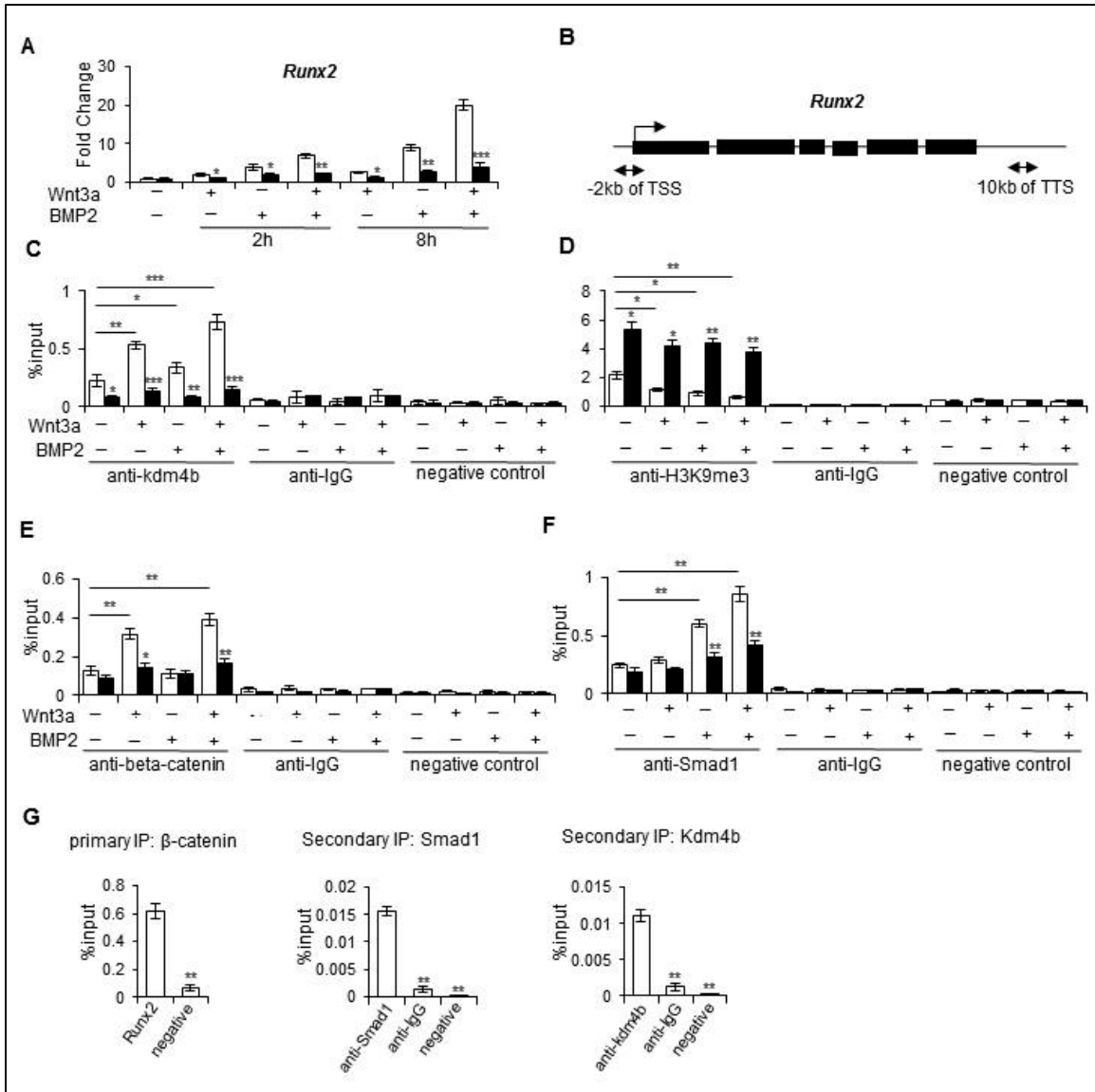
Figure 10. KDM4B was required for Runx2 expression induced by Wnt3a and BMP2 by removing H3K9me3 at Runx2 promoter. (A) qRT-PCR analysis of expression of Runx2 in Wnt3a and BMP2 treated primary MSCs from *Prx1-Cre;Kdm4b^{fl/fl}* mice and littermates. (B) Schematic diagram of primers at Runx2 promoter for Chip experiments. (C) Chip analysis of Kdm4b binding at Runx2 promoter in response to Wnt3a and BMP2 treatment. (D) Chip analysis of H3K9me3 levels at Runx2 promoter in response to Wnt3a and BMP2 treatment. (E) Chip analysis of β-catenin binding at Runx2 promoter in response to Wnt3a and BMP2 treatment. (F) Chip analysis of Smad1 binding at Runx2 promoter in response to Wnt3a and BMP2 treatment. (G) Re-Chip assay analysis showed β-catenin, Smad1, and Kdm4b may function in a complex to

47

activate Runx2 expression after treatment with Wnt3a and BMP2 for 4 hours.

3.7 Parathyroid hormone (PTH)-induced bone gain and adipose tissue loss is blunted by deletion of *Kdm4b* in mesenchymal progenitors

To further investigate the effect of PTH administration on aged Prx1-Cre;Kdm4b$^{fl/fl}$ mice, 12-month-old *Prx1-Cre;Kdm4b$^{fl/fl}$* male mice and wild-type littermates were subjected to daily injections of PTH(1–34) at 50 μg/kg or vehicle for 4 weeks. Consistently, PTH administration significantly increase trabecular bone mass in wild-type controls, but not in *Prx1-Cre;Kdm4b$^{fl/fl}$* mice, as determined by μCT analysis (Figure 11A). Histomorphometric analysis further revealed a blunted response to PTH administration in osteoblasts in *Prx1-Cre;Kdm4b$^{fl/fl}$* mice (Figure 11B-11D). More importantly, we noticed that the FABP4-stained rMAT was dramatically reduced by PTH administration in wild-type controls, but it remained almost unchanged in *Prx1-Cre;Kdm4b$^{fl/fl}$* mice (Figure 11E, 11F).
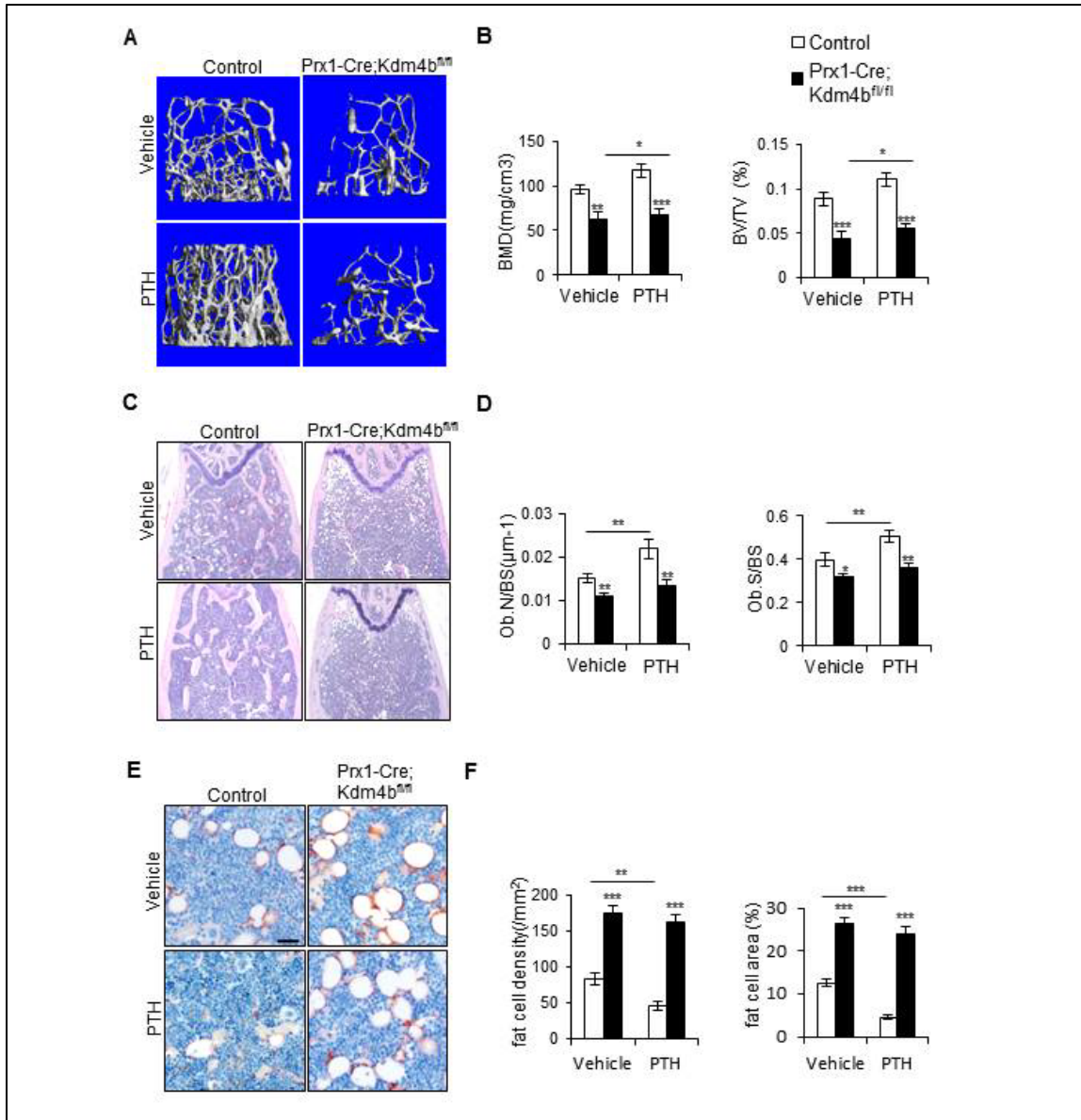
Figure 11. PTH-induced bone gain and adipose tissue loss was blunted by deletion of *Kdm4b* in mesenchymal progenitors. (A) μCT analysis of trabecular bone in femurs of *Prx1-Cre;Kdm4b^fl/fl* and littermates after 4 weeks of PTH administration. (B) BMD and BV/TV were analyzed. (C) HE-stained bone sections from *Prx1-Cre;Kdm4b^fl/fl* mice and littermates after 4 weeks of PTH administration. (D) Ob.N and Ob.S were normalized to the BS, respectively. (E) Representative images show FABP4 staining in femur sections. Bar indicates 40 μm. (F) Quantification of the adipocyte per millimeter^2.

Mechanistically, we found that we found expression of *Kdm4b* was upregulated in mBMSCs in response to treatment with 100 nM PTH (1-34) (Figure 12A). Deletion of *Kdm4b* in mesenchymal progenitors inhibited Runx2 expression induced by PTH treatment in primary MSCs (Figure 12B). KDM4B was recruited to the promoter of Runx2, and H3K9me3 marks were removed in response to PTH treatment in MSCs from control mice. However, in MSCs from Prx1-Cre;Kdm4b$^{fl/fl}$ mice, PTH treatment failed to remove the repressive H3K9me3 marks, due to lack of KDM4B (Figure12C, 12D). Our results indicate deletion of Kdm4b in mesenchymal progenitors significantly inhibited PTH-induced osteoblastic differentiation of MSCs, thereby resulted in a decrease in PTH-induced bone gain.
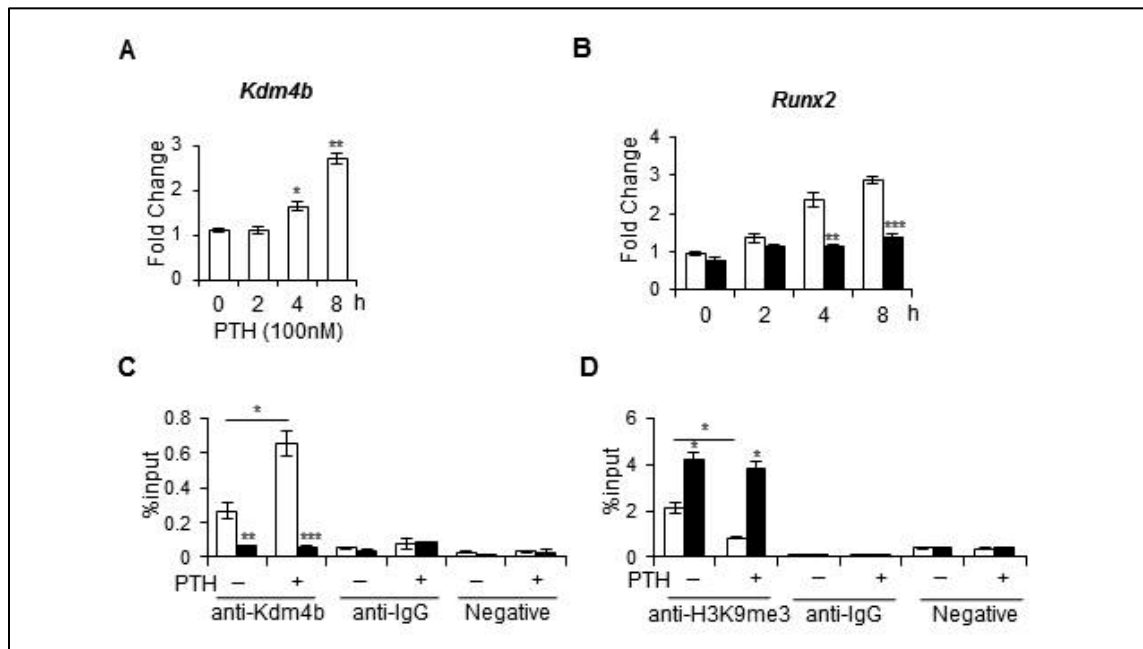
Figure 12. PTH treatment recruited KDM4B to Runx2 promoter to remove H3K9me3 marks. (A) qRT-PCR analysis of expression of Kdm4b in response to treatment with PTH in primary MSCs. (B) qRT-PCR analysis of expression of Runx2 in response to treatment with PTH in primary MSCs from *Prx1-Cre;Kdm4b$^{fl/fl}$* mice and littermates. (C) Chip analysis of Kdm4b binding at Runx2 promoter in response to PTH treatment. (D) Chip analysis of H3K9me3 levels at Runx2 promoter in response to PTH treatment.

PTH was reported to activate downstream PKA signaling and wnt/β-catenin signaling[169, 170]. To investigate the mechanism by which PTH treatment induced expression of *Kdm4b*, primary MSCs were pre-treated with H89 (a competitive PKA inhibitor) for 1 hour, followed by PTH treatment for 8 hours. qRT-PCR analysis showed H89 significantly inhibited PTH-induced expression of *Kdm4b* (Figure 13A). Similarly, siRNA-mediated depletion of β-catenin suppressed *Kdm4b* expression, in presence or absence of PTH treatment (Figure 13B). In order to further confirm whether PTH induces *Kdm4b* expression by PKA signaling and wnt/β-catenin signaling, we analyzed the promoter region of Kdm4b by using JASPAR profiles, and found two potential CREB (cAMP response element binding protein) binding sites (-2484~-2477; -2380~-2373) next to TCF/LEF1 binding sites (-2532~-2521; -2324~-2313)[171]. As evidenced by Chip assay, both CREB and β-catenin were recruited to the promoter region of Kdm4b in response to PTH (1-34) treatment (Figure13C, 13D).
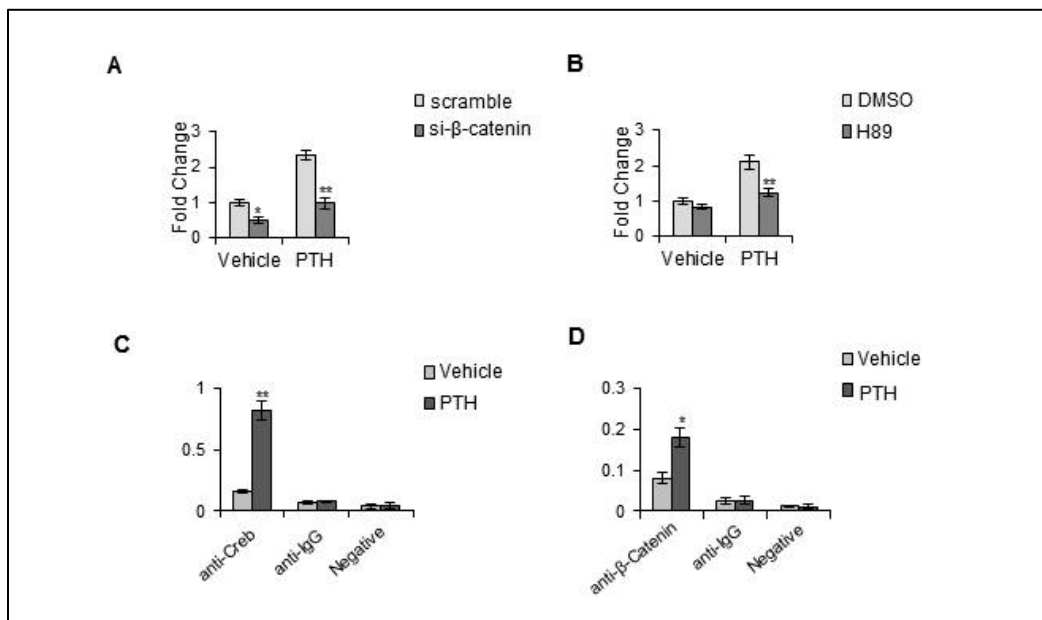
Figure 13. PTH induce KDM4B expression via activate downstream PKA signaling and wnt/β-catenin signaling. (A) qRT-PCR analysis of expression of Kdm4b in response to treatment with PTH in primary MSCs

after knockdown of β-catenin. (B) qRT-PCR analysis of expression of Kdm4b in response to treatment with PTH in primary MSCs that were pretreated with H89. (C) Chip analysis of Creb binding at Kdm4b promoter in response to PTH treatment. (D) Chip analysis of β-catenin binding at Kdm4b promoter in response to PTH treatment.

3.8 Kdm4b is required for the self-renewal of mouse MSCs

Giving the decreased bone mass in aged *Prx1-Cre;Kdm4b^{fl/fl}* mice, we suspected that deletion of *Kdm4b* not only led to an unbalanced differentiation potential, but also impaired the self-renewal capacity of MSCs. We found that deletion of *Kdm4b* in mesenchymal progenitors significantly reduced the number of colony-forming unit fibroblasts (CFU-Fs) (Figure 14A). In contrast, β-galactosidase activity, a senescence marker, was significantly enhanced by deletion of Kdm4b in primary MSCs (Figure 14B). GSEA further revealed that deletion of Kdm4b downregulated expression of stem-ness related genes in primary MSCs (Figure 14C)[128]. We then found expression of NANOG and SOX2, the essential transcription factor for maintenance of stem cells, was inhibited in Kdm4b-deficient MSCs, as evidenced by RT-qPCR and western blot (Figure 13D, 13E).
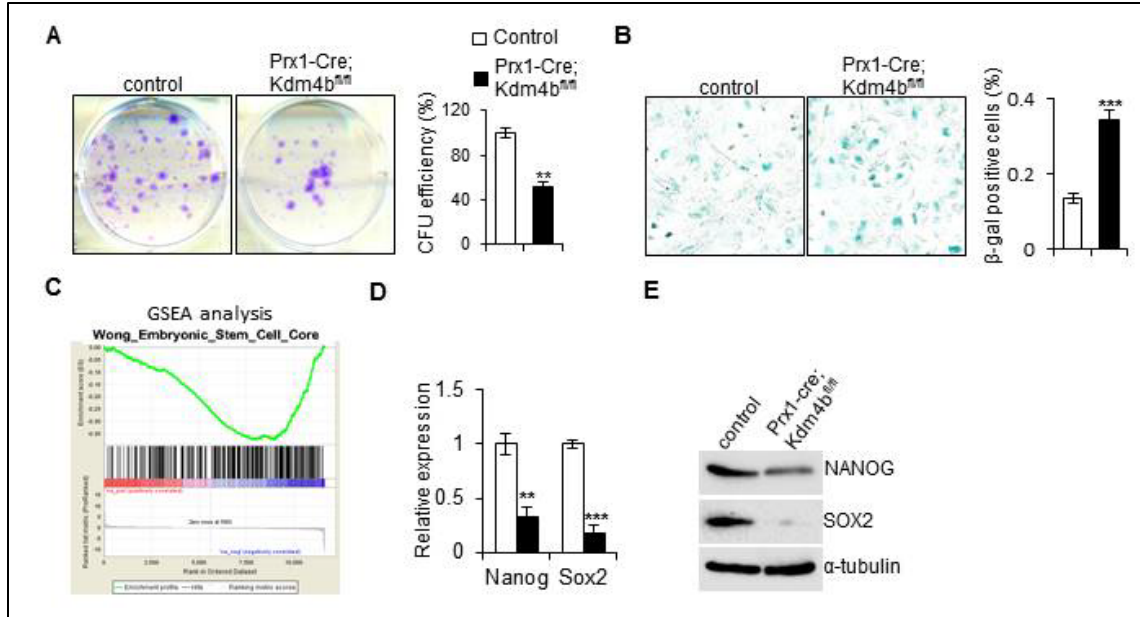
Figure 14. Kdm4b is required for the self-renewal of primary MSCs *in vitro*. (A) Crystal violet-stained colonies after 2 weeks of culture, and quantification of CFU-Fs. (B) β-galactosidase staining and quantification of β-galactosidase-positive primary MSCs. (C) GSEA revealed that deletion of Kdm4b downregulated stemness-related genes. (D) qRT-PCR analysis of expression of *Nanog* and *Sox2* in primary MSCs from *Prx1-Cre;Kdm4b^{fl/fl}* mice and littermates. (E) Western blot analysis of expression of NANOG and SOX2 in primary MSCs from *Prx1-Cre;Kdm4b^{fl/fl}* mice and littermates.

To further confirm this hypothesis *in vivo*, we isolated primary MSCs from *Prx1-Cre;Kdm4b^{wt/wt};tdTomato* and *Prx1-Cre;Kdm4b^{fl/fl};tdTomato* mice, and assessed the self-renewal capacity of tdTomato+ MSCs in serial transplantation[172, 173]. For the primary transplantation, tdTomato+ MSCs from *Prx1-Cre;Kdm4b^{wt/wt};tdTomato* and *Prx1-Cre;Kdm4b^{fl/fl};tdTomato* mice were incubated with gelform scaffold, and subcutaneously transplanted in the dorsal sites of nude mice (n=8). After 6 weeks, the mice were sacrificed and transplants were collected for histology analysis. Intriguingly, all the MSCs from *Prx1-Cre;Kdm4b^{wt/wt};tdTomato* and 7 out of 8 MSCs from *Prx1-Cre;Kdm4b^{fl/fl};tdTomato* gave rise to bone, fat, and stromal tissues in the transplants,

respectively (Figure 15A). Quantitative measurement of mineralized tissue areas revealed a 39% decrease in bone formation by MSCs from *Prx1-Cre;Kdm4b^{fl/fl};tdTomato* mice compared to MSCs from *Prx1-Cre;Kdm4b^{wt/wt};tdTomato* mice (Figure 15B). All the cells in bone tissues expressed tdTomato, indicating the bone were generated by the transplanted tdTomato+ MSCs (Figures 15C). Next, the tdTomato+ adipocytes were further confirmed by immunostaining for FABP4 (Figure 15D). And MSCs from *Prx1-Cre;Kdm4b^{fl/fl};tdTomato* mice generated more adipose tissue compared to the controls (Figure 6F). Importantly, the cells from the transplants with *Prx1-Cre;Kdm4b^{wt/wt};tdTomato* MSCs exhibited a significant decrease in CFU capacity, compared to the controls (Figure 15E). After *in vitro* expansion, the cells from the transplants were used for secondary transplantation (n=8). After 6 weeks, while 7 out of 8 transplants with *Prx1-Cre;Kdm4b^{wt/wt};tdTomato* MSCs generated bone, fat, and stromal tissues, only 3 out of 8 secondary transplants with *Prx1-Cre;Kdm4b^{fl/fl};tdTomato* cells MSCs have bone, fat, and stromal tissues (Figure 15F). Of note, because the scaffold was absorbed, we suspect that the rest transplants might be absorbed and were not found. Similarly, the cells from transplants with *Prx1-Cre;Kdm4b^{fl/fl};tdTomato* MSCs showed a showed a 90% decrease in bone formation, and a greater than 100% increase in adipose tissues formation in the secondary transplants (Figure 15G). Furthermore, the cells from transplants with *Prx1-Cre;Kdm4b^{fl/fl};tdTomato* MSCs were barely able to generate CFUs, indicating a fast loss of self-renewal capacity, compared to the controls (Figure 15H).
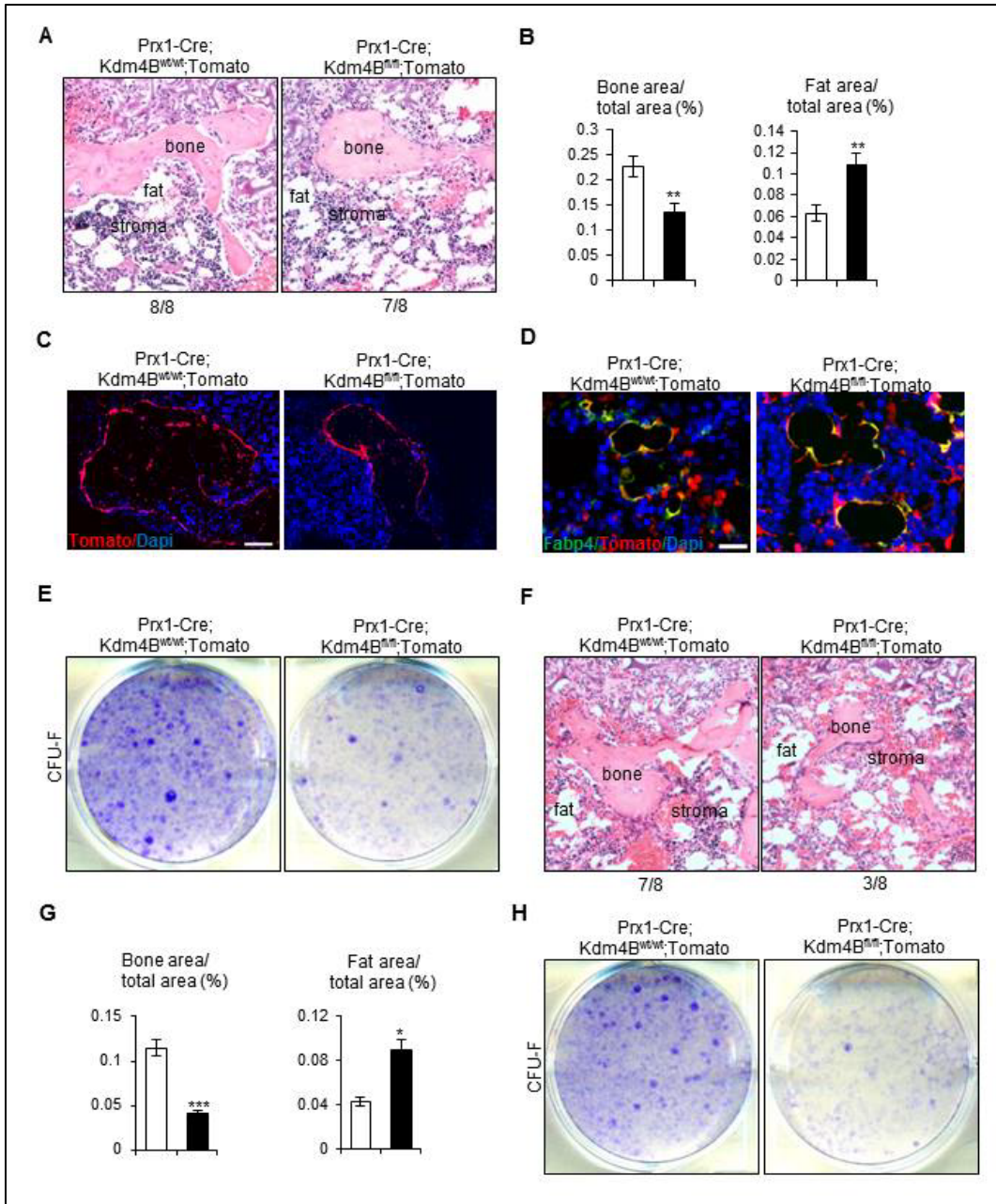
Figure 15. Kdm4b is required for the self-renewal of primary MSCs in serial transplantation. (A) HE-stained sections from transplants generated by MSCs from Prx1-Cre;Kdm4b$^{fl/fl}$ mice and littermates after 6 weeks, respectively. (B) Quantification of bone and adipose tissues in the primary transplants. (C) tdTomato-expressing bone tissue was found in the primary transplants. Bar indicates 150 μm. (D) IF staining for FABP4 of tomato-expressing adipocytes in transplants. Bar indicates 40 μm. (E) Crystal violet-stained colonies generated by the cells from the primary transplants after 2 weeks of culture, and

quantification of CFU-Fs. (F) HE-stained sections from secondary transplants generated by MSCs from Prx1-Cre;Kdm4b^{fl/fl} mice and littermates after 6 weeks, respectively. (G) Quantification of bone and adipose tissues in the secondary transplants. (H) Crystal violet-stained colonies generated by the cells from the secondary transplants after 2 weeks of culture, and quantification of CFU-Fs.

4. DISCUSSION

Osteoporosis is the most common bone metabolic diseases that associated with loss of bone mass and accumulation of adipose tissues in bone marrow[174]. Unbalanced differentiation of MSCs into osteoblasts or adipocytes contributes significantly to the development of osteoporosis. By using mouse model of aging and estrogen-deficiency, we found that deletion of Kdm4b in mesenchymal progenitors led to an enhanced bone loss by inhibition of the osteoblastic differentiation of MSCs, but promoted the adipogenic differentiation of MSCs. As determined the Chip assay, recruitment of KDM4B and removing of the H3K9me3 marks at the promoter regions of Runx2 are critical for osteogenic lineage commitment of MSCs. PTH (1-34) is the only FDA-approved anabolic bone treatment for treatment of osteoporosis in the United States[175]. We further revealed Kdm4b was upregulated by PTH (1-34) treatment in primary MSCs, and KDM4B deletion of Kdm4b in mesenchymal progenitors significantly attenuated the bone gain induced by PTH (1-34) administration in vivo.

The reverse relationship between osteogenic and adipogenic lineage specification of MSCs has been long realized, and the commitment to an osteogenic lineage of MSCs, in theory, requires inhibition of differentiation toward adipogenic lineages. In this study, we found the regulation of cell fate of MSCs could take place at epigenetic level by removing the repressing histone modification at regulation region of Runx2 gene. Previous studies have demonstrated RUNX2

represses adipogenesis, while deletion of Runx2 leads to the loss of the differentiated characters of chondrocytes and induced adipogenic differentiation *in vitro*[176, 177]. In the contrary, PPARγ, the master regulator of adipogenesis, inhibits expression of Runx2, and binds to the RUNX2 protein to inhibit transcription activator of Runx2 at osteogenic promoters[38, 176]. We suspect that KDM4B may promote osteogenic commitment of MSCs by RUNX2, thereby possibly inhibited adipogenic commitment of MSCs. One the other hand, we found KDM4B was required for activation of Wnt signaling that represses adipogenesis. It is also possible the enhanced adipogenesis was caused by the decrease in Wnt signaling in Kdm4b-deficient MSCs. However, whether KDM4B directly participates in the regulation of PPARγ and other adipogenic genes remains to be investigated.

MAT is not inert. Instead, adipocytes are capable of regulating bone remodeling by secreting endocrine and paracrine factors that strongly influence function and activities of other neighboring and distant cells. In particular, bone marrow adipocytes compose a unique adipose depot and express RANKL that promotes osteoclastogenesis[178]. On contrast, they can also produce the cytochrome P450 enzyme, aromatase, which can restrain osteoclastogenesis within the BMUs via converting testosterone into estradiol [179]. In addition, other factors secreted by adipocytes, such as leptin, adiponectin, and proinflammatory cytokines, can affect the osteoblastic differentiation of MSCs[180]. These studied highlighted the role of MAT in regulation of bone homeostasis, and partially explain the bone loss after menopause. In the present study, we found that deletion of Kdm4b resulted in an accumulation of MAT in aged mice. However, to what extent BMF actually affects bone remodeling requires further investigation. It is likely that the accumulated adipocytes secreted factors, like RANKL, which compensated the decreased RANKL from osteoblasts and maintain OC activities in Kdm4b-deficient mice at a comparable level as control mice. This may also accelerate the bone loss in Kdm4b-deficient mice.

In addition, recent studies have provoked a fundamental debate about the lineage restriction of skeletal stem cells. A small proportion of bone marrow cells are restricted to generate osteogenic and chondrogenic lineages, and reticular cells, namely osteochondroreticular (OCR) stem cells. OCR stem cells were reported to contribute to bone generation, maintenance, and repair during development and adulthood. Gremlin1^{+} cells and CD45^{-}Ter[-]119^{-}Tie2^{-}AlphaV^{+}Thy-6C3^{-}CD105^{-}CD200^{+} cells were identified as OCR stem cells by two different groups[181, 182]. However, as Grem1+ cells are also positive for CD105, they are distinct from CD45^{-}Ter[-]119^{-}Tie2^{-}AlphaV^{+}Thy-6C3^{-}CD105^{-}CD200^{+} cells. And obviously, OCR stem cell does not meet the minimal criteria of MSCs. As Worthley *et al.* suggested, there might be at least two types of skeletogenic stem cells, which contribute to postnatal bone formation[181]. Grem1+ OCR stem cells are major source of skeletal tissue in the early life, and the contribution of perivascular MSCs, such as LepR[+] MSCs, increases with age[149]. As Zhou *et al.* reported, in the marrow of mice limb bones, LepR^{+} cells uniformly express the Prx1. In this study, we used a Prx1 limb enhancer to drive expression of Cre recombinase, and to delete Kdm4b in mesenchymal progenitors. On the other hand, the proposed existence of two distinct skeletogenic stem cells (MSCs and OCR stem cells) may explain why deletion of Kdm4b had little effect on the bone mass at 3-month-old.

Finally, we demonstrated KDM4B was also required for self-renewal of MSCs. It is possible that deletion of Kdm4b resulted in a rapid aging process in MSCs, which eventually led to a decrease in osteoblast numbers. And osteoblast function declines in late life, further exaggerating the imbalance between bone resorption and formation [183]. However, a global decrease in H3K9me3 was associated with alterations in heterochromatin patterns and MSC senescence[144, 184, 185]. Notably, knocking in a catalytically inactive form of SUV39H1, a H3K9me3 methyl-transferase, in wild-type mesenchymal stem cells accelerated cellular senescence and led to a phenotype like

WRN-null MSCs[144]. These findings seem to conflict with our result that deletion of Kdm4b led to an increase in H3K9me3 levels and MSC senescence. We suspect that, compared to SUV39H1, KDM4B specifically promoted the differentiation- and stemness-related genes in MSCs. Also, deletion of Kdm4b may not affect heterochromatin patterns as strong as SUV39H1.

In conclusion, we found Histone Demethylases KDM4B promotes osteogenesis and reduces adipogenesis, and is required for self-renewal of MSCs. More importantly, KDM4B is required for bone gain induced by PTH administration. Our findings indicate Kdm4b is key regulator of bone homeostasis, and is a potential therapeutic target for osteoporosis and bone repair after injury.

CHAPTER 2

Inhibition of IKK/NF-κB Signaling Enhances Differentiation of Mesenchymal Stromal Cells from Human Embryonic Stem Cells

1. INTRODUCTION

Mesenchymal stem cells (MSCs) have generated a great amount of enthusiasm over the past decades for tissue engineering. Two properties of MSCs are highlighted during the bone regeneration: 1) to differentiate into mature osteocytes, 2) to secrete multiple bioactive molecules capable of stimulating recovery of injured cells, inhibiting inflammation and performing immune-modulatory functions[186, 187]. Many completed clinical trials have demonstrated that implantation of MSCs is an effective, safe and durable method for repair of bone defects [188-190].So far, MSCs for clinical use have been derived mostly from adult bone marrow[188, 190]. However, adult MSCs have been isolated from bone marrow and adipose tissues, the isolation procedure is invasive, and MSCs represent a very small fraction, 0.001–0.01% of the total population of nucleated cells in bone marrow. bone marrow may be detrimental due to the highly invasive donation procedure and the decline in MSC number and differentiation potential with aging[8].

Human embryonic stem cells (ESCs), derived from the inner cell mass of blastocyst, are characterized by their immortality and the potential to give rise to a large variety of cells and tissues from all 3 germ layers, including MSCs. Because of these unique properties, ESC might be the ideal candidate for regenerative medicine. However, with immunologic incompatibility and the risk to form neoplasms or teratomas, it has become clear that the pluripotency, at the same time, makes ESCs hard to control. Furthermore, the possible clinical application is also prevented by political and ethical concerns. Hence, In spite of the pluripotency of human ESCs, these

complicated controversies have restricted their use for therapeutic purposes. To free cell-based therapy of bone defects from this dilemma, there is an alternative detour: derivation of human MSCs from human ESCs. Since the first human ESC-derived MSC lineage was developed in 2007, many other ESC lines have been successfully employed to generate MSCs in vitro. These MSCs could be consistently derived in large amounts from ESCs, and they show similar properties with adult MSCs in their gene expression, surface markers, and differential potential, which means they also hold the promise for clinical application. In this review, we summarize the studies on derivation human MSCs from ESCs via EB formation, and the potential cell-based therapy of bone defects.

1.1 Derivation MSCs from ESCs

Basically, derivation of MSCs from hESCs consists of two steps: differentiation and purification. Human embryonic stem cells (ESCs) are pluripotent, which have the potential to provide unlimited supply of MSCs[191, 192]. Many differentiation strategies have been used to generate human MSCs, which can be classified into three categories: 1) embryoid body (EB)-based differentiation, 2) co-culture with stromal cells, 3) the culture of ESCs as monolayers[193-195]. hMSCs have been successfully derived from many human ES cell lines, such as CHA3hESC,H1,H9, HuES9,SNUhES3[196, 197].

EB formation is the most will-known method to induce differentiation of hESCs, which has been used to induce differentiation to all the three primary germ layers. When cultured in suspension, ES cells differentiate spontaneously, and form three-dimensional and round "ball" called EBs. An EB is the aggregate of ectodermal, mesodermal, and endodermal tissues. Generally, there are three methods to from EBs, culture in low-attachment plates, culture in methylcellose semisolid, and culture in hanging drops. To induce EB formation, colonies of hESCs are detached by collagenase

IV and then culture in suspension to form EBs in the low-attachment plates. After 7 to 14 days suspension, the EBs are attached on tissue culture plates. When the outgrowing cells reach confluent, these cells could be expanded with trypsin. After 2~3 passages, these cells are ready for cell sorting with MSCs makers. The isolation of hMSCs is performed through flow cytometry based on the specific surface makers, such as CD73, CD90, CD105, and CD146.

Compared to EB-based differentiation, it is recently reported that direct differentiation of human ESCs as cell aggregates enhanced osteogenesis potential, indicating more restricted mesenchymal or osteogenic progenitors in the derived cells[198].

1.2 Signaling Pathway Governing ESC Cell Fate

Canonical Wnt signaling plays an essential role in regulation of stem cells, including ESCs. Previously, it has been implicated in the maintenance of both mouse and human ESCs[199, 200]. It has also been demonstrated to promote the reprogramming of somatic cells into iPSCs (induced pluripotent stem cells)[201]. Several studies have revealed that Wnt/β-catenin signaling is capable of promoting self-renewal of mouse ESCs. However, recent loss-of-function studies suggested that β-catenin is dispensable for self-renewal, but is required for multilineage differentiation, such as cardiac differentiation in hESCs[202]. Davidson et al. further reported Wnt/β-catenin signaling was repressed by Oct4 in hESCs, and activation of Wnt/β-catenin signaling promotes differentiation[203]. Specifically, Ctnnb1(β-catenin)-deficient mESCs failed to give rise to mesendodermal germ layer and neuroepithelial formation, indicating Wnt/β-catenin signaling is required for the differentiation of ESCs into MSCs[204].

Several TGF-β family genes also play crucial roles in the maintenance of self-renewal in both human and mouse ESCs. When co-culturing ESCs with mouse embryonic fibroblasts (MEFs),

MEFs provide an essential cytokine, like LIF (leukemia inhibitory factor) and BMP4. Mechanistically, BMP4 inhibits extracellular receptor kinase (ERK) and p38 mitogen-activated protein kinase (MAPK) pathway to maintain ESC identity[205]. Furthermore, treatment with TGF-β and activin induced nuclear localization of phosphorylated Smad2 in ESCs, but the phosphorylated Smad2 decreased upon differentiation[206]. Conversely, treatment with SB-43154, a chemical inhibitor of Smad2 phosphorylation, resulted in downregulation of the expression of pluripotent markers in ESCs[207]. On the other hand, TGF family members also contribute to diverse processes during embryogenesis by regulating ESC differentiation. In general, TGF-β signaling inhibits ectodermal differentiation, but promotes mesodermal and endodermal differentiation of human and mouse ESCs[208]. For instance, treatment with BMP4 and VEGF (vascular endothelial growth factor) induced hematopoietic differentiation of mESCs in serum free culture[209]. Lengerke et al. reported that BMP signals induced mesoderm and blood lineages by activation of Wnt signaling and Cdx-Hox pathway[210]. Moveover, BMPs inhibits the formation of neuroectoderm, but induces its epidermal differentiation of mESCs[211]. However, the role of TGF-β family genes in regulation of differentiation of ESCs to MSCs remains large unknown.

FGFs and their receptors, FGFRs, have long been known for important roles in embryonic development. To date, 23 members have been found in FGF family, and 5 different FGFRs have been identified in vertebrates[212]. The divergent effects of FGF signaling may depend on the states of differentiation of the cells, the expression of FGFRs, and the presence of other factors. Recent studies have shown that hESCs express several isoforms of FGFs, such as FGF-2, 11 and 13, and all the FGFRs[213]. FGF-2, also known as basic fibroblast growth factor (bFGF), is a key factor to support the maintenance of hMSCs at undifferentiated state in the presence or absence of a feeder layer in vitro. And several studies suggested FGF signaling might be important for self-renewal of

hESCs[214, 215]. In contrast, treatment with synthetic inhibitor of FGFRs, SU5402, resulted in downregulation of Oct4 expression and rapid differentiation. Interestingly, more recently have highlighted an important role in lineage specification during early embryonic development. For instance, FGF-2 promoted mesendoderm over trophoectoderm differentiation during BMP4-induced hESC differentiation[216]. And after hESCs differentiated into a primitive ectoderm-like fate, FGF signaling further promoted neural differentiation[217].

NFκB (nuclear factor kappa-light-chain-enhancer of activated B cells) plays an essential role in regulation of inflammation response, tumor development, as well as stem cell self-renewal and differentiation[218, 219]. In resting cells, the majority of NFκB subunits are associated with inhibitors of NFκB (IκB). Activation of NFκB is caused by the IκB kinase-mediated phosphorylation of IkB, which then allows the active form of NFκB to translocate into the nucleus and initiate gene transcription[220]. Previously, it was shown that the principal NFκB subunits p65, p50, IκB-α, and IκB-β are present throughout differentiation of human ESCs[221]. Although NFκB signaling is very low in the undifferentiated human ESCs, inhibition of NFκB signaling led to significant cell death and differentiation [221, 222], which suggests that NFκB is required for human ESC viability and maintenance. In addition, NFκB signaling strongly increases during differentiation of human ESCs [223]. However, its role in lineage specification of human ESCs remains to be investigated.

In this study, we investigated the role of NFκB signaling in regulation of human ESC differentiation, and provided an efficient method to derive functional MSC from human ESCs by inhibition of NFκB signaling. A specific inhibitor targeting IκB kinase beta (IKKi), which suppressed phosphorylation of p65, was used to inhibit NFκB signaling transduction. We found that treatment with IKKi promoted human ESC differentiation and enhanced MSC marker expression. The derived cells with treatment of IKKi showed stronger osteogenic and

chondrogenic differentiation potential. Further, MSCs were sorted and used to generate ectopic bone in vivo. Thereby, we discovered the role of NFκB in mesenchymal lineage specification of human ESCs, and the derived MSCs have the potential to be used for bone regeneration in the future.

2. METHODS AND MATERIALS

hESC Culture

This research was approved by UCLA Embryonic stem cells research oversight (ESCRO) committee.H1 Human ESCs (WA-01, XY) were obtained from UCLA Broad Stem Cell Research Center. Human ESCs (passages 35–45) were cultured as cell aggregates on a mitotically inactivated mouse embryonic feeder (MEF) layer, as previously described [192]. The hESCs were passaged every week using 1 mg/ml type IV collagenase (Invitrogen). To induce differentiation of human ESCs, ESC aggregates were directly plated into tissue culture dishes, and grown in DMEM, containing 15% fetal bovine serum (FBS), 1% L-Glutamine, 1% non-essential amino acid, and 1% Penicillin-Streptomycin (MSC medium, all from Invitrogen). IKKi (1μM, Calbiochem) was added during ESC differentiation as indicated. After 7 days of differentiation, the derived cells were trypsinized to generate a single-cell suspension, and $1x\ 10^5$ cells were seeded into each well in 12-well plates for further differentiation.

Viral infection

To knockdown p65 during differentiation of human ESCs, we constructed a p65 shRNA (shp65) and a scrambled shRNA (Scr). The shRNA was subcloned into a pLKO.1 lentiviral vector, and lentiviruses were packaged and generated in 293T cells as described previously[224]. For viral infection, ESC aggregates plated overnight and then infected with lentiviruses in the presence of

polybrene for 24 hours. The target sequences for shRNA were: 5'-GTGACAAGGTGCAGAAAGA-3'.

Induction of Osteogenic, Chondrogenic, and Adipogenic Differentiation

To induce osteogenic differentiation, cells were grown in osteogenic induction (OI) medium containing 1 nM dexamethasone, 100 μM ascorbic acid, and 5 mM beta-Glycerophosphate (all from Sigma). To induce chondrogenic differentiation, cells were cultured in chondrogenic induction (CI) medium containing 100 mM sodium pyruvate, 40 μg/mL proline, 100 nM dexamethasone, 200 μM ascorbic acid (all from Sigma), and 10 ng/mL TGF-β3 (R&D systems). To induce adipogenic differentiation, the cells were cultured in adipogenic induction (AI) medium containing 1 μM dexamethasone, 10 μg/mL insulin, 0.5 mM 3-isobutyl-1-methylxanthine, and 0.2 mM indomethacin (all from Sigma).

ALP, Alizarin Red Staining, Alcian Blue Staining and Oil-Red O Staining

ALP activity assay and Alizarin Red Staining were performed as described previously. For Alcian blue staining, cells were fixed with 10% neutral buffered formalin (Fisher) for 15 min at room temperature, and then incubated in Alcian staining solution (1% Alcian blue in 3% Acetic acid, Fihser) for 30 min. The plates were then photographed, and the stained cultures were destained by 6 M guanidine hydrochloride (Fisher). The absorbance of the solution was read at 620 nM using a microplate reader (Bio-Rad). After adipogenic induction, Oil-Red-O staining was performed to detect the lipid droplets using an OIL-RED-O STAIN KIT according to the manufacturer's instruction (Diagnostic BioSystems), and then destained by 100% isopropanol (Fisher). The absorbance of the solution was measured at 450nM.

Quantitative RT-PCR

Total RNA was isolated using the Trizol reagents (Invitrogen) according to manufacturer's instructions. cDNA was synthesized from 2 ug aliquots of RNA using random hexamer primers and reverse transcriptase (New England Biolabs). SYBR Green PCR master mix (EuroClone) was used for quantitative PCR (qPCR) analysis. The primers for GAPDH are: 5'-GGAGCGAGATCCCTCCAAAAT -3' (forward), 5'-GGCTGTTGTCATACTTCTC ATGG -3' (reverse). The primers for PAX6 are: 5'-TGGGCAGGTATTACGAGACTG -3' (forward), 5'-ACTCCCGCTTATAC TGGGCTA -3' (reverse). The primers for PDGFR-α are: 5'-TATGTGCCAGACCC AGATGT -3' (forward), 5'-GGAGTCTCGGGATCAGTTGT -3' (reverse). The primers for T-Brachyury (T) are: 5'-TATGAGCCTCGAATCCACATAGT -3' (forward), 5'-CCTCGTTCTGATAAGCAGTCAC -3' (reverse). The primers for FOXA2 are: 5'-GGAGCAGCTACTATGCAGAGC -3' (forward), 5'-CGTGTTCATGCCGTTCATCC -3' (reverse). The primers for CD73 are: 5'-TTACACAGGCAATCCACCTTC -3' (forward), 5'-TTACACAGGCAATCCACCT TC -3' (reverse). The primers for CD146 are: 5'-CTGCTGAGTGAACCACAGGA -3' (forward), 5'-CACCTGGCCTGTCTCTTC TC -3' (reverse).

Western Blot Analysis

Protein was isolated from SCAP using CelLytic MT solution (sigma), supplemented with protease inhibitor cocktail (PIC, Promega). 40 ug aliquots of protein were separated by a 7.5% SDS-polyacrylamide (PAGE) gel. The following primary antibodies and reagents were used: rabbit anti-human phosphorylated p65 (S536, cell signaling), rabbit anti-human p65 (Santa Cruz Biotech), mouse anti-human α-tubulin (Santa Cruz Biotech). Detection was performed with using Luminal/Enhancer Solution and Super Signal West Stable Peroxide Solution (Thermo). Blots were then exposed to HyBlot CL autoradiography films (Denville).

Flow Cytometry and Fluorescence-Activated Cell Sorting (FACS)

Cells were digested with trypsin (Gbico) for 2 min at 37°C, neutralized and passed through a 40 µm cell strainer. Then, Cells were washed twice with FACS buffer (PBS, 10 mM EDTA, and 2% FBS) and resuspended at a maximum concentration of 2×10^5 cells per 100 µl. Cells were stained with indicated antibodies for 30 min on ice in dark, washed, and resuspended in PBS. Samples were analyzed on a BD LSR II analyzer or sorted on a BD FACS Aria III. Cell gating was based on comparison with isotype negative controls and single stained controls. Cells were sorted into serum-free DMEM media for gene expression analysis or into complete media for cell culture. Antibodies used include CD34 (PE), CD45 (PerCP), CD51 (PE), CD73 (APC), CD90 (FITC), CD146 (PE) (all from Biolegend).

3. RESULT

3.1 Human ESC aggregates spontaneously differentiate without the feeder cell layer

To induce differentiation of human ESCs, the ESC aggregates were detached by digestion with collegenase IV, and seeded into tissue culture dishes in MSC medium without feeder cells. We found the alp activities of human ESCs decreased dramatically in the following 7 days (Figure 16A). And the expression levels of pluripotent markers, such as NANOG, POU5F1, SOX2, reduced in parallel with the alp activity during human ESC differentiation (Figure 16B). We then examined the expression pattern of germ layer-specific markers. While the expression of PAX6 and FOXA2 slightly increased, the expression of PDGFR-α and T was significantly elevated, indicating the differentiated ESCs are more restricted to mesodermal lineages (Figure 16C). Further, the expression levels of positive and negative MSC markers were assessed after 7 days of differentiation. More than 95% of the derived cells are positive for CD51 and CD90, but negative for CD34 and CD45 (Figure 16D). However, the percentages of CD73-positive cells and CD146-

positive cells are relatively low (Figure 1D). Based on these results, we selected the combination markers of $CD73^+CD90^+CD146^+CD45^-$ to isolate ES-MSCs, excluding CD51 due to its high level of expression at 99% (Figure 16D). We were able to obtain 3.6% $CD73^+CD90^+CD146^+CD45^-$ ES-MSCs of the total differentiated cells from hESCs (Figure 16E).
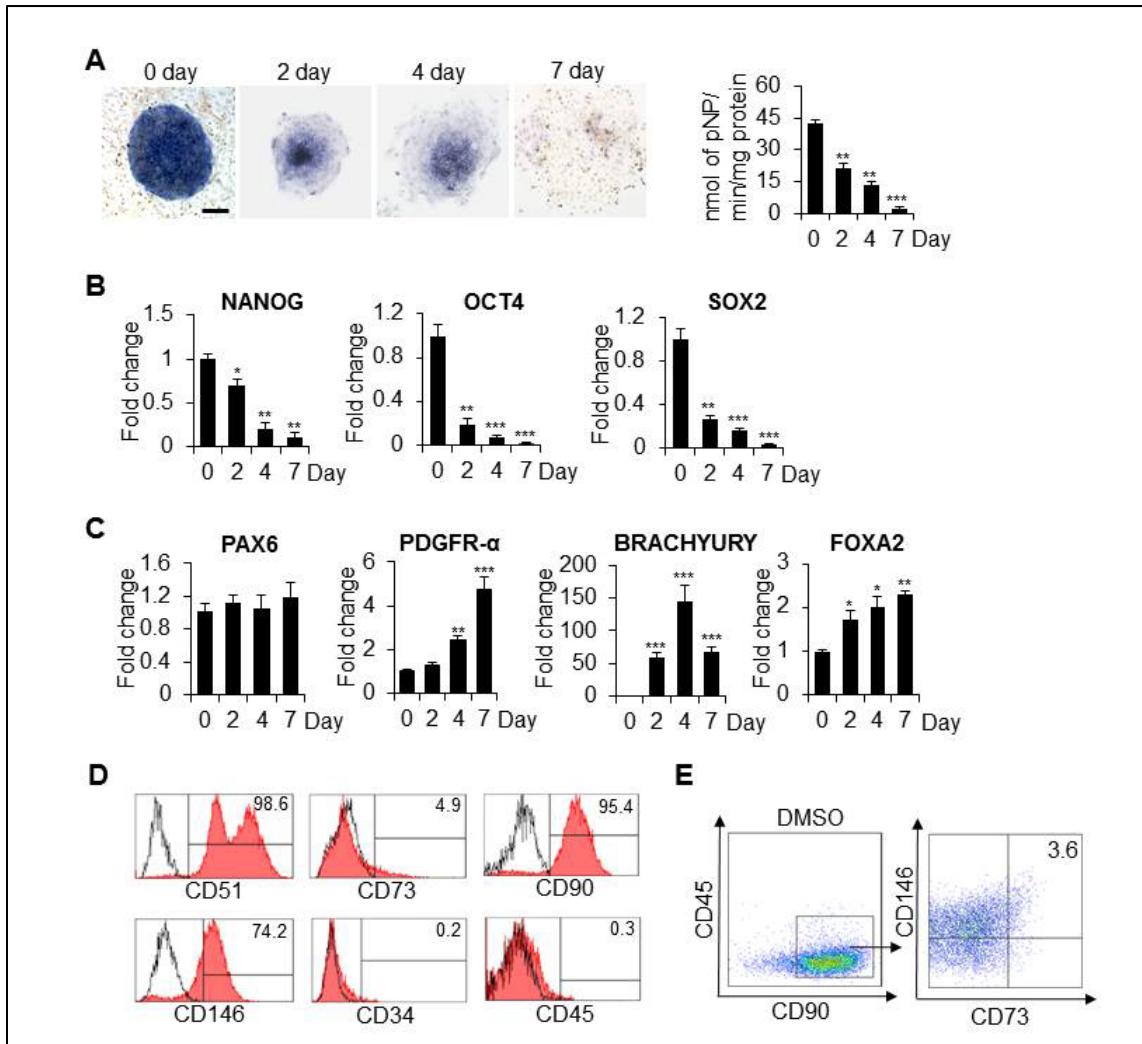
Figure 16. Human ESC aggregates spontaneously differentiate without the feeder cell layer. (A) ALP staining and quantitative ALP activity assay for differentiation of human ESC aggregates at 0, 2, 4, 7 days. Bar indicates 200 μm. (B) RT-qPCR analysis of NANOG, OCT4, POU5F1 (pluripotent markers) expression of human ESC aggregates at 0, 2, 4, 7 days during differentiation. (C) RT-qPCR analysis of PAX6 (ectoderm),

PDGFR-α (mesoderm), T (mesoderm), FOXA2 (endoderm) expression of human ESC aggregates at 0, 2, 4, 7 days during differentiation. (D) Flow cytometry schema of MSC marker expression of cells after 7 days of differentiation. (E) Western blot analysis of p65 and phosphorylated p65 during differentiation of human ESCs at 0, 2, 4, 7 days. * p< 0.05.

To examine the status of the IKK/NF-κB signaling pathway, we evaluated phosphorylated p65 and IκBα during hESC differentiation. Consistent with previous studies[223, 225], we found NFκB signaling was up-regulated upon differentiation of hESCs in the first 4 days of differentiation. Interestingly, it decreased to basal level on day 7 (Figure 17A, 17B). In contrast, the components of non-canonical NF-κB signaling, p100 and p52[226], were minimally affected (Figure 17C).
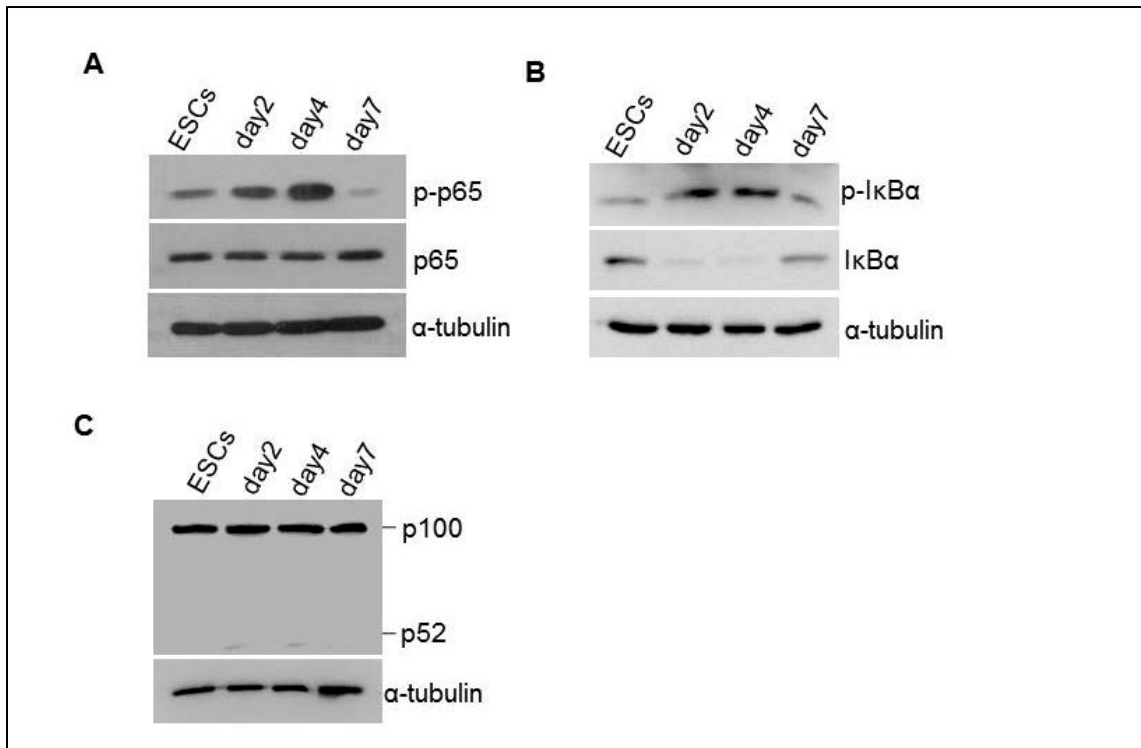
Figure 17. Activity of Canonical and non-canonical NF-κB signaling pathway during human ESC aggregates spontaneous differentiation without the feeder cell layer. (A) Western blot of p65 and phosphorylated p65 at 0, 2, 4, and 7 days of hESC differentiation. (B) Western blot of IκBα and

phosphorylated IκBα at 0, 2, 4, and 7 days of hESC differentiation. (C) Western blot of p100 and p52 at 0, 2, 4, and 7 days of hESC differentiation.

3.2 Inhibition of NFκB signaling promotes human ESC differentiation and enhances MSC marker expression

To investigate if inhibition of NFκB signaling promotes human ESC differentiation into MSCs, human ESC colonies were plated overnight and the exposed to 1μM IKK-beta inhibitor (IKKi) for 3 days (d1-d4) (Figure 18A, 18B). The Alp activity of the cells was reduced by treatment with IKKi (Figure 18C). Accordingly, inhibition of NFκB signaling promoted loss of pluripotent marker expression during human ESC differentiation (Figure 18D). Germ layer marker examination revealed that mesodermal markers *PDGFR-α* and *BRACHYURY* were found to be significantly upregulated as a result of treatment at day 2 and 4 of hESC differentiation (Figure 18E). The endodermal marker *FOXA2* was also upregulated at day 4 (Figure 18E). In contrast, the ectodermal marker *PAX6* gene expression remained unchanged (Figure 18E).
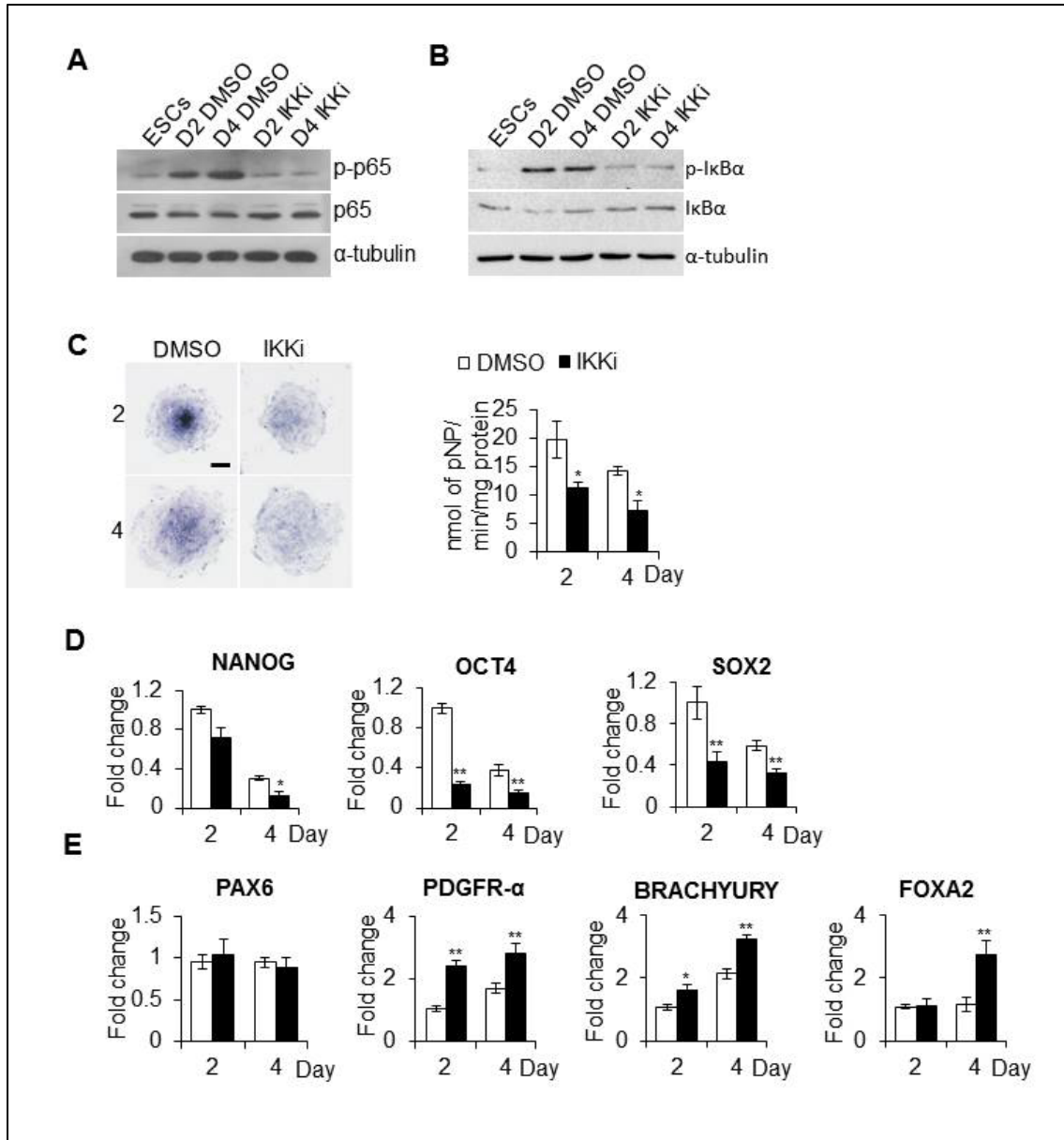
Figure 18. Inhibition of NFκB signaling promotes human ESC differentiation to mesoderm and endoderm.

(A) Western blot of p65 and phosphorylated p65 at 0, 2, and 4 days of hESC differentiation in presence or absence of IKKi. (B) Western blot of IκBα and phosphorylated IκBα at 0, 2, and 4 days of hESC differentiation in presence or absence of IKKi.. (C) ALP staining and quantitative ALP activity assay at 2 and 4 days. Bar indicates 200 μm. (D) qRT-PCR results of NANOG, OCT4, POU5F1 at 2 and 4 days in presence or absence of IKKi.. (E) qRT-PCR results of PAX6 (ectoderm), PDGFR-α (mesoderm), BRACHYURY

(mesoderm), and FOXA2 (endoderm) at 2 and 4 days in presence or absence of IKKi.

MSC marker assessment showed that CD73 and CD146 were significantly upregulated following 4 days of IKKi treatment (Figure 19A); such upregulation was further confirmed by flow cytometry analysis (Figure 19B). IKKi treatment also generated a three-fold increase in the proportion of $CD73^+CD90^+CD146^+CD45^-$ ES-MSCs in the total differentiated hESC population, as compared to vehicle control treatment (Figure 19C). These data indicate that inhibition of the NF-κB signaling pathway enhances hESC differentiation into the MSC lineage.
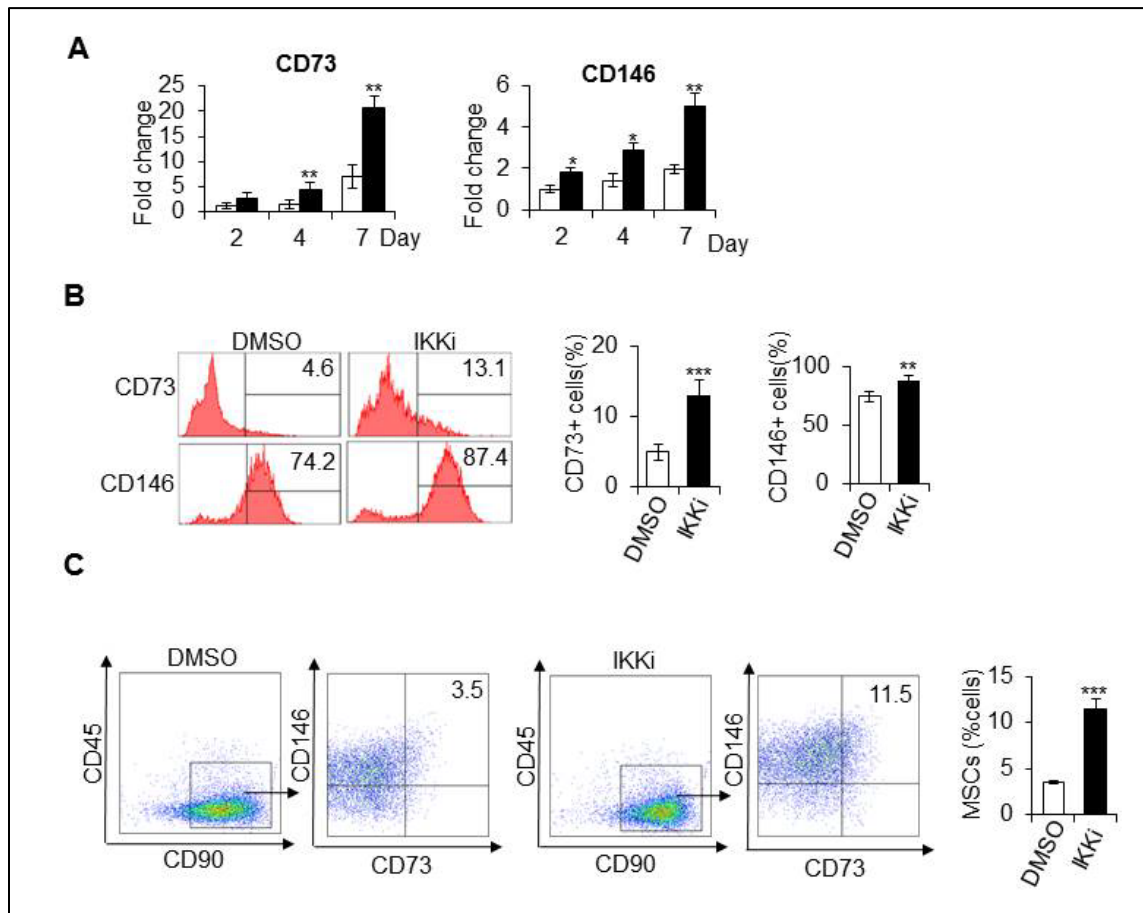
Figure 19. Inhibition of NFκB signaling during human ESC differentiation enhanced MSC marker expression. (A) qRT-PCR results of CD73 and CD146 at 2, 4, and 7 days. (B) Flow cytometry analysis of cells

with or without IKKi treatment examining MSC marker expression. (C) Four-color flow cytometry analysis for CD45, CD90, CD73, CD146 expression to isolate CD73+CD90+CD146+CD45- ES-MSCs following 7 days of hESC differentiation with or without IKKi. Proportions of CD73+CD90+CD146+CD45- ES-MSCs generated. Three independent experiments were performed.

3.3 IKKi-treated cells showed enhanced osteogenic and chondrogenic potentials

To determine the further differentiation potential of derived cells, the cells were seed into 12-well plates and cultured in osteogenic induction (OI) medium, chondrogenic induction (CI) medium, and adipogenic induction (AI) medium, respectively. We found that the IKKi treated cells showed stronger alp activity and higher expression levels of osteogenic markers, such as RUNX2 and BGLAP (Figure 20A-20C) after 7 days of OI. The mineralization was also enhanced by treatment with IKKi, as assessed by Alizarin Red staining (Figure 20D). Similarly, the IKKi treated cells also exhibited stronger chondrogenic potential, as determined by Alcian blue staining and expression of chondrogenic markers, such as SOX9 and COL2A1 (Figure 20D, 20E). However, despite our several trails, we failed to generate lipid deposits with AI for 4 weeks in these cells (data not shown). Collectively, the derived cells treated with IKKi have higher percentage of CD73-positive cells and CD146-positive cells, and possess stronger osteogenic and chondrogenic differentiation potential.
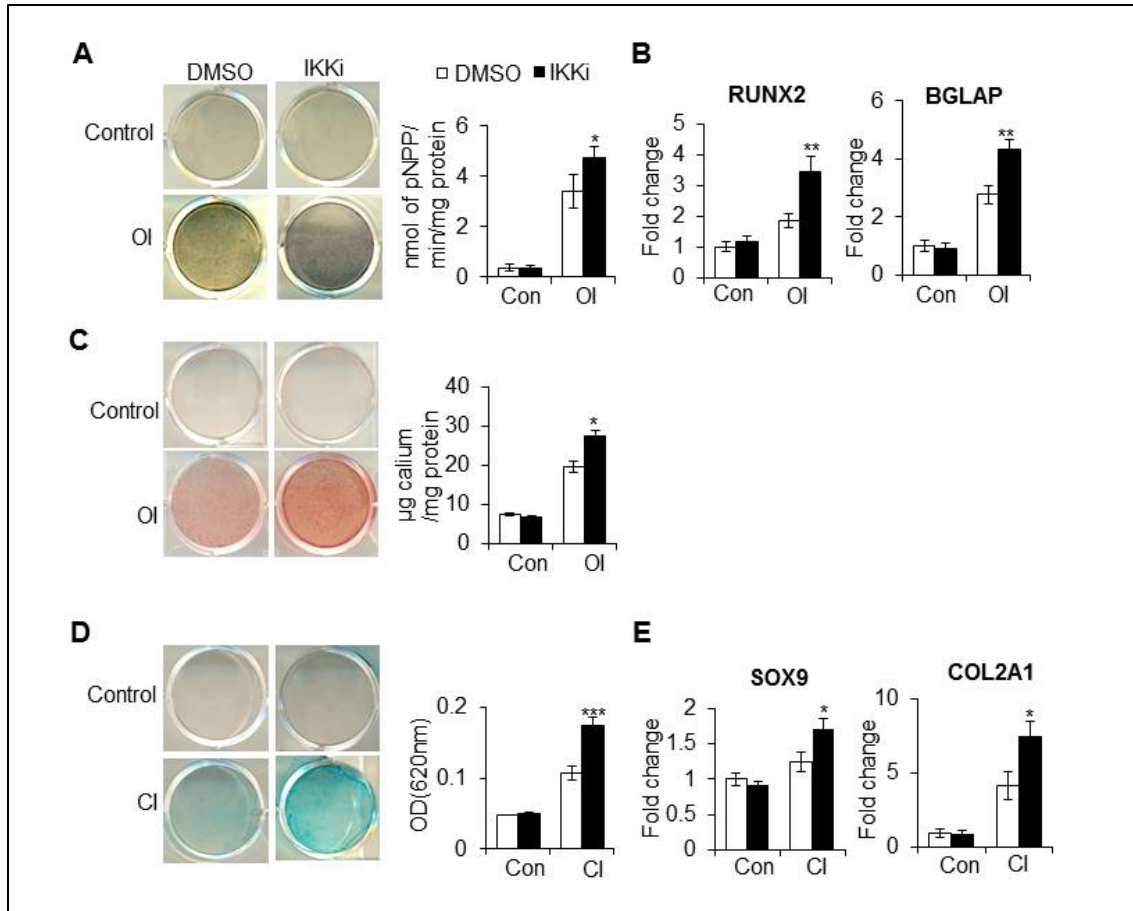
Figure 20. IKKi-treated cells showed enhanced osteogenic and chondrogenic potentials. (A) ALP staining and quantitative ALP activity assay for derived cells with IKKi or vehicle treatment after 14 days of osteogenic induction (OI). (B) RT-qPCR analysis of RUNX2 and BGLAP (osteogenic markers) expression of derived cells after 7 days of OI. (C) ARS staining and quantification of derived cells with DMSO or IKKi treatment after 21 days of OI. (D) Alcian blue staining and quantification of derived cells with DMSO or IKKi treatment after 21 days of chondrogenic induction (CI). (E) RT-qPCR analysis of SOX2 and COL2a1 (chondrogenic markers) expression of derived cells after 14 days of CI.

3.4 Inhibition of NF-κB signaling by p65 depletion promotes hESC differentiation and enhances MSC marker expression

To further confirm that inhibition of NF-κB promotes hESC differentiation, we constructed a specific shRNA targeting p65 targeting the 3' untranslated region, to exclude the possibility that the observed effect is due to off-target effects of IKKi. The knockdown efficacy was confirmed by RT-PCR (Figure 21A). The depletion of p65 in hESCs was confirmed by significantly suppressed expression of NF-κB target genes, including cIAP2, IL-6, and IL-8 (Figure 21B). Consistently, depletion of p65 promoted the loss of alp activity and pluripotent markers (Figure 21C). Consistent with our IKKi treatment results, p65 deficiency also led to the decline of ALP activity at days 2 and 4 of the differentiation process (Figure 21D). Furthermore, RT-qPCR showed accelerated loss of the pluripotent markers (NANOG, OCT4, and SOX2) during hESC differentiation (Figure 21D). Similar to IKKi treatment, the endodermal marker FOXA2 and two mesodermal markers PDGFR-α and BRACHYURY were found to be significantly elevated, while the ectodermal marker PAX6 remained unchanged (Figure 21E).

We also evaluated MSC marker expression in p65-depleted ESC aggregates after 7 days of differentiation, and found that CD73 and CD146 were significantly upregulated The in a time-dependent manner with the most drastic differences at day 7 of hESC differentiation (Figure 22A); such upregulation was further confirmed by flow cytometry analysis (Figure 22B). Finally, similar to IKKi treatment, NF-κB inhibition by p65 depletion increased the proportion of CD73+CD90+CD146+CD45- MSCs by approximately three-fold (Figure 22C). These data indicate that inhibition of the NF-κB signaling pathway enhances hESC differentiation into the MSC lineage.
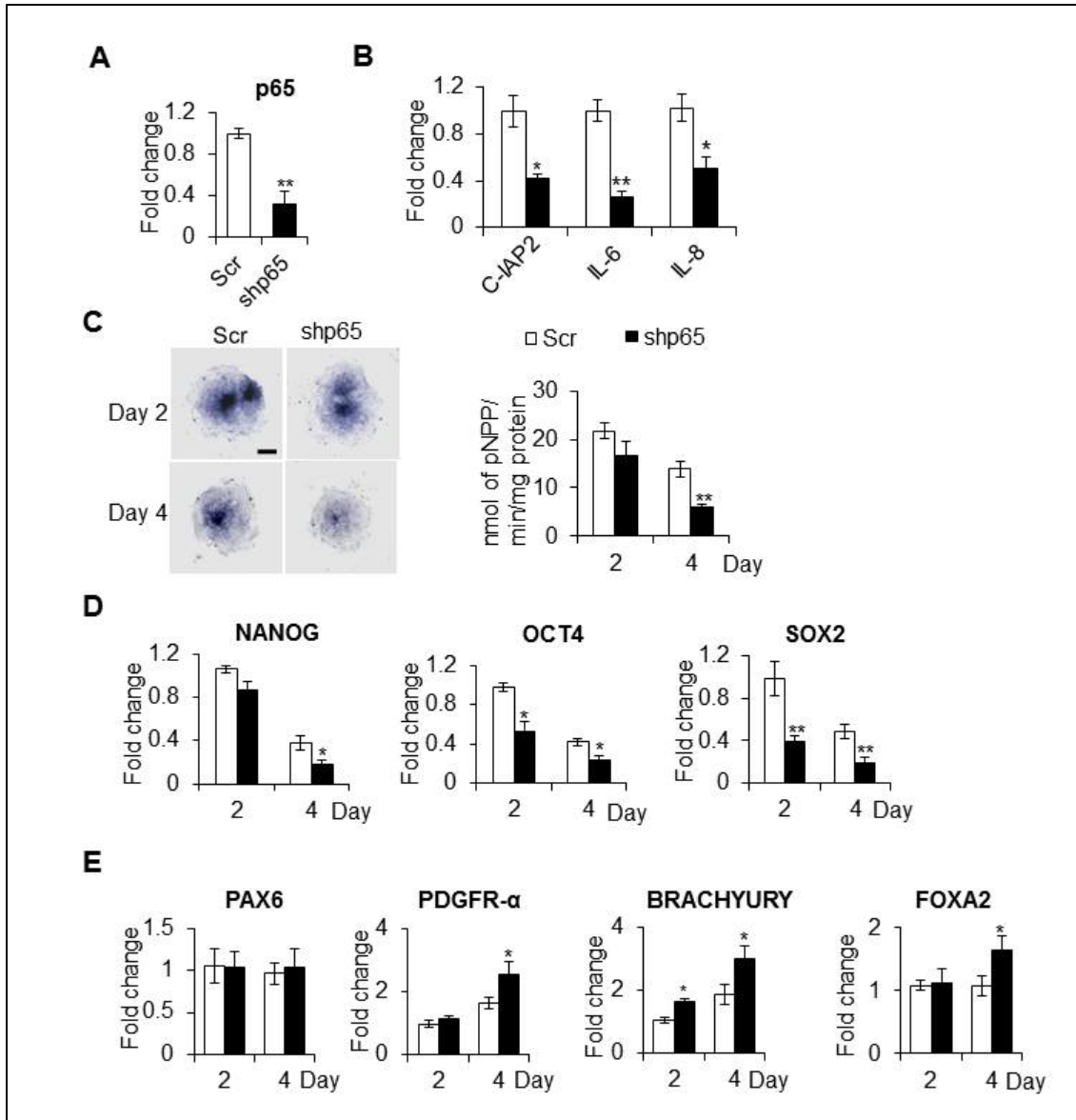
**Figure 21. Inhibition of NF-κB signaling by p65 depletion promotes hESC differentiation.** (A) RT-qPCR analysis of p65 in Scr or shp65 transfected human ESC aggregates after 7 days of differentiation. (B) RT-qPCR results of NF-κB target genes (cIAP2, IL-6, IL-8) in Scr or shp65 transduced hESCs at 2, 4 days. (C) ALP staining and quantitative ALP activity assay at 2 and 4 days. Bar indicates 200 μm. (D) qRT-PCR results of NANOG, OCT4, POU5F1 at 2 and 4 days. (E) qRT-PCR results of PAX6 (ectoderm), PDGFR-α (mesoderm), BRACHYURY (mesoderm), and FOXA2 (endoderm) at 2 and 4 days.
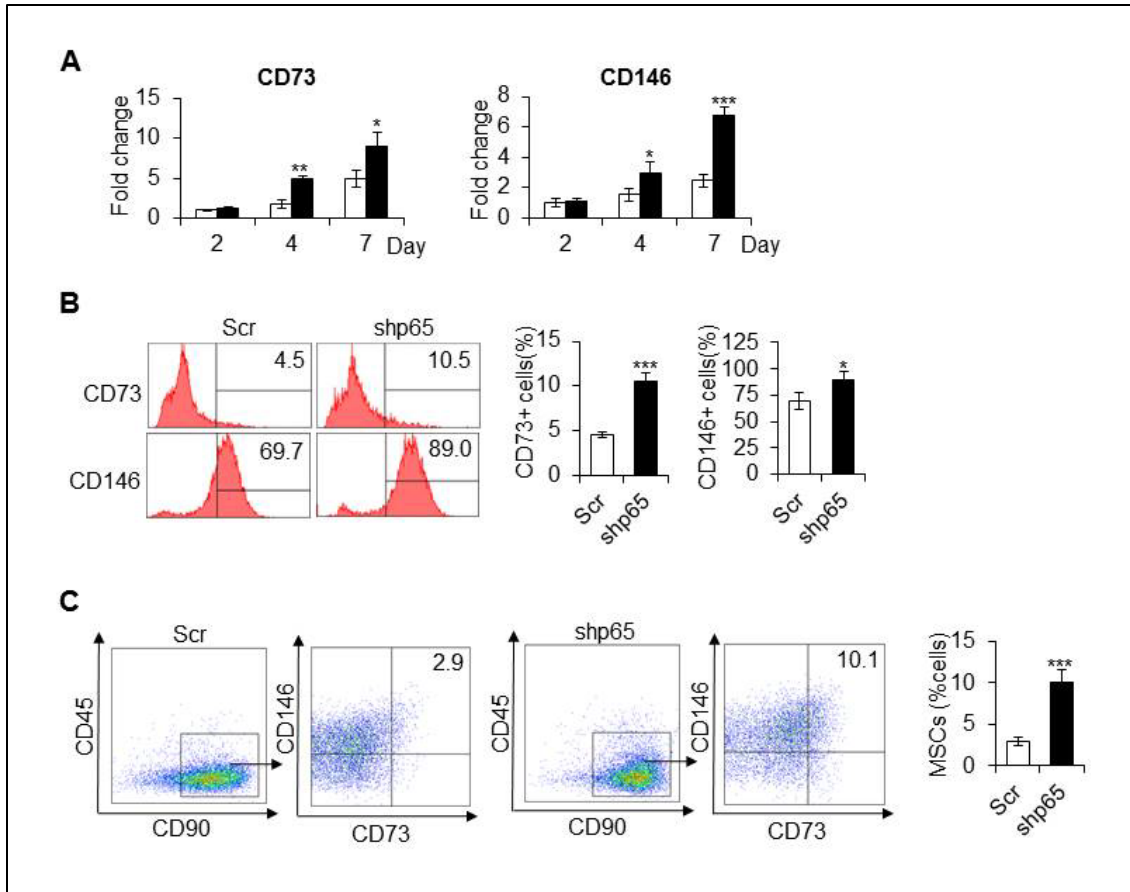
Figure 22. Inhibition of NF-κB signaling by p65 depletion enhances MSC marker expression. (A) qRT-PCR results of CD73 and CD146 at 2, 4, 7 days. (B) Flow cytometry analysis of cells expressing MSC markers. (C) Four-color flow cytometry analysis for CD45, CD90, CD73, CD146 to isolate CD73+CD90+CD146+CD45- ES-MSCs following 7 days of hESC differentiation. Three independent experiments were performed.

3.5 Purified MSCs show similar differentiation potential in vitro and form ectopic bone in scaffolds in vivo

We next asked whether the enhanced differentiation potential of the derived cells was because there are more MSCs of the total population, or because the derived MSCs have stronger differentiation potential. The CD73+CD90+CD146+CD45- cells were sorted after 2~3 passages

for expansion, and differentiation assays were performed. Interestingly, we found that the derived MSCs with DMSO or IKKi treatment displayed similar alp activity, mineralization, and similar pattern of expression of osteogenic markers with OI (Figure 23A-23C). And no significant differences in chondrogenic potential were observed in sorted MSCs treated with DMSO or IKKi, as determined by Alcian blue staining and expression of SOX9 and COL2A1 (Figure 23D, 23E). Similar lipid deposits were detected and quantified by Oil Red O staining after 3 weeks of AI (Figure 23F). There is no significant difference in expression of adipogenic markers, such as PPAR-γ and LPL (Figure 23G). Taken together, treatment with IKKi increased the MSC yield from human ESCs, but did not affect the differentiation potential of the derived MSCs.
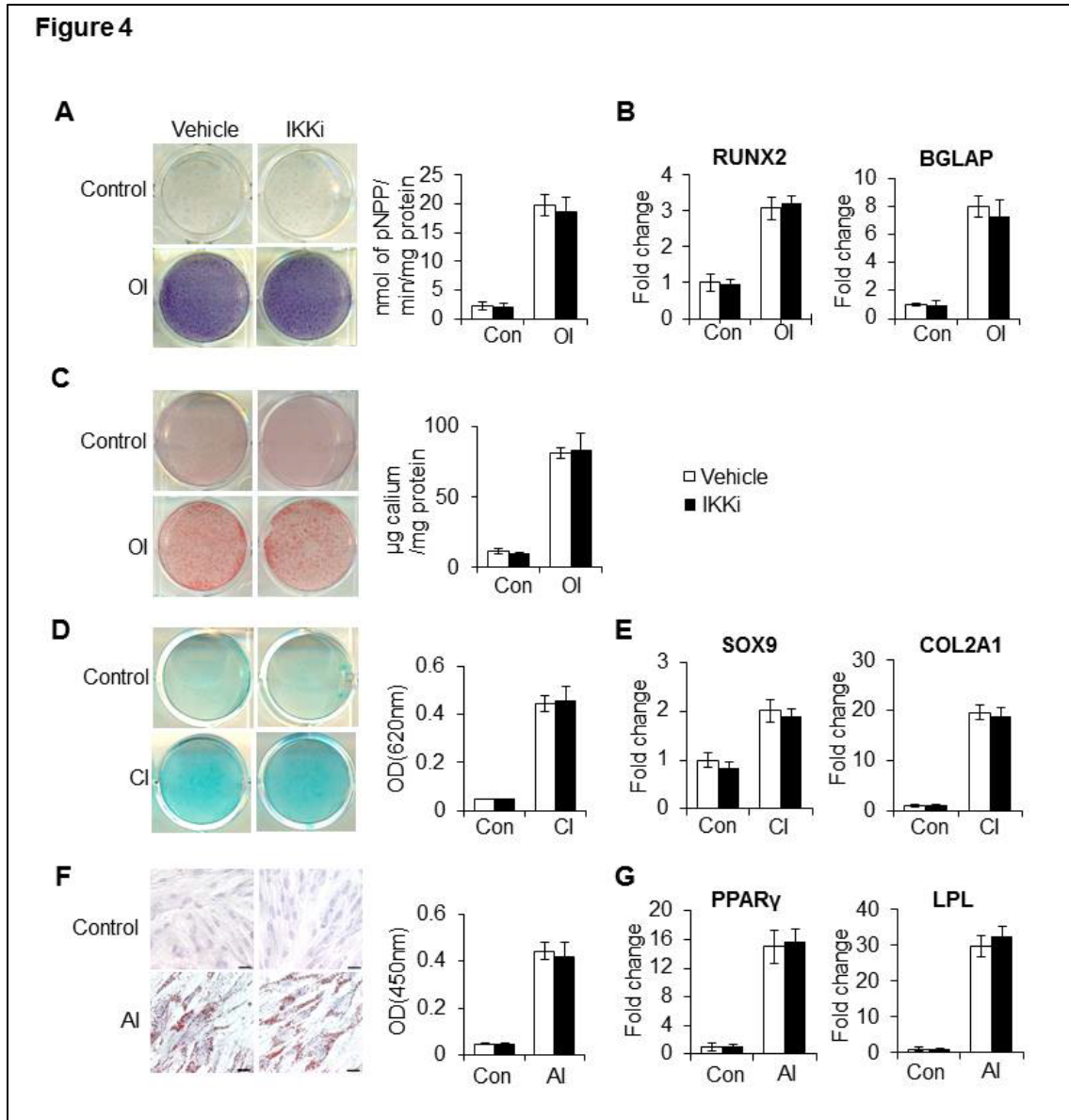
Figure 23. Purified MSCs show similar differentiation potential in vitro. (A) ALP staining and quantitative

ALP activity assay for sorted MSCs from DMSO or IKKi treated human ESC aggregates after 14 days of OI.

(C) RT-qPCR analysis of RUNX2 and BGLAP (osteogenic markers) expression of sorted MSCs after 7 days of

OI. (D) ARS staining and quantification of sorted MSCs after 21 days of OI. (E) Alcian blue staining and

quantification of sorted MSCs from DMSO or IKKi treated human ESC aggregates after 21 days of CI. (F) RT-

qPCR analysis of SOX2 and COL2a1 (chondrogenic markers) expression of sorted MSCs after 14 days of CI.

(G) Oil Red O staining and quantification of sorted MSCs from DMSO or IKKi treated human ESC aggregates

80

after 21 days of adipogenic induction (AI). Bar indicates 200 μm. (H) RT-qPCR analysis of PPAR-γ and LPL (adipogenic markers) expression of sorted MSCs after 14 days of AI.

Importantly, both populations were able to form bone in vivo (Figure 24A, 24B). In order to confirm that the ectopic bone was formed by human cells, we examined the expression of human osteocalcin in these mineralized tissues. Osteocytes and lining osteoblasts were positively stained in both groups (figure 24C). In addition, both sorted MSCs showed a normal male karyotpye (Figure 24D). These results indicate that the derived MSCs with IKKi treatment have the potential to be used in bone repair. Our results therefore demonstrate that treatment with IKKi increases MSC yield without causing chromosomal abnormality and negatively affecting differentiation potential, suggesting that MSCs derived with hESCs with IKKi pretreatment may be used in regenerative medicine.
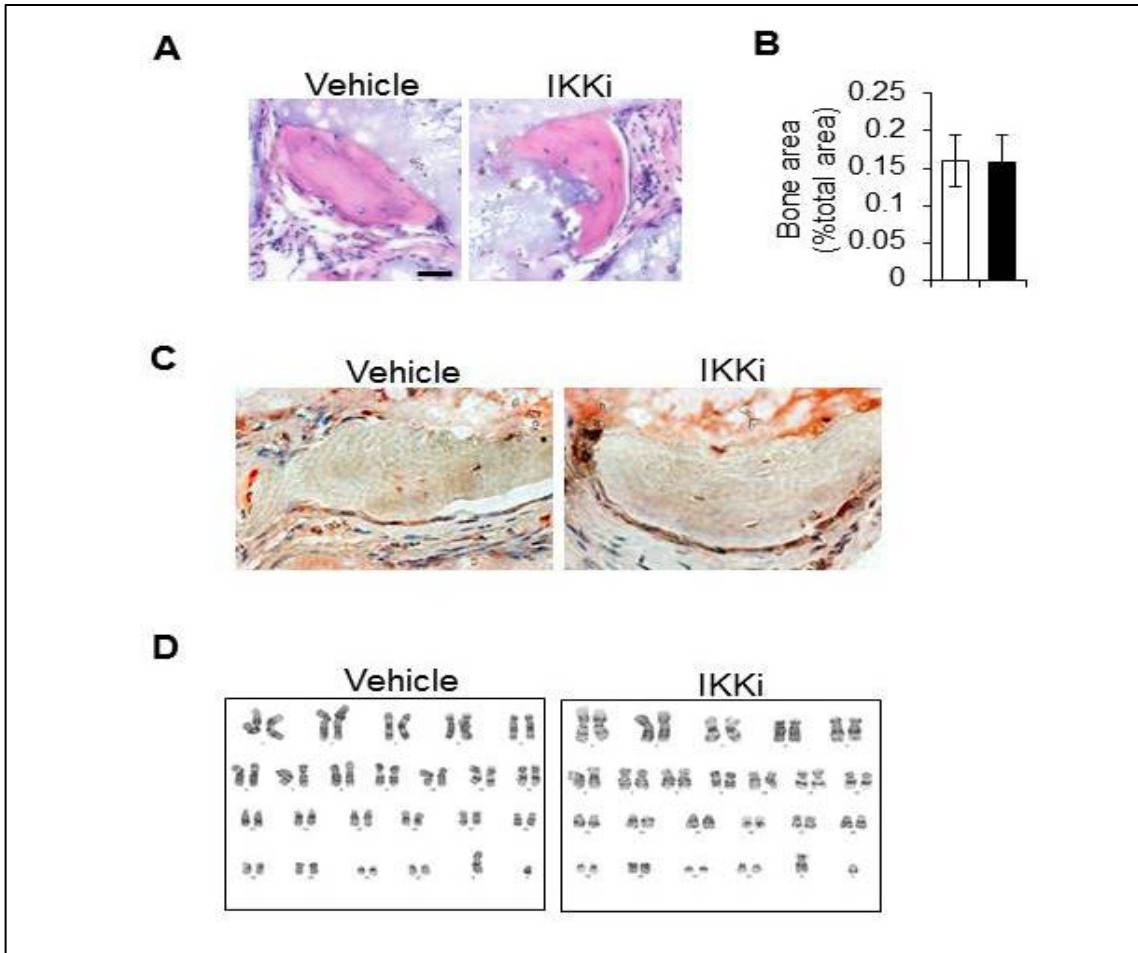
Figure 24. Purified MSCs form ectopic bone in scaffolds in vivo, and show a normal male karyotpye.

(A) Bone formation *in vivo* by sorted ES-MSCs derived from IKKi-treated hESCs in 6 immunocompromised mice. (B) Immunostaining of human osteocalcin the ectopic bone. (C) Karyotype analysis of sorted ES-MSCs derived from IKKi-treated hESCs. For all *in-vitro* experiments, three independent experiments were performed.

4. DISCUSSION

Human ESCs are derived from the inner cell mass of the early embryo, and are characterized by their immortality and the potential to give rise to a large variety of cells and tissues from all 3 germ layers, including MSCs[191, 227]. However, the plasticity that permits ESCs to become any somatic

cell type also makes them hard to control, and transplantation of ESCs may lead to generation of undesired cell types and tissues, including teratomas[195, 228, 229]. Thus, a two-step differentiation is necessary for ESC-based regenerative medicine: 1) lineage-specific differentiation of human ESCs is induced in vitro, 2) purified progenitors are transplanted into the patient for further differentiation[230]. To achieve this, it is essential to understand the molecular regulation of ESC differentiation and to direct the lineage-specific development of these cells along specific pathways.

NFκB signaling is associated with ESC self-renewal and differentiation [231]. A low but detectable level of NFκB activity was found in both mouse and human ESCs [221, 232]. However, the role of NFκB in pluripotency maintenance is different in mouse ESCs and human ESCs. In mouse ESCs, Nanog binds to NFκB proteins, inhibits NFκB activity and cooperates with Stat3 to maintain pluripotency[232]. In addition, it recently defined p65 as a target gene of miR-290, an ESC-specific mircoRNA cluster[233]. NFκB inhibition increases expression of pluripotency markers, while forced expression of p65 causes loss of pluripotency, and promotes differentiation in mouse ESCs[233, 234]. In human ESCs, inhibition of NFκB leads to massive cell differentiation within ESC colonies, as well as significant cell death [221, 222]. Regard to ESC differentiation, knockdown of IKK1/2 promotes differentiation of mouse ESCs into neuroectoderm at the expense of mesoderm [235], indicating a regulatory role of NFκB in ESC differentiation. In this study, to induce mesenchymal differentiation, human ESC aggregates were cultured in monolayer without feeder cells in presence of FBS. Under this condition, human ESCs differentiate rapidly as shown in Figure 1. However, the expression of PAX6 did not up-regulated during the process, which suggests the differentiation to ectoderm is blocked or at a very low level.

Our findings show that inhibition of NFκB signaling enhanced human ESC differentiation into mesenchymal lineages. However, the role of NFκB in mesodermal lineage specification of human ESCs is still elusive to us. It is reported that inhibition of canonical NFκB signaling during EB formation resulted in suppression of differentiation toward mesoderm, as shown by diminished induction of T gene[221]. A recent study showed that TNFα activates the Notch and NF-κB signaling pathways to establish hematopoietic stem cells fate during embryonic development of zebrafish[236], which suggests NFκB is required for emergence of mesodermal lineages, at least in part. In our study, the expression levels of common mesodermal markers are differential. It is possible that inhibition of NFκB promotes mesenchymal differentiation of human ESCs, but suppresses other mesodermal lineages, such as HSCs.

In our microarray analysis, the result suggests a cross-talk among NFκB, TGF-β, and Wnt signaling during human ESC differentiation. Kassem et al. reported that inhibition of TGF-β/Activin/Nodal signaling pathway differentiation of hESCs into mesenchymal progenitors[237]. In addition, TGFβ/activin/nodal signaling is necessary for the maintenance of pluripotency in human embryonic stem cells [238, 239]. Consistently, as IKKi treatment enhances mesenchymal differentiation of human ESCs, many TGF-β target genes are down-regulated (72% in Table S2). Combination treatment with inhibitors or activators of different signaling pathway may be used to direct the differentiation into MSCs in the future.

The differentiation potential of MSCs is essential for application in tissue engineering. In our study, the derived cells with IKKi treatment possess stronger osteogenic and chondrogenic differentiation potential. We further assessed the differentiation potential of purified MSCs. As expected, the purified MSCs from DMSO or IKKi treated group showed similar differentiation potential to osteogenic, chondrogenic, and adipogenic lineage. Importantly, the sorted MSCs are able to

generate mineralized bone tissue in vivo. Together with other studies[192, 194, 240, 241], we demonstrated that human ESCs are a reliable resource to generate functional MSCs. The induced pluripotent stem cells (iPSCs) provide powerful new tools to develop patient-specific pluripotent stem cells [242]. MSCs have already been derived from iPSCs [243, 244], and used for bone repair in animal models [245]. The role of NFκB in iPSC differentiation may be investigated in the further, and our method could facilitate studies on derivation of MSCs from iPSCs.

In summary, we found that inhibition of NFκB signaling promotes human ESCs differentiation into mesenchymal stem cells. Further, inhibition of NFκB significantly increased the yield of MSCs from human ESCs, and the purified MSCs showed multipotency in vitro. Thus, we provide a novel and efficient method to derive functional MSCs from human ESCs, which hold the promise for regenerative medicine in the future.

5. OUTLOOK

MSCs are characterized by the self-renewal capacity and differentiation potential into multiple tissues, including osteoblasts and adipocytes. The differentiation of MSCs contributes significantly to the maintenance of bone mass during bone remodeling. In addition, MSCs represent an important paradigm of cell-based therapy for a variety of diseases, because of their multipotent differentiation capacities, immune privilege, and anti-inflammation effects.

5.1 The identification of MSCs

Although all definition of stem cells is functional in nature, the use of the term MSC may often indistinctively refer to both in vivo precursors and their expanded cells in vitro[5]. To avoid misunderstandings at work, International Society for Cellular Therapy (ISCT) suggested to restrict

the term stem cell to in vivo precursor cells, and to use the name multipotent mesenchymal stromal cells for their cultured progeny [246]. Accordingly, ISCT has issued a statement on minimal criteria for defining multipotent mesenchymal stromal cells in vitro [10]. First, they must be plastic-adherent when maintained in standard culture conditions. Secondly, they must express CD73, CD105, and CD90 and lack expression of CD45, CD34, CD14 or CD11b, CD79a or CD19, and HLA-DR surface molecules. Thirdly, they must be capable of differentiating into osteoblasts, adipocytes, and chondrocytes in vitro [10]. Furthermore, a functional assay defines multipotent mesenchymal stromal cells by generation of a heterotopic ossicle (bone marrow organ) upon transplantation in vivo [120, 247]. According to these criteria, multipotent mesenchymal stromal cells have been isolated from various postnatal tissues, including bone marrow, umbilical cord blood [248], adipose tissue [249], muscle [250] and so on.

However, questions have been raised about the existence of a common mesenchymal progenitor. First, the developmental origin of mesenchymal tissues is not uniform. For example, bone and muscle derive from different precursors during embryonic development [9]. Secondly, the heterogeneity of mesenchymal stromal cells derived from different tissues has been observed in proliferation rate, mutlipotency in vitro, and the ability to generate ectopic bone [7, 8]. In addition, whether MSCs in different tissues in vivo give rise to the same lineages has not been well demonstrated [5]. In other words, the "inducible" multipotency in multipotent mesenchymal stromal cells does not mean that their precursor cells are also "determined" to spontaneous differentiation into all the skeletal tissues [6].

All these considerations demand an unequivocal identification of MSCs in vivo, and a lineage tracing approach to study their lineage specification. However, identification of MSC in vivo has been long hindered, because of their low frequency in bone marrow and the lack of exclusive

surface markers [120]. Isolation of MSCs from mouse bone marrow largely depends on their plastic adherent properties [251]. Although the isolated cells are capable of differentiating into osteoblasts, adipocytes, and chondrocytes in vitro, they can be contaminated by hematopoietic cells, such as macrophages [252]. In recent years, intensive research has tried to unveil the nature and function of MSCs in vivo, and different markers have been used to identify and isolate purified MSCs. However, there are no suitable markers that allow us to establish a hierarchical relationship among MSCs, committed progenitors, and terminal differentiated cells.

5.2 The interaction between epigenetic regulations

Eukaryotic chromatins are organized in euchromatin (active) and heterochromatin (inactive) and forms. Histone methylation marks are key in defining these functional states, particularly in promoter regions. Physically, the lysine residues in histone tails are extremely close to each other. However, during MSC differentiation, the cross-talk among the histone methylation marks is still elusive to us, and should be take into account in future studies. For instance, the euchromatic mark H3K4me3 prevents tri-methylation of H3K9 by SETDB1[253]. Conversely, the heterochromatin mark H3K9me3 prevents mono-methylation H3K4 by SET7[254]. Notably, the cross-talk among histone methylation marks is not restricted in methylation at lysine residues. More information can be found in previous reviews [64, 255-257].

Another question we need to pay attention to is that the histone methylation status is established by the opposite functions of KMTs and KDMs. Both KMTs and KDMs may take part in MSC differentiation at the same time. It is plausible that both methylation and demethylation happens in the promoters of different lineage-specific genes. For instance, EZH2 and KDM6A, which both target to H3K27, act as an epigenetic switch to regulate MSC lineage specification[71]. However,

the methyltransferase activity of SET domain-containing KMTs seems to be specific to one site, while JmjC domain-containing KDMs exhibit more redundancy and tissue specificity.

Interestingly, the KMTs and KDMs could interact with each other. For instance, JMJ is shown to be required for efficient binding of PRC2 complex[258]. A study on mouse embryonic stem cells revealed that Kdm4c could interact with the components of PRC2 and assist Ezh2 to fully repress target genes[258]. In addition, KDM5C, a H3K4 demethylase, could interact with H3K9 methylases, which may couple H3K9 methylation to H3K4 demethylation[90]. The interaction may also be critical in MSC differentiation, especially for the initiation of lineage determination.

5.3 The association between self-renewal and lineage specification of MSCs

The idea that aged MSCs are of reduced osteogenesis and enhanced adipogenesis potential has been long implicated, as aging induces bone loss and adipose accumulation in both mice and human. Indeed, several studies support this idea. For instance, conditional of Foxp1 in MSCs led to impaired MSC self-renewal capacity and premature aging characteristics in mice, such as decreased bone mass, increased bone marrow adiposity[259]. Our study also showed KDM4B was required for self-renewal of MSCs, and promoted osteogenesis at expense of adipogenesis. However, whether natural aging process without gene edition directly induced reduced osteogenesis and enhanced adipogenesis potential of MSCs is still in debates, as some studies reported MSCs from older donors exhibited no difference or even a decrease in differentiation potential to adipogenic lineage[260-262].

The transcription factors in self-renewal can also affect differentiation of MSCs. As mentioned above, NANOG and SOX2 have been found to promote self-renewal of MSCs and to be required for inhibition of spontaneous differentiation in MSCs. However, the impact of their expression

levels on differentiation potential is distinct. Knockdown Nanog at early passage inhibited the differentiation potential of all the three lineages (osteoblasts, chondrocytes, and adipocytes)[263]. Overexpression of SOX2 inhibited osteogenesis and enhanced adipogenesis, and knockout of Sox2 enhanced osteogenesis and inhibited adipogenesis of MSCs[130].

5.4 Clinical applications of MSCs

To date, MSCs has been used in about 350 clinical trials for the treatment of various diseases, including osteogenesis imperfecta, bone and cartilage defects, heamtopoietic stem cell transplantation, chronic graft versus host disease, myocardial infarction, and so on[264, 265]. Both allogeneic and autologous MSCs have been used in these clinic trails. Although some studies showed disappointing results, several trials have suggested MSCs is promising for clinical use. The studies have also raised the concern about the immune property of MSCs. Due to the lack of the expression of the major histocompatibility complex class II and low expression of major histocompatibility complex class I, MSCs was initially considered to be immunoprivileged. However, recent studies revealed allogeneic MSCs may stimulate innate immune responses[266]. And allogeneic MSCs can be targeted by activated NK cells and induce immune memory, which led to the rejection of allogeneic MSC grafts[267, 268].

Taken together, MSCs have generated a great amount of enthusiasm over the past decade for regenerative medicine and other stem cell based therapies. In this manuscript, we revealed the critical role of histone demethylase KDM4B in regulation of cell fate decision and self-renewal of MSCs, provided new insights into the role of NF-κB in mesenchymal lineage specification during hESC differentiation, and described a novel efficient method to derive MSCs from human ESCs,

and. These finding may facilitate the prevention and therapy of osteoporosis, and also be used in

MSC-based bone regeneration.

6. REFERENCE

1. Masi, L. Epidemiology of osteoporosis. *Clinical Cases in Mineral and Bone Metabolism* **5**, 11-13 (2008).

2. Kanis, J.A. *et al.* Assessment of fracture risk. *Osteoporosis International* **16**, 581-589 (2005).

3. Riggs, B.L., Khosla, S. & Melton III, L.J. Sex steroids and the construction and conservation of the adult skeleton. *Endocrine reviews* **23**, 279-302 (2002).

4. Garnero, P., Sornay-Rendu, E., Chapuy, M.-C. & Delmas, P.D. Increased bone turnover in late postmenopausal women is a major determinant of osteoporosis. *Journal of Bone and Mineral Research* **11**, 337-349 (1996).

5. Nombela-Arrieta, C., Ritz, J. & Silberstein, L.E. The elusive nature and function of mesenchymal stem cells. *Nature reviews. Molecular cell biology* **12**, 126-131 (2011).

6. Kassem, M. & Bianco, P. Skeletal stem cells in space and time. *Cell* **160**, 17-19 (2015).

7. Yoshimura, H. *et al.* Comparison of rat mesenchymal stem cells derived from bone marrow, synovium, periosteum, adipose tissue, and muscle. *Cell and tissue research* **327**, 449-462 (2007).

8. Kern, S., Eichler, H., Stoeve, J., Kluter, H. & Bieback, K. Comparative analysis of mesenchymal stem cells from bone marrow, umbilical cord blood, or adipose tissue. *Stem cells* **24**, 1294-1301 (2006).

9. Buckingham, M. *et al.* The formation of skeletal muscle: from somite to limb. *J Anat* **202**, 59-68 (2003).

10.   Dominici, M. *et al.* Minimal criteria for defining multipotent mesenchymal stromal cells. The International Society for Cellular Therapy position statement. *Cytotherapy* **8**, 315-317 (2006).

11.   Chen, J.-Y., Mou, X.-Z., Du, X.-C. & Xiang, C. Comparative analysis of biological characteristics of adult mesenchymal stem cells with different tissue origins. *Asian Pacific Journal of Tropical Medicine* **8**, 739-746 (2015).

12.   Mendez-Ferrer, S. *et al.* Mesenchymal and haematopoietic stem cells form a unique bone marrow niche. *Nature* **466**, 829-834 (2010).

13.   Morikawa, S. *et al.* Prospective identification, isolation, and systemic transplantation of multipotent mesenchymal stem cells in murine bone marrow. *The Journal of experimental medicine* **206**, 2483-2496 (2009).

14.   Houlihan, D.D. *et al.* Isolation of mouse mesenchymal stem cells on the basis of expression of Sca-1 and PDGFR-alpha. *Nature protocols* **7**, 2103-2111 (2012).

15.   Zhou, B.O., Yue, R., Murphy, M.M., Peyer, J.G. & Morrison, S.J. Leptin-receptor-expressing mesenchymal stromal cells represent the main source of bone formed by adult bone marrow. *Cell stem cell* **15**, 154-168 (2014).

16.   James, A.W. Review of Signaling Pathways Governing MSC Osteogenic and Adipogenic Differentiation. *Scientifica* **2013**, 684736 (2013).

17.   Neve, A., Corrado, A. & Cantatore, F.P. Osteoblast physiology in normal and pathological conditions. *Cell and tissue research* **343**, 289-302 (2011).

18.   Ali, A.T., Hochfeld, W.E., Myburgh, R. & Pepper, M.S. Adipocyte and adipogenesis. *European journal of cell biology* **92**, 229-236 (2013).

19.   Lefterova, M.I. & Lazar, M.A. New developments in adipogenesis. *Trends in endocrinology and metabolism: TEM* **20**, 107-114 (2009).

20.   Kawai, M., de Paula, F.J.A. & Rosen, C.J. New Insights into Osteoporosis: The Bone-Fat Connection. *Journal of internal medicine* **272**, 317-329 (2012).

21.   Vande Berg, B.C., Malghem, J., Lecouvet, F.E. & Maldague, B. Magnetic resonance imaging of normal bone marrow. *European Radiology* **8**, 1327-1334 (1998).

22.   Machann, J., Stefan, N. & Schick, F. 1H MR spectroscopy of skeletal muscle, liver and bone marrow. *European Journal of Radiology* **67**, 275-284 (2008).

23.   Ye, L. *et al.* Histone demethylases KDM4B and KDM6B promotes osteogenic differentiation of human MSCs. *Cell stem cell* **11**, 50-61 (2012).

24.   Rosen, C.J. & Bouxsein, M.L. Mechanisms of disease: is osteoporosis the obesity of bone? *Nature clinical practice. Rheumatology* **2**, 35-43 (2006).

25.   Otto, F., Kanegane, H. & Mundlos, S. Mutations in the RUNX2 gene in patients with cleidocranial dysplasia. *Human Mutation* **19**, 209-216 (2002).

26.   Choi, J.Y. *et al.* Subnuclear targeting of Runx/Cbfa/AML factors is essential for tissue-specific differentiation during embryonic development. *Proceedings of the National Academy of Sciences of the United States of America* **98**, 8650-8655 (2001).

27.   Takarada, T. *et al.* Genetic analysis of Runx2 function during intramembranous ossification. *Development* **143**, 211-218 (2016).

28.   Zheng, H., Guo, Z., Ma, Q., Jia, H. & Dang, G. Cbfa1/osf2 Transduced Bone Marrow Stromal Cells Facilitate Bone Formation In Vitro and In Vivo. *Calcified Tissue International* **74**, 194-203 (2004).

29.   Liu, W. *et al.* Overexpression of Cbfa1 in osteoblasts inhibits osteoblast maturation and causes osteopenia with multiple fractures. *The Journal of Cell Biology* **155**, 157-166 (2001).

30.   Seifert, A., Werheid, D.F., Knapp, S.M. & Tobiasch, E. Role of Hox genes in stem cell differentiation. *World Journal of Stem Cells* **7**, 583-595 (2015).

31.   Lee, M.H. *et al.* BMP-2-induced Runx2 expression is mediated by Dlx5, and TGF-beta 1 opposes the BMP-2-induced osteoblast differentiation by suppression of Dlx5 expression. *The Journal of biological chemistry* **278**, 34387-34394 (2003).

32.   Lee, M.-H., Kwon, T.-G., Park, H.-S., Wozney, J.M. & Ryoo, H.-M. BMP-2-induced Osterix expression is mediated by Dlx5 but is independent of Runx2. *Biochemical and Biophysical Research Communications* **309**, 689-694 (2003).

33.   Hassan, M.Q. *et al.* HOXA10 controls osteoblastogenesis by directly activating bone regulatory and phenotypic genes. *Molecular and cellular biology* **27**, 3337-3352 (2007).

34.   Carapuço, M., Nóvoa, A., Bobola, N. & Mallo, M. Hox genes specify vertebral types in the presomitic mesoderm. *Genes & Development* **19**, 2116-2121 (2005).

35.   Kubota, N. *et al.* PPARG Mediates High-Fat Diet Induced Adipocyte Hypertrophy and Insulin Resistance. *Molecular Cell* **4**, 597-609.

36.   Barroso, I. *et al.* Dominant negative mutations in human PPAR[gamma] associated with severe insulin resistance, diabetes mellitus and hypertension. *Nature* **402**, 880-883 (1999).

37.   Jones, J.R. *et al.* Deletion of PPARgamma in adipose tissues of mice protects against high fat diet-induced obesity and insulin resistance. *Proceedings of the National Academy of Sciences of the United States of America* **102**, 6207-6212 (2005).

38.   Rosen, E.D. & MacDougald, O.A. Adipocyte differentiation from the inside out. *Nat Rev Mol Cell Biol* **7**, 885-896 (2006).

39.   Linhart, H.G. *et al.* C/EBPalpha is required for differentiation of white, but not brown, adipose tissue. *Proceedings of the National Academy of Sciences of the United States of America* **98**, 12532-12537 (2001).

40.   Tanaka, T., Yoshida, N., Kishimoto, T. & Akira, S. Defective adipocyte differentiation in mice lacking the C/EBPbeta and/or C/EBPdelta gene. *The EMBO Journal* **16**, 7432-7443 (1997).

41.   Siersbaek, R., Nielsen, R. & Mandrup, S. PPARgamma in adipocyte differentiation and metabolism--novel insights from genome-wide studies. *FEBS letters* **584**, 3242-3249 (2010).

42.   Canalis, E. Wnt signalling in osteoporosis: mechanisms and novel therapeutic approaches. *Nature reviews. Endocrinology* **9**, 575-583 (2013).

43.   Balemans, W. *et al.* Increased bone density in sclerosteosis is due to the deficiency of a novel secreted protein (SOST). *Human molecular genetics* **10**, 537-543 (2001).

44.   Padhi, D., Jang, G., Stouch, B., Fang, L. & Posvar, E. Single-dose, placebo-controlled, randomized study of AMG 785, a sclerostin monoclonal antibody. *Journal of Bone and Mineral Research* **26**, 19-26 (2011).

45.   Kang, S. *et al.* Wnt signaling stimulates osteoblastogenesis of mesenchymal precursors by suppressing CCAAT/enhancer-binding protein alpha and peroxisome proliferator-activated receptor gamma. *The Journal of biological chemistry* **282**, 14515-14524 (2007).

46.   Bilkovski, R. *et al.* Role of Wnt-5a in the Determination of Human Mesenchymal Stem Cells into Preadipocytes. *Journal of Biological Chemistry* **285**, 6170-6178 (2010).

47.   Yu, B. *et al.* Wnt4 signaling prevents skeletal aging and inflammation by inhibiting nuclear factor-kappaB. *Nature medicine* **20**, 1009-1017 (2014).

48.   Ross, S.E. *et al.* Inhibition of Adipogenesis by Wnt Signaling. *Science* **289**, 950 (2000).

49.   Liu, J. & Farmer, S.R. Regulating the Balance between Peroxisome Proliferator-activated Receptor γ and β-Catenin Signaling during Adipogenesis: A GLYCOGEN SYNTHASE KINASE 3β PHOSPHORYLATION-DEFECTIVE MUTANT OF β-CATENIN INHIBITS EXPRESSION OF A SUBSET OF ADIPOGENIC GENES. *Journal of Biological Chemistry* **279**, 45020-45027 (2004).

50.   Moldes, M. *et al.* Peroxisome-proliferator-activated receptor gamma suppresses Wnt/beta-catenin signalling during adipogenesis. *Biochemical Journal* **376**, 607-613 (2003).

51.   Kawai, M. *et al.* Wnt/Lrp/β-catenin signaling suppresses adipogenesis by inhibiting mutual activation of PPARγ and C/EBPα. *Biochemical and Biophysical Research Communications* **363**, 276-282 (2007).

52.   Beederman, M. *et al.* BMP signaling in mesenchymal stem cell differentiation and bone formation. *Journal of biomedical science and engineering* **6**, 32-52 (2013).

53.   Shu, B. *et al.* BMP2, but not BMP4, is crucial for chondrocyte proliferation and maturation during endochondral bone development. *Journal of Cell Science* **124**, 3428 (2011).

54.   Zhao, G.-Q. Consequences of knocking out BMP signaling in the mouse. *genesis* **35**, 43-56 (2003).

55.   Canalis, E., Brunet, L.J., Parker, K. & Zanotti, S. Conditional Inactivation of Noggin in the Postnatal Skeleton Causes Osteopenia. *Endocrinology* **153**, 1616-1626 (2012).

56.   Zimmerman, L.B., De Jesús-Escobar, J.M. & Harland, R.M. The Spemann Organizer Signal noggin Binds and Inactivates Bone Morphogenetic Protein 4. *Cell* **86**, 599-606 (1996).

57.   Lee, K.-S. *et al.* Runx2 Is a Common Target of Transforming Growth Factor β1 and Bone Morphogenetic Protein 2, and Cooperation between Runx2 and Smad5 Induces Osteoblast-Specific Gene Expression in the Pluripotent Mesenchymal Precursor Cell Line C2C12. *Molecular and cellular biology* **20**, 8783-8792 (2000).

58.   Sottile, V. & Seuwen, K. Bone morphogenetic protein-2 stimulates adipogenic differentiation of mesenchymal precursor cells in synergy with BRL 49653 (rosiglitazone). *FEBS letters* **475**, 201-204 (2000).

59.   Huang, H. *et al.* BMP signaling pathway is required for commitment of C3H10T1/2 pluripotent stem cells to the adipocyte lineage. *Proceedings of the National Academy of Sciences* **106**, 12670-12675 (2009).

60.   Hata, K. *et al.* Differential Roles of Smad1 and p38 Kinase in Regulation of Peroxisome Proliferator-activating Receptor γ during Bone Morphogenetic Protein 2-induced Adipogenesis. *Molecular Biology of the Cell* **14**, 545-555 (2003).

61.   Wu, H. & Sun, Y.E. Epigenetic Regulation of Stem Cell Differentiation. *Pediatric Research* **59**, 21R-25R (2006).

62.   Jenuwein, T. Translating the Histone Code. *Science* **293**, 1074-1080 (2001).

63.   Lunyak, V.V. & Rosenfeld, M.G. Epigenetic regulation of stem cell fate. *Human Molecular Genetics* **17**, R28-R36 (2008).

64.   Binda, O. On your histone mark, SET, methylate! *Epigenetics* **8**, 457-463 (2013).

65.   Klose, R.J. & Zhang, Y. Regulation of histone methylation by demethylimination and demethylation. *Nature Reviews Molecular Cell Biology* **8**, 307-318 (2007).

66.   Allfrey, V.G., Faulkner, R., & Mirsky, A. E. (1964).., 51(5), 786 Acetylation and methylation of histones and their possible role in the regulation of RNA synthesis.

Proceedings of the National Academy of Sciences of the United States of America **51**, 9 (1964).

67. Strahl, B.D., Ohba, R., Cook, R. G., & Allis, C. D. Methylation of histone H3 at lysine 4 is highly conserved and correlates with transcriptionally active nuclei in Tetrahymena. . *Proceedings of the National Academy of Sciences* **96**, 6 (1999).

68. Chou, R.H., Yu, Y. L., & Hung, M. C. (2011). . , 3(3), 243. The roles of EZH2 in cell lineage commitment. *American journal of translational research* **3**, 8 (2011).

69. Wei, Y. *et al.* CDK1-dependent phosphorylation of EZH2 suppresses methylation of H3K27 and promotes osteogenic differentiation of human mesenchymal stem cells. *Nature Cell Biology* **13**, 87-94 (2010).

70. Tonini, T., D'Andrilli, G., Fucito, A., Gaspa, L., & Bagella, L. Importance of Ezh2 polycomb protein in tumorigenesis process interfering with the pathway of growth suppressive key elements. *Journal of cellular physiology* **214**, 6 (2008).

71. Hemming, S. *et al.* EZH2andKDM6AAct as an Epigenetic Switch to Regulate Mesenchymal Stem Cell Lineage Specification. *Stem Cells* **32**, 802-815 (2014).

72. Schwarz, D. *et al.* Ezh2 is required for neural crest-derived cartilage and bone formation. *Development* **141**, 867-877 (2014).

73. Wang, L., Jin, Q., Lee, J.E., Su, I.h. & Ge, K. Histone H3K27 methyltransferase Ezh2 represses Wnt genes to facilitate adipogenesis. *Proceedings of the National Academy of Sciences* **107**, 7317-7322 (2010).

74. Chen, Y.H. *et al.* Myocyte Enhancer Factor-2 Interacting Transcriptional Repressor (MITR) Is a Switch That Promotes Osteogenesis and Inhibits Adipogenesis of Mesenchymal Stem

Cells by Inactivating Peroxisome Proliferator-activated Receptor -2. *Journal of Biological Chemistry* **286**, 10671-10680 (2011).

75.   Lawson, K.A. *et al.* ESET histone methyltransferase regulates osteoblastic differentiation of mesenchymal stem cells during postnatal bone development. *FEBS Letters* **587**, 3961-3967 (2013).

76.   Yang, L. *et al.* ESET histone methyltransferase is essential to hypertrophic differentiation of growth plate chondrocytes and formation of epiphyseal plates. *Developmental Biology* **380**, 99-110 (2013).

77.   Liu, W. Overexpression of Cbfa1 in osteoblasts inhibits osteoblast maturation and causes osteopenia with multiple fractures. *The Journal of Cell Biology* **155**, 157-166 (2001).

78.   Okamura, M., Inagaki, T., Tanaka, T., & Sakai, J. (2010).,6(1), 24. Role of histone methylation and demethylation in adipogenesis and obesity. *Organogenesis* **6**, 9 (2010).

79.   Lee, J. *et al.* Targeted inactivation of MLL3 histone H3-Lys-4 methyltransferase activity in the mouse reveals vital roles for MLL3 in adipogenesis. *Proceedings of the National Academy of Sciences* **105**, 19229-19234 (2008).

80.   Cho, Y.-W. *et al.* Histone Methylation Regulator PTIP Is Required for PPARγ and C/EBPα Expression and Adipogenesis. *Cell Metabolism* **10**, 27-39 (2009).

81.   Ge, W. *et al.* Inhibition of Osteogenic Differentiation of Human Adipose-Derived Stromal Cells by Retinoblastoma Binding Protein 2 Repression of RUNX2-Activated Transcription. *Stem Cells* **29**, 1112-1125 (2011).

82.   Krivtsov, A.V. *et al.* H3K79 Methylation Profiles Define Murine and Human MLL-AF4 Leukemias. *Cancer Cell* **14**, 355-368 (2008).

83.   Cristancho, A.G. & Lazar, M.A. Forming functional fat: a growing understanding of adipocyte differentiation. *Nature Reviews Molecular Cell Biology* **12**, 722-734 (2011).

84.   Wakabayashi, K.i. *et al.* The Peroxisome Proliferator-Activated Receptor /Retinoid X Receptor Heterodimer Targets the Histone Modification Enzyme PR-Set7/Setd8 Gene and Regulates Adipogenesis through a Positive Feedback Loop. *Molecular and Cellular Biology* **29**, 3544-3555 (2009).

85.   Yu, B.D., Hess, J. L., Horning, S. E., Brown, G. A., & Korsmeyer, S. J. Altered Hox expression and segmental identity in Mll-mutant mice. *Nature* **378**, 4 (1995).

86.   Terranova, R., Agherbi, H., Boned, A., Meresse, S. & Djabali, M. Histone and DNA methylation defects at Hox genes in mice expressing a SET domain-truncated form of Mll. *Proceedings of the National Academy of Sciences* **103**, 6629-6634 (2006).

87.   Shi, Y. *et al.* Histone Demethylation Mediated by the Nuclear Amine Oxidase Homolog LSD1. *Cell* **119**, 941-953 (2004).

88.   Martin, C. & Zhang, Y. The diverse functions of histone lysine methylation. *Nature Reviews Molecular Cell Biology* **6**, 838-849 (2005).

89.   Lu, F. *et al.* Comparative Analysis of JmjC Domain-containing Proteins Reveals the Potential Histone Demethylases inArabidopsisand Rice. *Journal of Integrative Plant Biology* **50**, 886-896 (2008).

90.   Lan, F., Nottke, A.C. & Shi, Y. Mechanisms involved in the regulation of histone lysine demethylases. *Current Opinion in Cell Biology* **20**, 316-325 (2008).

91.   Shi, Y. Histone lysine demethylases: emerging roles in development, physiology and disease. *Nature Reviews Genetics* **8**, 5 (2007).

92. Tsukada, Y.-i. *et al.* Histone demethylation by a family of JmjC domain-containing proteins. *Nature* **439**, 811-816 (2005).

93. Gao, R. *et al.* Depletion of histone demethylase KDM2A inhibited cell proliferation of stem cells from apical papilla by de-repression of p15INK4B and p27Kip1. *Molecular and Cellular Biochemistry* **379**, 115-122 (2013).

94. Dong, R., Yao, R., Du, J., Wang, S. & Fan, Z. Depletion of histone demethylase KDM2A enhanced the adipogenic and chondrogenic differentiation potentials of stem cells from apical papilla. *Experimental Cell Research* **319**, 2874-2882 (2013).

95. Fan, Z. *et al.* BCOR regulates mesenchymal stem cell function by epigenetic mechanisms. *Nature Cell Biology* **11**, 1002-1009 (2009).

96. Du, J., Ma, Y., Ma, P., Wang, S. & Fan, Z. Demethylation of Epiregulin Gene by Histone Demethylase FBXL11 and BCL6 Corepressor Inhibits Osteo/dentinogenic Differentiation. *Stem Cells* **31**, 126-136 (2013).

97. Labbé, R.M., Holowatyj, A., & Yang, Z. Q. (2014). , 6(1), 1. Histone lysine demethylase (KDM) subfamily 4: structures, functions and therapeutic potential. *American journal of translational research* **6**, 15 (2014).

98. Lorbeck, M.T. *et al.* The histone demethylase Dmel\Kdm4A controls genes required for life span and male-specific sex determination in Drosophila. *Gene* **450**, 8-17 (2010).

99. Iwamori, N., Zhao, M., Meistrich, M.L. & Matzuk, M.M. The Testis-Enriched Histone Demethylase, KDM4D, Regulates Methylation of Histone H3 Lysine 9 During Spermatogenesis in the Mouse but Is Dispensable for Fertility. *Biology of Reproduction* **84**, 1225-1234 (2011).

100. Pedersen, M.T. *et al.* The Demethylase JMJD2C Localizes to H3K4me3-Positive Transcription Start Sites and Is Dispensable for Embryonic Development. *Molecular and Cellular Biology* **34**, 1031-1045 (2014).

101. Shioda, T. *et al.* Histone Demethylase JMJD2B Functions as a Co-Factor of Estrogen Receptor in Breast Cancer Proliferation and Mammary Gland Development. *PLoS ONE* **6**, e17830 (2011).

102. Cox, G.A. *et al.* A New Isoform of the Histone Demethylase JMJD2A/KDM4A Is Required for Skeletal Muscle Differentiation. *PLoS Genetics* **7**, e1001390 (2011).

103. Strobl-Mazzulla, P.H., Sauka-Spengler, T. & Bronner-Fraser, M. Histone Demethylase JmjD2A Regulates Neural Crest Specification. *Developmental Cell* **19**, 460-468 (2010).

104. Johansson, C., Tumber, A., Che, K., Cain, P., Nowak, R., Gileadi, C., & Oppermann, U. The roles of Jumonji-type oxygenases in human disease. *Epigenomics* **6**, 32 (2014).

105. Ye, L. *et al.* Histone Demethylases KDM4B and KDM6B Promotes Osteogenic Differentiation of Human MSCs. *Cell Stem Cell* **11**, 50-61 (2012).

106. Guo, L. *et al.* Histone demethylase Kdm4b functions as a co-factor of C/EBPβ to promote mitotic clonal expansion during differentiation of 3T3-L1 preadipocytes. *Cell Death and Differentiation* **19**, 1917-1927 (2012).

107. Chisholm, A.D. *et al.* The C. elegans H3K27 Demethylase UTX-1 Is Essential for Normal Development, Independent of Its Enzymatic Activity. *PLoS Genetics* **8**, e1002647 (2012).

108. Sinha, K.M., Yasuda, H., Coombes, M.M., Dent, S.Y.R. & de Crombrugghe, B. Regulation of the osteoblast-specific transcription factor Osterix by NO66, a Jumonji family histone demethylase. *The EMBO Journal* **29**, 68-79 (2009).

109. Tao, Y. *et al.* Structural Insights into Histone Demethylase NO66 in Interaction with Osteoblast-specific Transcription Factor Osterix and Gene Repression. *Journal of Biological Chemistry* **288**, 16430-16437 (2013).

110. Christensen, J. *et al.* RBP2 Belongs to a Family of Demethylases, Specific for Tri-and Dimethylated Lysine 4 on Histone 3. *Cell* **128**, 1063-1076 (2007).

111. Klose, R.J. *et al.* The Retinoblastoma Binding Protein RBP2 Is an H3K4 Demethylase. *Cell* **128**, 889-900 (2007).

112. Benevolenskaya, E.V., Murray, H.L., Branton, P., Young, R.A. & Kaelin, W.G. Binding of pRB to the PHD Protein RBP2 Promotes Cellular Differentiation. *Molecular Cell* **18**, 623-635 (2005).

113. Lopez-Bigas, N. *et al.* Genome-wide Analysis of the H3K4 Histone Demethylase RBP2 Reveals a Transcriptional Program Controlling Differentiation. *Molecular Cell* **31**, 520-530 (2008).

114. Pasini, D. *et al.* Coordinated regulation of transcriptional repression by the RBP2 H3K4 demethylase and Polycomb-Repressive Complex 2. *Genes & Development* **22**, 1345-1355 (2008).

115. Pedersen, M.T. & Helin, K. Histone demethylases in development and disease. *Trends in Cell Biology* **20**, 662-671 (2010).

116. Okuno, Y., Ohtake, F., Igarashi, K., Kanno, J., Matsumoto, T., Takada, I.& Imai, Y. Epigenetic regulation of adipogenesis by PHF2 histone demethylase. *Diabetes* **62**, 9 (2013).

117. Lu, C. *et al.* IDH mutation impairs histone demethylation and results in a block to cell differentiation. *Nature* **483**, 474-478 (2012).

118. Sinha, K.M., Yasuda, H., Zhou, X. & deCrombrugghe, B. Osterix and NO66 Histone Demethylase Control the Chromatin of Osterix Target Genes During Osteoblast Differentiation. *Journal of Bone and Mineral Research* **29**, 855-865 (2014).

119. Challen, G.A., Boles, N., Lin, K.K. & Goodell, M.A. Mouse hematopoietic stem cell identification and analysis. *Cytometry. Part A : the journal of the International Society for Analytical Cytology* **75**, 14-24 (2009).

120. Bianco, P., Robey, P.G. & Simmons, P.J. Mesenchymal stem cells: revisiting history, concepts, and assays. *Cell stem cell* **2**, 313-319 (2008).

121. Bianco, P. *et al.* The meaning, the sense and the significance: translating the science of mesenchymal stem cells into medicine. *Nature medicine* **19**, 35-42 (2013).

122. Sacchetti, B. *et al.* Self-Renewing Osteoprogenitors in Bone Marrow Sinusoids Can Organize a Hematopoietic Microenvironment. *Cell* **131**, 324-336 (2007).

123. Yew, T.-L. *et al.* Knockdown of p21Cip1/Waf1 enhances proliferation, the expression of stemness markers, and osteogenic potential in human mesenchymal stem cells. *Aging Cell* **10**, 349-361 (2011).

124. Zhou, S. *et al.* Age-related intrinsic changes in human bone-marrow-derived mesenchymal stem cells and their differentiation to osteoblasts. *Aging Cell* **7**, 335-343 (2008).

125. Roobrouck, V.D., Ulloa-Montoya, F. & Verfaillie, C.M. Self-renewal and differentiation capacity of young and aged stem cells. *Experimental cell research* **314**, 1937-1944 (2008).

126. Tsai, C.C., Su, P.F., Huang, Y.F., Yew, T.L. & Hung, S.C. Oct4 and Nanog directly regulate Dnmt1 to maintain self-renewal and undifferentiated state in mesenchymal stem cells. *Mol Cell* **47**, 169-182 (2012).

127. Tsai, C.-C. & Hung, S.-C. Functional roles of pluripotency transcription factors in mesenchymal stem cells. *Cell Cycle* **11**, 3711-3712 (2012).

128. Zhang, P. *et al.* Loss of Asxl1 Alters Self-Renewal and Cell Fate of Bone Marrow Stromal Cell, Leading to Bohring-Opitz-like Syndrome in Mice. *Stem Cell Reports* **6**, 914-925 (2016).

129. Takahashi, K. & Yamanaka, S. Induction of Pluripotent Stem Cells from Mouse Embryonic and Adult Fibroblast Cultures by Defined Factors. *Cell* **126**, 663-676 (2006).

130. Seo, E. *et al.* SOX2 Regulates YAP1 to Maintain Stemness and Determine Cell Fate in the Osteo-Adipo Lineage. *Cell reports* **3**, 2075-2087 (2013).

131. Basu-Roy, U. *et al.* The transcription factor Sox2 is required for osteoblast self-renewal. *Cell death and differentiation* **17**, 1345-1353 (2010).

132. Park, S.B. *et al.* SOX2 has a crucial role in the lineage determination and proliferation of mesenchymal stem cells through Dickkopf-1 and c-MYC. *Cell Death and Differentiation* **19**, 534-545 (2012).

133. Holmes, G., Bromage, T.G. & Basilico, C. The Sox2 high mobility group transcription factor inhibits mature osteoblast function in transgenic mice. *Bone* **49**, 653-661 (2011).

134. Mansukhani, A., Ambrosetti, D., Holmes, G., Cornivelli, L. & Basilico, C. Sox2 induction by FGF and FGFR2 activating mutations inhibits Wnt signaling and osteoblast differentiation. *The Journal of Cell Biology* **168**, 1065-1076 (2005).

135. Seo, E., Basu-Roy, U., Zavadil, J., Basilico, C. & Mansukhani, A. Distinct Functions of Sox2 Control Self-Renewal and Differentiation in the Osteoblast Lineage. *Molecular and cellular biology* **31**, 4593-4608 (2011).

136. Pan, G. & Thomson, J.A. Nanog and transcriptional networks in embryonic stem cell pluripotency. *Cell Res* **17**, 42-49 (2007).

137. Enrico Pierantozzi, B.G., Ivana Manini, Franco Roviello, Giuseppe Marotta,Mario Chiavarelli, and Vincenzo Sorrentino Pluripotency Regulators in Human Mesenchymal Stem Cells: Expression of NANOG But Not of OCT-4 and SOX-2. *STEM CELLS AND DEVELOPMENT* **20** (2011).

138. Liu, T.M. *et al.* Effects of Ectopic Nanog and Oct4 Overexpression on Mesenchymal Stem Cells. *Stem Cells and Development* **18**, 1013-1021 (2009).

139. Han, J. *et al.* Nanog reverses the effects of organismal aging on mesenchymal stem cell proliferation and myogenic differentiation potential. *Stem cells (Dayton, Ohio)* **30**, 2746-2759 (2012).

140. Lengner, C.J. *et al.* Oct4 expression is not required for mouse somatic stem cell self-renewal. *Cell stem cell* **1**, 403-415 (2007).

141. Biniszkiewicz, D. *et al.* Dnmt1 Overexpression Causes Genomic Hypermethylation, Loss of Imprinting, and Embryonic Lethality. *Molecular and cellular biology* **22**, 2124-2135 (2002).

142. Fouse, S.D. *et al.* Promoter CpG methylation contributes to ES cell gene regulation in parallel with Oct4/Nanog, Polycomb binding and histone H3 lys4/lys27 trimethylation. *Cell stem cell* **2**, 160-169 (2008).

143. Sen, G.L., Reuter, J.A., Webster, D.E., Zhu, L. & Khavari, P.A. DNMT1 Maintains Progenitor Function in Self-Renewing Somatic Tissue. *Nature* **463**, 563-567 (2010).

144. Zhang, W. *et al.* A Werner syndrome stem cell model unveils heterochromatin alterations as a driver of human aging. *Science* **348**, 1160-1163 (2015).

145.   Li Z, L.C., Xie Z, Song P, Zhao RCH, Guo L, et al. Epigenetic Dysregulation in Mesenchymal Stem Cell Aging and Spontaneous Differentiation. *PLoS ONE* **6** (2011).

146.   Yu, K.R. & Kang, K.S. Aging-Related Genes in Mesenchymal Stem Cells: A Mini-Review. *Gerontology* **59**, 557-563 (2013).

147.   Jung, J.-W. *et al.* Histone deacetylase controls adult stem cell aging by balancing the expression of polycomb genes and jumonji domain containing 3. *Cellular and Molecular Life Sciences* **67**, 1165-1176 (2010).

148.   Logan, M. *et al.* Expression of Cre recombinase in the developing mouse limb bud driven by a Prxl enhancer. *genesis* **33**, 77-80 (2002).

149.   Zhou, Bo O., Yue, R., Murphy, Malea M., Peyer, J.G. & Morrison, Sean J. Leptin-Receptor-Expressing Mesenchymal Stromal Cells Represent the Main Source of Bone Formed by Adult Bone Marrow. *Cell stem cell* **15**, 154-168 (2014).

150.   Zhang, M. *et al.* Osteoblast-specific Knockout of the Insulin-like Growth Factor (IGF) Receptor Gene Reveals an Essential Role of IGF Signaling in Bone Matrix Mineralization. *Journal of Biological Chemistry* **277**, 44005-44012 (2002).

151.   Madisen, L. *et al.* A robust and high-throughput Cre reporting and characterization system for the whole mouse brain. *Nat Neurosci* **13**, 133-140 (2010).

152.   Scheller, E.L. *et al.* Region-specific variation in the properties of skeletal adipocytes reveals regulated and constitutive marrow adipose tissues. *Nat Commun* **6**, 7808 (2015).

153.   Scheller, E.L. *et al.* Use of Osmium Tetroxide Staining with Microcomputerized Tomography to Visualize and Quantify Bone Marrow Adipose Tissue In Vivo. *Methods in enzymology* **537**, 123-139 (2014).

154. Egan, K.P., Brennan, T.A. & Pignolo, R.J. Bone histomorphometry using free and commonly available software. *Histopathology* **61**, 1168-1173 (2012).

155. Chang, J. *et al.* Inhibition of Osteoblast Functions by IKK/NF-κB in Osteoporosis. *Nature medicine* **15**, 682-689 (2009).

156. Suire, C., Brouard, N., Hirschi, K. & Simmons, P.J. Isolation of the stromal-vascular fraction of mouse bone marrow markedly enhances the yield of clonogenic stromal progenitors. *Blood* **119**, e86-e95 (2012).

157. Wysocka, J., Reilly, P.T. & Herr, W. Loss of HCF-1–Chromatin Association Precedes Temperature-Induced Growth Arrest of tsBN67 Cells. *Molecular and Cellular Biology* **21**, 3820-3829 (2001).

158. Klose, R.J., Kallin, E.M. & Zhang, Y. JmjC-domain-containing proteins and histone demethylation. *Nat Rev Genet* **7**, 715-727 (2006).

159. Labbé, R.M., Holowatyj, A. & Yang, Z.-Q. Histone lysine demethylase (KDM) subfamily 4: structures, functions and therapeutic potential. *American Journal of Translational Research* **6**, 1-15 (2014).

160. Scheller, E.L. *et al.* Region-specific variation in the properties of skeletal adipocytes reveals regulated and constitutive marrow adipose tissues. *Nat Commun* **6** (2015).

161. Soleimani, M. & Nadri, S. A protocol for isolation and culture of mesenchymal stem cells from mouse bone marrow. *Nat. Protocols* **4**, 102-106 (2009).

162. Sweis, R.F. *et al.* Discovery and Development of Potent and Selective Inhibitors of Histone Methyltransferase G9a. *ACS Medicinal Chemistry Letters* **5**, 205-209 (2014).

163. Huang, D.W., Sherman, B.T. & Lempicki, R.A. Systematic and integrative analysis of large gene lists using DAVID bioinformatics resources. *Nat. Protocols* **4**, 44-57 (2008).

164. Huang da, W., Sherman, B.T. & Lempicki, R.A. Bioinformatics enrichment tools: paths toward the comprehensive functional analysis of large gene lists. *Nucleic Acids Res* **37**, 1-13 (2009).

165. Subramanian, A. *et al.* Gene set enrichment analysis: A knowledge-based approach for interpreting genome-wide expression profiles. *Proceedings of the National Academy of Sciences of the United States of America* **102**, 15545-15550 (2005).

166. Schroeder, T.M., Jensen, E.D. & Westendorf, J.J. Runx2: a master organizer of gene transcription in developing and maturing osteoblasts. *Birth defects research. Part C, Embryo today : reviews* **75**, 213-225 (2005).

167. Komori, T. *et al.* Targeted Disruption of Cbfa1 Results in a Complete Lack of Bone Formation owing to Maturational Arrest of Osteoblasts. *Cell* **89**, 755-764 (1997).

168. Rodriguez-Carballo, E. *et al.* Conserved regulatory motifs in osteogenic gene promoters integrate cooperative effects of canonical Wnt and BMP pathways. *Journal of bone and mineral research : the official journal of the American Society for Bone and Mineral Research* **26**, 718-729 (2011).

169. Kulkarni, N.H. *et al.* Effects of parathyroid hormone on Wnt signaling pathway in bone. *Journal of Cellular Biochemistry* **95**, 1178-1190 (2005).

170. Wan, M. *et al.* Parathyroid hormone signaling through low-density lipoprotein-related protein 6. *Genes Dev* **22**, 2968-2979 (2008).

171. Mathelier, A. *et al.* JASPAR 2016: a major expansion and update of the open-access database of transcription factor binding profiles. *Nucleic Acids Research* (2015).

172. Chan, Charles K.F. *et al.* Identification and Specification of the Mouse Skeletal Stem Cell. *Cell* **160**, 285-298 (2015).

173. Worthley, Daniel L. *et al.* Gremlin 1 Identifies a Skeletal Stem Cell with Bone, Cartilage, and Reticular Stromal Potential. *Cell* **160**, 269-284 (2015).

174. Kawai, M., de Paula, F.J. & Rosen, C.J. New insights into osteoporosis: the bone-fat connection. *Journal of internal medicine* **272**, 317-329 (2012).

175. Augustine, M. & Horwitz, M.J. Parathyroid hormone and parathyroid hormone-related protein analogs as therapies for osteoporosis. *Current osteoporosis reports* **11**, 400-406 (2013).

176. Jeon, M.J. *et al.* Activation of Peroxisome Proliferator-activated Receptor-γ Inhibits the Runx2-mediated Transcription of Osteocalcin in Osteoblasts. *Journal of Biological Chemistry* **278**, 23270-23277 (2003).

177. Enomoto, H. *et al.* Runx2 deficiency in chondrocytes causes adipogenic changes in vitro. *Journal of Cell Science* **117**, 417-425 (2004).

178. Fan, Y. *et al.* Parathyroid Hormone Directs Bone Marrow Mesenchymal Cell Fate. *Cell metabolism* **25**, 661-672 (2017).

179. Cohen, P.G. Aromatase, adiposity, aging and disease. The hypogonadal-metabolic-atherogenic-disease and aging connection. *Medical Hypotheses* **56**, 702-708 (2001).

180. Pino, A.M. *et al.* Concentration of adipogenic and proinflammatory cytokines in the bone marrow supernatant fluid of osteoporotic women. *Journal of Bone and Mineral Research* **25**, 492-498 (2010).

181. Worthley, D.L. *et al.* Gremlin 1 Identifies a Skeletal Stem Cell with Bone, Cartilage, and Reticular Stromal Potential. *Cell* **160**, 269-284 (2015).

182. Chan, C.K.F. *et al.* Identification and Specification of the Mouse Skeletal Stem Cell. *Cell* **160**, 285-298 (2015).

183. Gimble, J.M., Robinson, C.E., Wu, X. & Kelly, K.A. The function of adipocytes in the bone marrow stroma: an update. *Bone* **19**, 421-428 (1996).

184. Faial, T. Heterochromatin and human aging. *Nat Genet* **47**, 568-568 (2015).

185. Mendelsohn, A.R. & Larrick, J.W. Stem Cell Depletion by Global Disorganization of the H3K9me3 Epigenetic Marker in Aging. *Rejuvenation Research* **18**, 371-375 (2015).

186. Stappenbeck, T.S. & Miyoshi, H. The role of stromal stem cells in tissue regeneration and wound repair. *Science* **324**, 1666-1669 (2009).

187. Kode, J.A., Mukherjee, S., Joglekar, M.V. & Hardikar, A.A. Mesenchymal stem cells: immunobiology and role in immunomodulation and tissue regeneration. *Cytotherapy* **11**, 377-391 (2009).

188. Kim, N. & Cho, S.G. Clinical applications of mesenchymal stem cells. *The Korean journal of internal medicine* **28**, 387-402 (2013).

189. Wang, S., Qu, X. & Zhao, R.C. Clinical applications of mesenchymal stem cells. *Journal of hematology & oncology* **5**, 19 (2012).

190. Quarto, R., Maddalena Mastrogiacomo, Ranieri Cancedda, Sergei M. Kutepov, Vladimir Mukhachev, Alexander Lavroukov, Elizaveta Kon, and Maurilio Marcacci. Repair of large bone defects with the use of autologous bone marrow stromal cells. *New England Journal of Medicine* **344**, 2 (2001).

191. Thomson, J.A. Embryonic Stem Cell Lines Derived from Human Blastocysts. *Science* **282**, 1145-1147 (1998).

192. Choo, A. & Lim, S.K. Derivation of mesenchymal stem cells from human embryonic stem cells. *Methods in molecular biology* **690**, 175-182 (2011).

193. Lee, E.J., Ha-Neul Lee, Hyun-Jae Kang, Keum-Hyun Kim, Jin Hur, Hyun-Jai Cho, Jaewon Lee et al. Novel Embryoid Body-Based Method to Derive Mesenchymal Stem Cells from Human Embryonic Stem Cells. *Tissue Engineering* **16**, 11 (2009).

194. Barberi, T., Willis, L.M., Socci, N.D. & Studer, L. Derivation of multipotent mesenchymal precursors from human embryonic stem cells. *PLoS medicine* **2**, e161 (2005).

195. Murry, C.E. & Keller, G. Differentiation of embryonic stem cells to clinically relevant populations: lessons from embryonic development. *Cell* **132**, 661-680 (2008).

196. Moon, S.-H. *et al.* Differentiation of hESCs into Mesodermal Subtypes: Vascular-, Hematopoietic- and Mesenchymal-lineage Cells. *International Journal of Stem Cells* **4**, 24-34 (2011).

197. Trivedi, P. & Hematti, P. Derivation and Immunological Characterization of Mesenchymal Stromal Cells from Human Embryonic Stem Cells. *Experimental hematology* **36**, 350-359 (2008).

198. Karp, J.M. *et al.* Cultivation of human embryonic stem cells without the embryoid body step enhances osteogenesis in vitro. *Stem cells* **24**, 835-843 (2006).

199. Hao, J., Li, T.-G., Qi, X., Zhao, D.-F. & Zhao, G.-Q. WNT/β-catenin pathway up-regulates Stat3 and converges on LIF to prevent differentiation of mouse embryonic stem cells. *Developmental Biology* **290**, 81-91 (2006).

200. ten Berge, D. *et al.* Embryonic stem cells require Wnt proteins to prevent differentiation to epiblast stem cells. *Nat Cell Biol* **13**, 1070-1075 (2011).

201. Marson, A. *et al.* Wnt signaling promotes reprogramming of somatic cells to pluripotency. *Cell stem cell* **3**, 132-135 (2008).

202. Paige, S.L. *et al.* Endogenous Wnt/β-Catenin Signaling Is Required for Cardiac Differentiation in Human Embryonic Stem Cells. *PLOS ONE* **5**, e11134 (2010).

203. Davidson, K.C. *et al.* Wnt/β-catenin signaling promotes differentiation, not self-renewal, of human embryonic stem cells and is repressed by Oct4. *Proceedings of the National Academy of Sciences* **109**, 4485-4490 (2012).

204. Lyashenko, N. *et al.* Differential requirement for the dual functions of [beta]-catenin in embryonic stem cell self-renewal and germ layer formation. *Nat Cell Biol* **13**, 753-761 (2011).

205. Qi, X. *et al.* BMP4 supports self-renewal of embryonic stem cells by inhibiting mitogen-activated protein kinase pathways. *Proceedings of the National Academy of Sciences of the United States of America* **101**, 6027-6032 (2004).

206. James, D., Levine, A.J., Besser, D. & Hemmati-Brivanlou, A. TGFβ/activin/nodal signaling is necessary for the maintenance of pluripotency in human embryonic stem cells. *Development* **132**, 1273 (2005).

207. Vallier, L., Alexander, M. & Pedersen, R.A. Activin/Nodal and FGF pathways cooperate to maintain pluripotency of human embryonic stem cells. *Journal of Cell Science* **118**, 4495 (2005).

208. Park, K.-S. TGF-beta Family Signaling in Embryonic Stem Cells. *International Journal of Stem Cells* **4**, 18-23 (2011).

209. Park, C. *et al.* A hierarchical order of factors in the generation of FLK1- and SCL-expressing hematopoietic and endothelial progenitors from embryonic stem cells. *Development* **131**, 2749 (2004).

210. Lengerke, C. *et al.* BMP and Wnt Specify Hematopoietic Fate by Activation of the Cdx-Hox Pathway. *Cell stem cell* **2**, 72-82 (2008).

211. Watanabe, K. *et al.* Directed differentiation of telencephalic precursors from embryonic stem cells. *Nat Neurosci* **8**, 288-296 (2005).

212. Böttcher, R.T. & Niehrs, C. Fibroblast Growth Factor Signaling during Early Vertebrate Development. *Endocrine Reviews* **26**, 63-77 (2005).

213. Dvorak, P. *et al.* Expression and Potential Role of Fibroblast Growth Factor 2 and Its Receptors in Human Embryonic Stem Cells. *STEM CELLS* **23**, 1200-1211 (2005).

214. Levenstein, M.E. *et al.* Basic FGF Support of Human Embryonic Stem Cell Self-Renewal. *Stem cells (Dayton, Ohio)* **24**, 568-574 (2006).

215. Xu, C. *et al.* Basic Fibroblast Growth Factor Supports Undifferentiated Human Embryonic Stem Cell Growth Without Conditioned Medium. *STEM CELLS* **23**, 315-323 (2005).

216. Yu, P., Pan, G., Yu, J. & Thomson, J.A. FGF2 Sustains NANOG and Switches the Outcome of BMP4 Induced Human Embryonic Stem Cell Differentiation. *Cell stem cell* **8**, 326-334 (2011).

217. Cohen, M.A., Itsykson, P. & Reubinoff, B.E. The role of FGF-signaling in early neural specification of human embryonic stem cells. *Developmental biology* **340**, 450-458 (2010).

218. Doyle, S.L. & O'Neill, L.A. Toll-like receptors: from the discovery of NFkappaB to new insights into transcriptional regulations in innate immunity. *Biochemical pharmacology* **72**, 1102-1113 (2006).

219. Guttridge, D.C., Chris Albanese, Julie Y. Reuther, Richard G. Pestell, and Albert S. Baldwin. NF-κB controls cell growth and differentiation through transcriptional regulation of cyclin D1. *Molecular and cellular biology* **19**, 15 (1999).

220. Li, X., and George R. Stark. NFκB-dependent signaling pathways. *Experimental hematology* **30**, 12 (2002).

221. Yang, C. *et al.* Opposing putative roles for canonical and noncanonical NFkappaB signaling on the survival, proliferation, and differentiation potential of human embryonic stem cells. *Stem cells* **28**, 1970-1980 (2010).

222. Armstrong, L. *et al.* The role of PI3K/AKT, MAPK/ERK and NFkappabeta signalling in the maintenance of human embryonic stem cell pluripotency and viability highlighted by transcriptional profiling and functional analysis. *Human molecular genetics* **15**, 1894-1913 (2006).

223. Kang, H.B., Kim, Y.E., Kwon, H.J., Sok, D.E. & Lee, Y. Enhancement of NF-kappaB expression and activity upon differentiation of human embryonic stem cell line SNUhES3. *Stem cells and development* **16**, 615-623 (2007).

224. Ramadoss, S., Li, J., Ding, X., Al Hezaimi, K. & Wang, C.Y. Transducin beta-like protein 1 recruits nuclear factor kappaB to the target gene promoter for transcriptional activation. *Molecular and cellular biology* **31**, 924-934 (2011).

225. Foldes, G. *et al.* Innate immunity in human embryonic stem cells: comparison with adult human endothelial cells. *PloS one* **5** (2010).

226. Bakkar, N. *et al.* IKKα and alternative NF-κB regulate PGC-1β to promote oxidative muscle metabolism. *The Journal of cell biology* **196**, 497-511 (2012).

227. Reubinoff, B.E., Martin F. Pera, Chui-Yee Fong, Alan Trounson, and Ariff Bongso. Embryonic stem cell lines from human blastocysts: somatic differentiation in vitro. *Nature biotechnology* **18**, 6 (2000).

228. Keller, G. Embryonic stem cell differentiation: emergence of a new era in biology and medicine. *Genes & development* **19**, 27 (2005).

229. Herberts, C.A., Kwa, M.S. & Hermsen, H.P. Risk factors in the development of stem cell therapy. *Journal of translational medicine* **9**, 29 (2011).

230. Reubinoff, B.E., Pavel Itsykson, Tikva Turetsky, Martin F. Pera, Etti Reinhartz, Anna Itzik, and Tamir Ben-Hur Neural progenitors from human embryonic stem cells. *Nature biotechnology* **19**, 7 (2001).

231. Dreesen, O. & Brivanlou, A.H. Signaling Pathways in Cancer and Embryonic Stem Cells. *Stem Cell Reviews* **3**, 7-17 (2007).

232. Torres, J. & Watt, F.M. Nanog maintains pluripotency of mouse embryonic stem cells by inhibiting NFkappaB and cooperating with Stat3. *Nature cell biology* **10**, 194-201 (2008).

233. Luningschror, P., Stocker, B., Kaltschmidt, B. & Kaltschmidt, C. miR-290 cluster modulates pluripotency by repressing canonical NF-kappaB signaling. *Stem cells* **30**, 655-664 (2012).

234. Dutta, D. *et al.* Self-renewal versus lineage commitment of embryonic stem cells: protein kinase C signaling shifts the balance. *Stem cells* **29**, 618-628 (2011).

235. Luningschror, P., Kaltschmidt, B. & Kaltschmidt, C. Knockdown of IKK1/2 promotes differentiation of mouse embryonic stem cells into neuroectoderm at the expense of mesoderm. *Stem Cell Rev* **8**, 1098-1108 (2012).

236. Espin-Palazon, R. *et al.* Proinflammatory signaling regulates hematopoietic stem cell emergence. *Cell* **159**, 1070-1085 (2014).

237. Mahmood, A., Harkness, L., Schroder, H.D., Abdallah, B.M. & Kassem, M. Enhanced differentiation of human embryonic stem cells to mesenchymal progenitors by inhibition

of TGF-beta/activin/nodal signaling using SB-431542. *Journal of bone and mineral research : the official journal of the American Society for Bone and Mineral Research* **25**, 1216-1233 (2010).

238.   Saha, S., Ji, L., de Pablo, J.J. & Palecek, S.P. TGFbeta/Activin/Nodal pathway in inhibition of human embryonic stem cell differentiation by mechanical strain. *Biophysical journal* **94**, 4123-4133 (2008).

239.   James, D., Levine, A.J., Besser, D. & Hemmati-Brivanlou, A. TGFbeta/activin/nodal signaling is necessary for the maintenance of pluripotency in human embryonic stem cells. *Development* **132**, 1273-1282 (2005).

240.   Trivedi, P. & Hematti, P. Derivation and immunological characterization of mesenchymal stromal cells from human embryonic stem cells. *Exp Hematol* **36**, 350-359 (2008).

241.   Liu, Y.P. & Hematti, P. Generation of mesenchymal stromal cells from HOXB4-expressing human embryonic stem cells. *Cytotherapy* **11**, 716-725 (2009).

242.   Takahashi, K. & Yamanaka, S. Induction of pluripotent stem cells from mouse embryonic and adult fibroblast cultures by defined factors. *Cell* **126**, 663-676 (2006).

243.   Villa-Diaz, L.G. *et al.* Derivation of mesenchymal stem cells from human induced pluripotent stem cells cultured on synthetic substrates. *Stem cells* **30**, 1174-1181 (2012).

244.   Zhao, Q. *et al.* MSCs derived from iPSCs with a modified protocol are tumor-tropic but have much less potential to promote tumors than bone marrow MSCs. *Proceedings of the National Academy of Sciences of the United States of America* (2014).

245.   Lian, Q. *et al.* Functional mesenchymal stem cells derived from human induced pluripotent stem cells attenuate limb ischemia in mice. *Circulation* **121**, 1113-1123 (2010).

246. Horwitz, E.M. *et al.* Clarification of the nomenclature for MSC: The International Society for Cellular Therapy position statement. *Cytotherapy* **7**, 393-395 (2005).

247. Bianco, P. *et al.* The meaning, the sense and the significance: translating the science of mesenchymal stem cells into medicine. *Nature medicine* **19**, 35-42 (2013).

248. Lee, O.K. *et al.* Isolation of multipotent mesenchymal stem cells from umbilical cord blood. *Blood* **103**, 1669-1675 (2004).

249. Lee, R.H. *et al.* Characterization and expression analysis of mesenchymal stem cells from human bone marrow and adipose tissue. *Cellular physiology and biochemistry : international journal of experimental cellular physiology, biochemistry, and pharmacology* **14**, 311-324 (2004).

250. Jankowski, R.J., Deasy, B.M. & Huard, J. Muscle-derived stem cells. *Gene Ther* **9**, 642-647 (2002).

251. Soleimani, M. & Nadri, S. A protocol for isolation and culture of mesenchymal stem cells from mouse bone marrow. *Nature protocols* **4**, 102-106 (2009).

252. Peister, A. *et al.* Adult stem cells from bone marrow (MSCs) isolated from different strains of inbred mice vary in surface epitopes, rates of proliferation, and differentiation potential. *Blood* **103**, 1662-1668 (2004).

253. Binda, O. *et al.* Trimethylation of histone H3 lysine 4 impairs methylation of histone H3 lysine 9: Regulation of lysine methyltransferases by physical interaction with their substrates. *Epigenetics* **5**, 767-775 (2010).

254. Wang, H., Cao, R., Xia, L., Erdjument-Bromage, H., Borchers, C., Tempst, P., & Zhang, Y. Purification and functional characterization of a histone H3-lysine 4-specific methyltransferase. *Molecular cell* **8**, 11 (2001).

255.   Fischle, W., Wang, Y. & Allis, C.D. Histone and chromatin cross-talk. *Current Opinion in Cell Biology* **15**, 172-183 (2003).

256.   Bannister, A.J. & Kouzarides, T. Regulation of chromatin by histone modifications. *Cell Research* **21**, 381-395 (2011).

257.   Shukla, A., Chaurasia, P. & Bhaumik, S.R. Histone methylation and ubiquitination with their cross-talk and roles in gene expression and stability. *Cellular and Molecular Life Sciences* **66**, 1419-1433 (2008).

258.   Shen, X. *et al.* Jumonji Modulates Polycomb Activity and Self-Renewal versus Differentiation of Stem Cells. *Cell* **139**, 1303-1314 (2009).

259.   Li, H. *et al.* FOXP1 controls mesenchymal stem cell commitment and senescence during skeletal aging. *The Journal of Clinical Investigation* **127**, 1241-1253 (2017).

260.   Liu, H., Xia, X. & Li, B. Mesenchymal stem cell aging: Mechanisms and influences on skeletal and non-skeletal tissues. *Experimental Biology and Medicine* **240**, 1099-1106 (2015).

261.   Baxter, M.A. *et al.* Study of Telomere Length Reveals Rapid Aging of Human Marrow Stromal Cells following In Vitro Expansion. *STEM CELLS* **22**, 675-682 (2004).

262.   Stolzing, A., Jones, E., McGonagle, D. & Scutt, A. Age-related changes in human bone marrow-derived mesenchymal stem cells: Consequences for cell therapies. *Mechanisms of Ageing and Development* **129**, 163-173 (2008).

263.   Tsai, C.-C., Su, P.-F., Huang, Y.-F., Yew, T.-L. & Hung, S.-C. Oct4 and Nanog Directly Regulate Dnmt1 to Maintain Self-Renewal and Undifferentiated State in Mesenchymal Stem Cells. *Molecular Cell* **47**, 169-182 (2012).

264. Kim, N. & Cho, S.-G. Clinical applications of mesenchymal stem cells. *The Korean Journal of Internal Medicine* **28**, 387-402 (2013).

265. Ankrum, J.A., Ong, J.F. & Karp, J.M. Mesenchymal stem cells: immune evasive, not immune privileged. *Nat Biotech* **32**, 252-260 (2014).

266. Grinnemo, K.H. *et al.* Xenoreactivity and engraftment of human mesenchymal stem cells transplanted into infarcted rat myocardium. *The Journal of Thoracic and Cardiovascular Surgery* **127**, 1293-1300 (2004).

267. Schu, S. *et al.* Immunogenicity of allogeneic mesenchymal stem cells. *Journal of Cellular and Molecular Medicine* **16**, 2094-2103 (2012).

268. Zangi, L. *et al.* Direct Imaging of Immune Rejection and Memory Induction by Allogeneic Mesenchymal Stromal Cells. *STEM CELLS* **27**, 2865-2874 (2009).